The Abdus Salam
International Centre for Theoretical Physics

United Nations
Educational, Scientific and
Cultural Organization

IAEA
International Atomic Energy Agency

1932-18

Winter College on Micro and Nano Photonics for Life Sciences

11 - 22 February 2008

Coherent Anti-Stokes Raman Scattering Microscopy (CARS): from fundamentals to applications (Part I, II and III)

Herve Rigneault
Institut Fresnel Marseille
Marseille, France

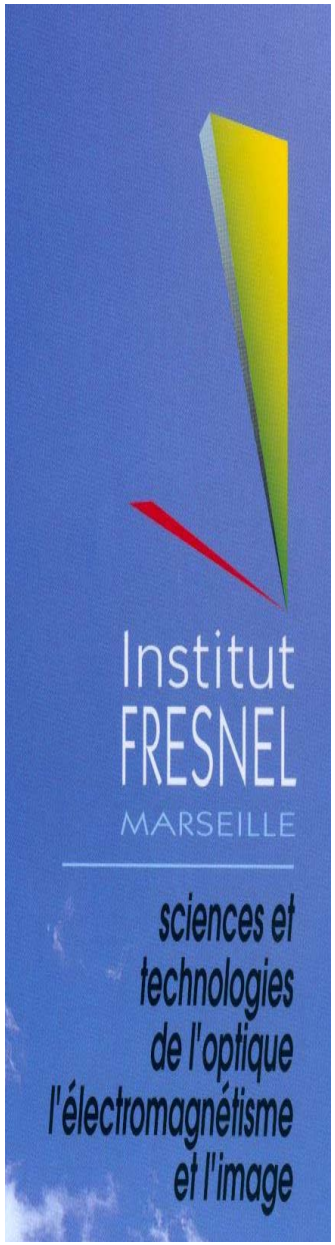

Coherent anti-Stokes Raman scattering (CARS) microscopy: from principles to applications

Hervé Rigneault

Mosaic group, Institut Fresnel – Marseille, France

Thanks to: N. Djaker, D. Gachet, N. Sandeau, F. Billard

Light

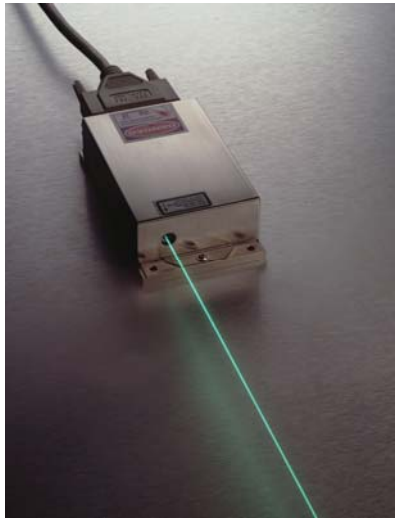

+

molecule

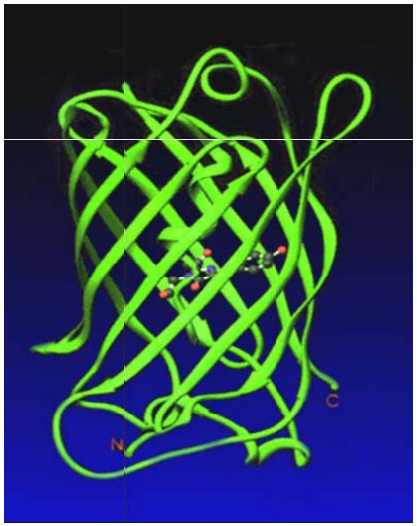

Contrast mechanism

Refraction
Scattering
Raman
Fluorescence
Nonlinear

+

Image

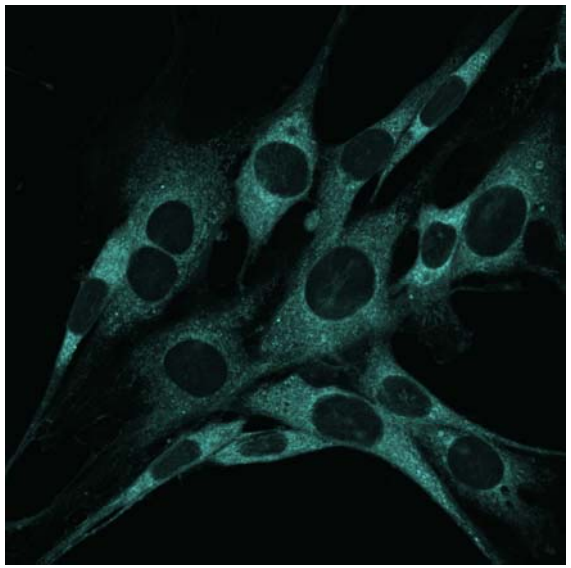

Light Microscopy

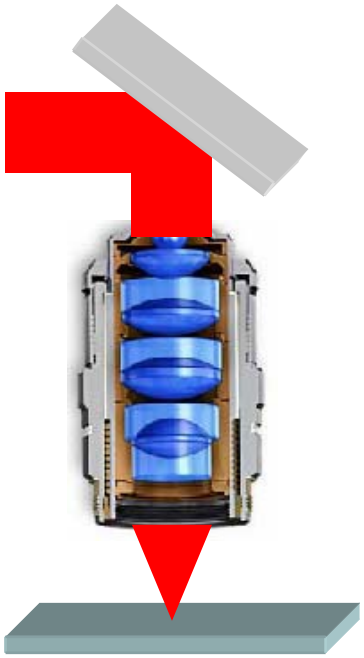

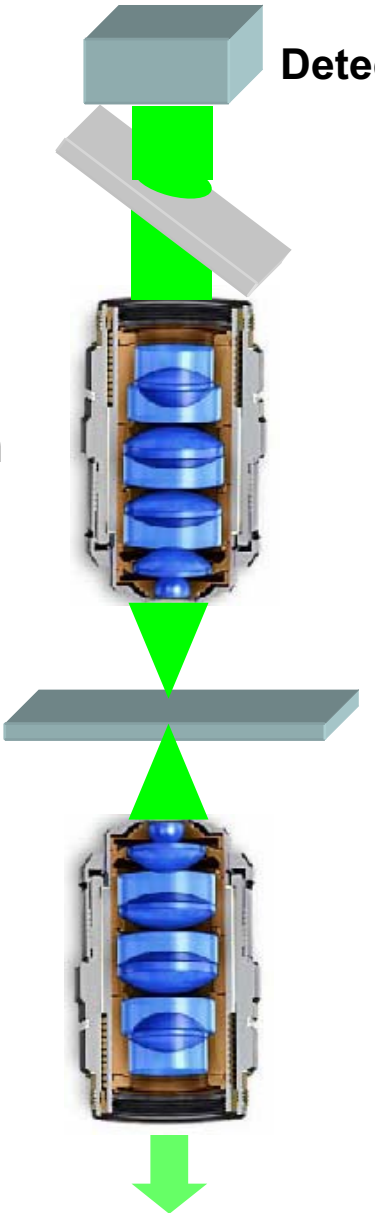

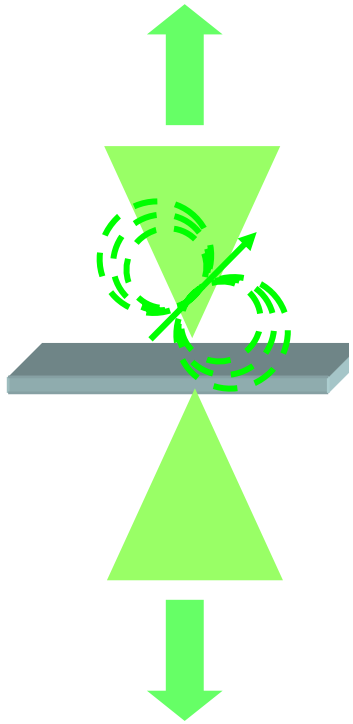

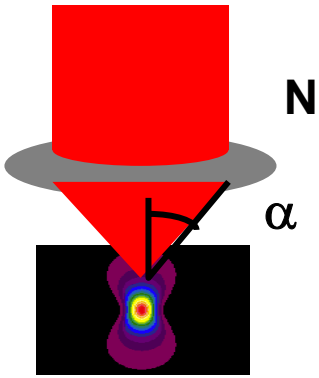

Numerical aperture

$NA = n \sin\alpha$

Typical NA ~ 0.5 – 1.4
(immersion objective)

$$r = \frac{1.22\lambda}{2 \cdot NA}$$

$$d = \frac{0.22\lambda}{n \sin^2(\alpha/2)}$$

Light microscopy: excitation field

Excitation

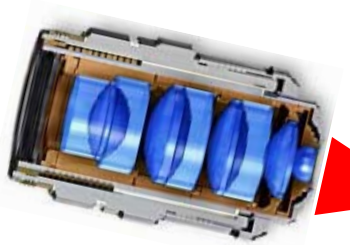

?

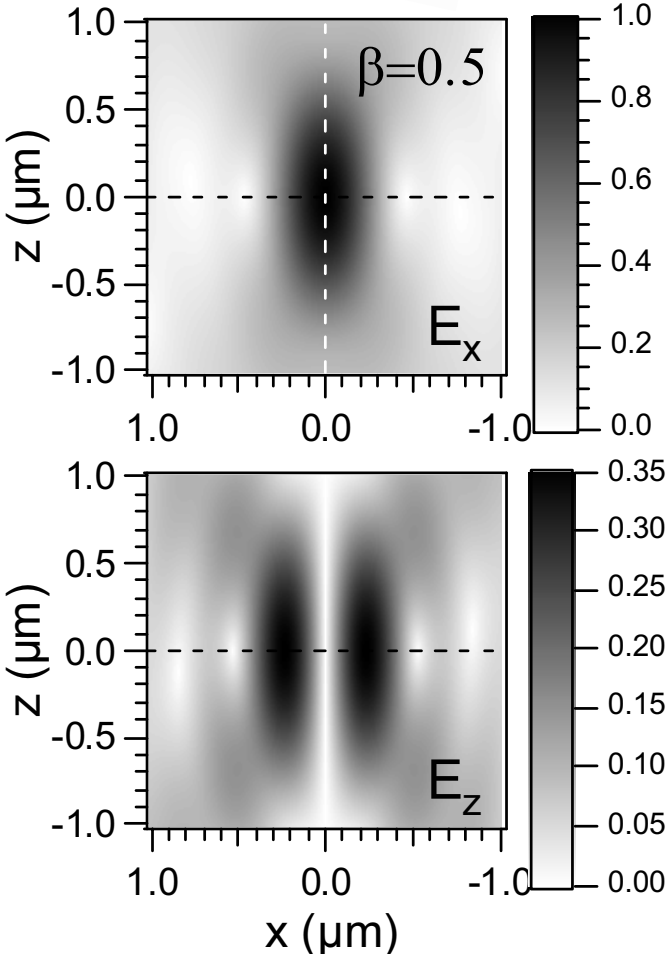

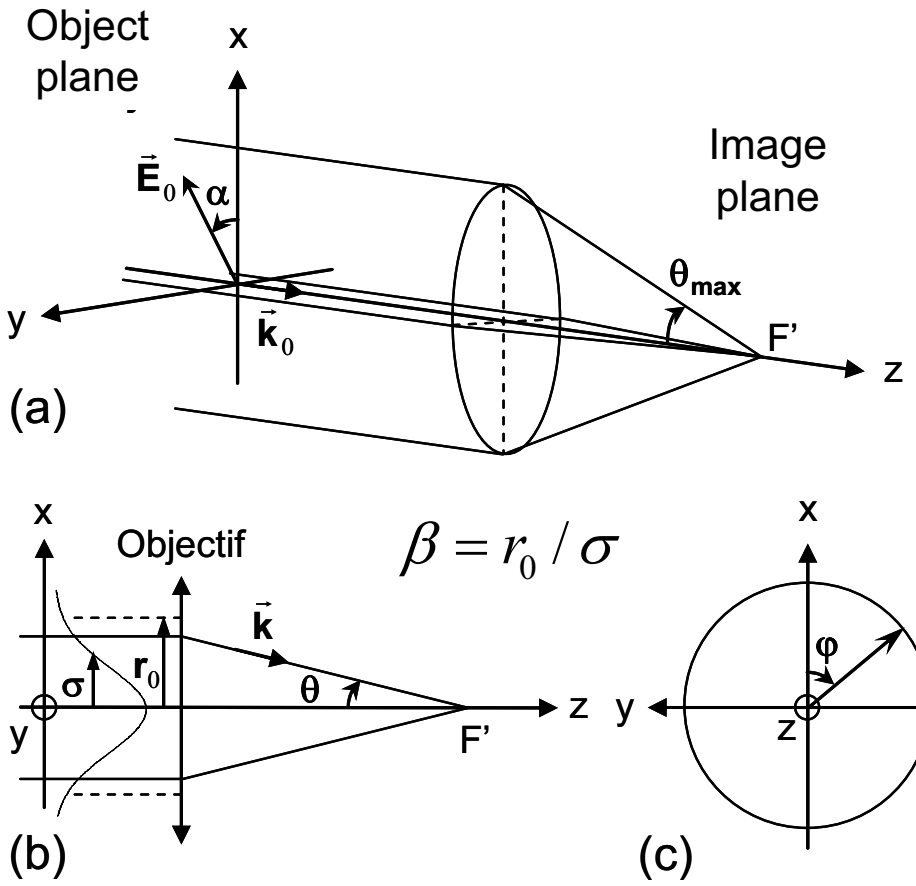

$$\beta = r_0 / \sigma$$

References:

Richards & Wolf, "Electromagnetic diffraction in optical systems. II. Structure of the image field in an aplanetic system", *Royal Society of London Proceedings Series A, Proceedings of the Royal Society of London,* **1959**, *253*, 358-379

Novotny & Hecht, "Principles of Nano-Optics", *Cambridge University Press,* **2006**

Light microscopy: emission field

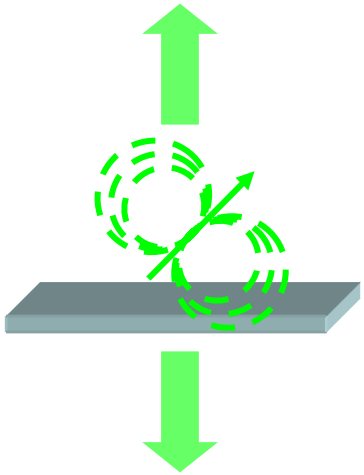

Contrast mechanism dependent

-Fluorescence 1P, 2P

-SHG (TWM), THG, CARS (FWM)

Far-field approximation (r >> λ):

$$\vec{E} \approx \frac{1}{4\pi\varepsilon_0}\left(\frac{-k^2 p_0 \sin\theta}{r}\right)\exp\left(i\vec{k}\cdot\vec{r}\right)\vec{e}_\theta$$

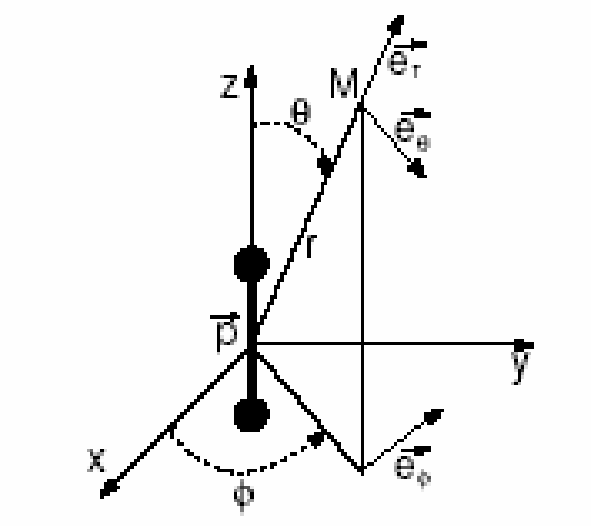

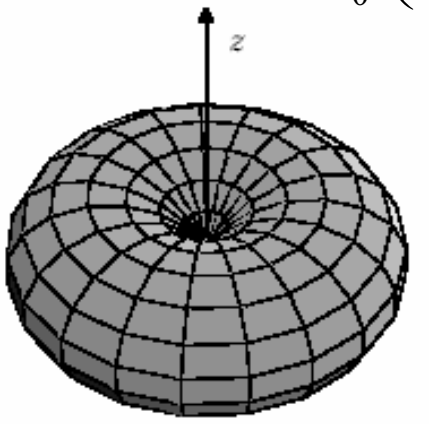

From J.M. Raimond, electromagnetism & relativity's lesson (2000)

Far-field radiation pattern of a single z-oriented Hertzian dipole

Light emission in incoherent processes

…to an assembly of dipoles.

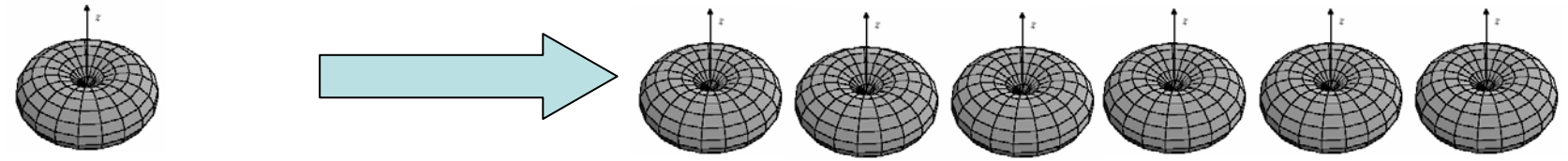

From a single dipole…

≡

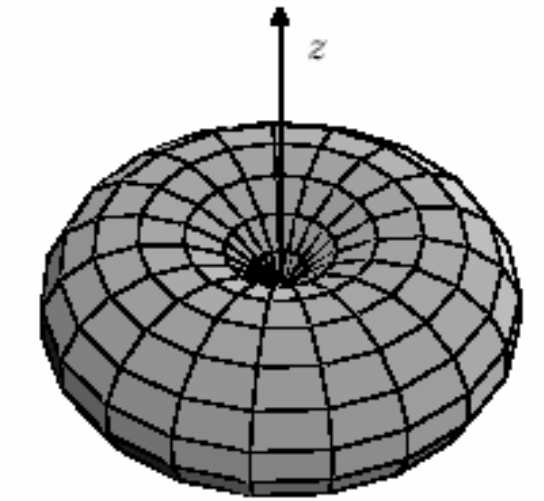

- **Incoherent emission =>** each dipole emits light with a random phase.
- The **total intensity** equals the sum of individual intensities.

For an incoherent process: Fluorescence

Light emission in coherent process

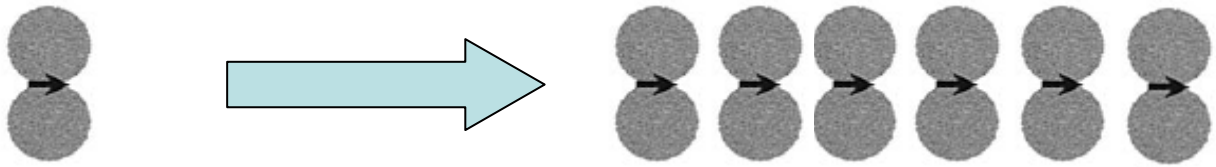

Adapted from J.X. Cheng and al.,
Biophys. J. **83**, 502 (2002)

- **Coherent emission =>** the phase of each dipole is fixed by a phase relation.
- Locally, the **total field** is the sum of the fields emitted by each dipole (interference).
- The intensity is the square modulus of the total field

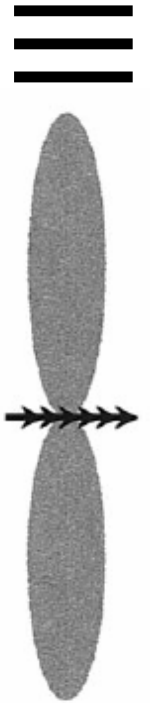

Radiation pattern depends on the phase relationship between emitters !

For a coherent process: SHG (TWM), **THG, CARS** (FWM)

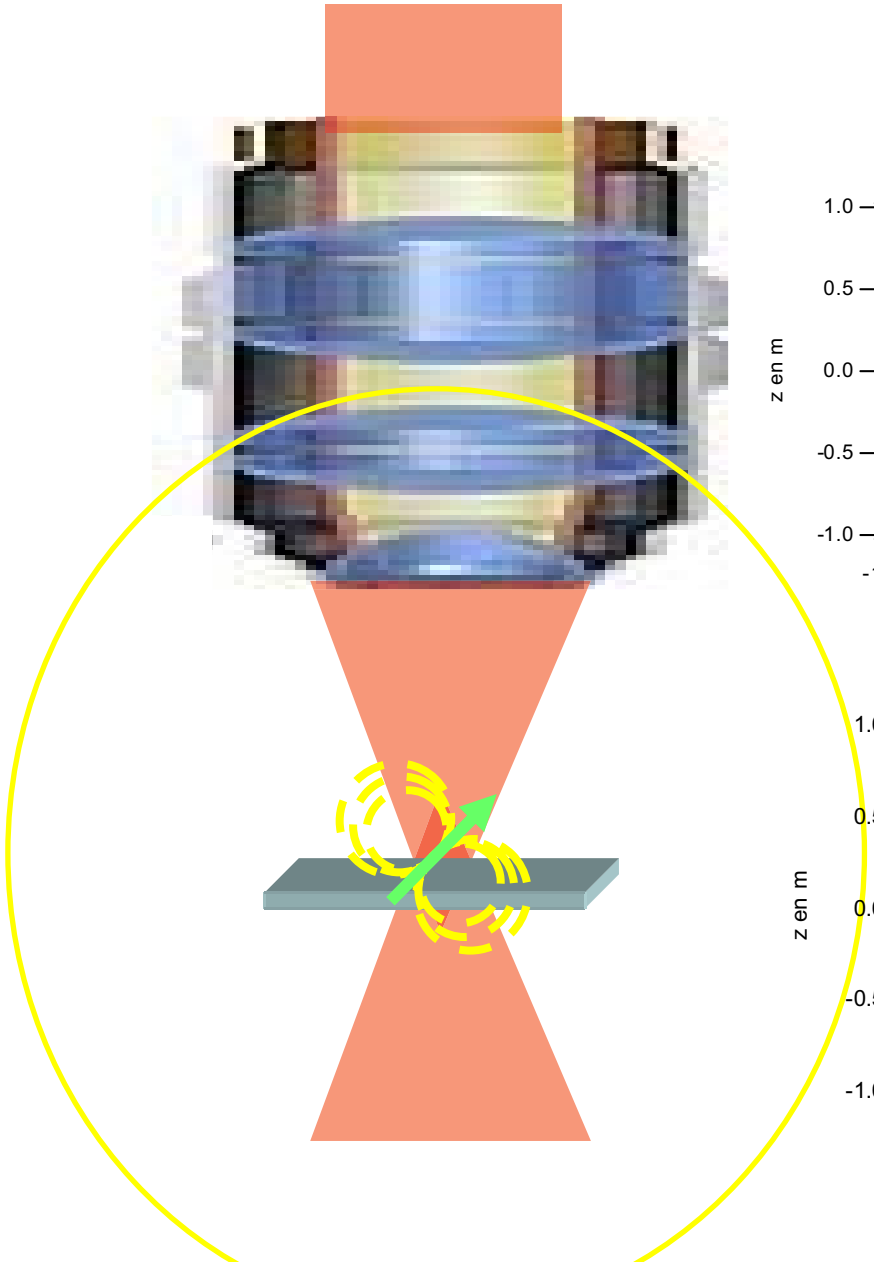

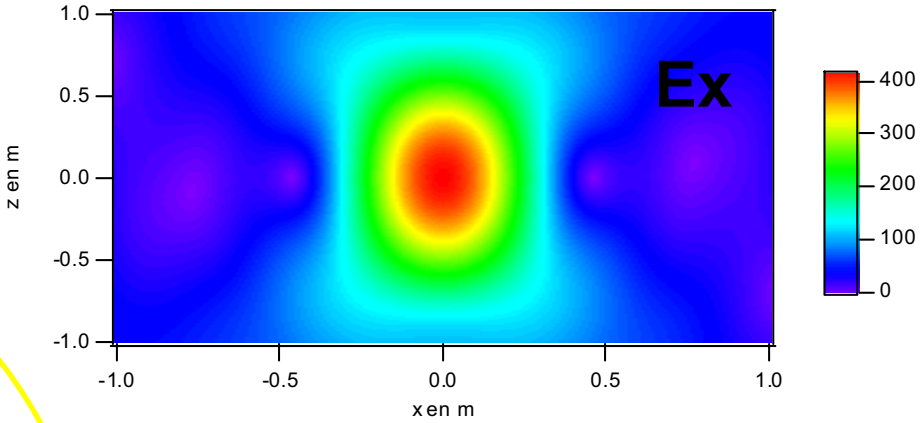
Ex
1.0
0.5
0.0
-0.5
-1.0
z en m
-1.0
-0.5
0.0
0.5
1.0
x en m
400
300
200
100
0

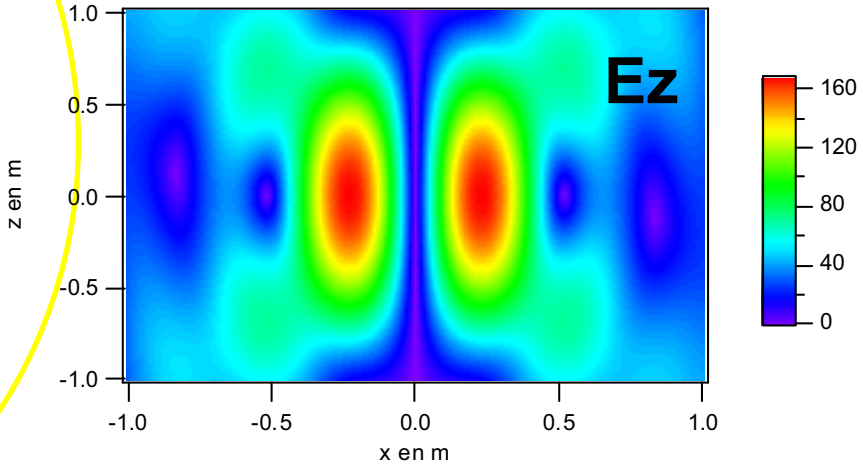
Ez
1.0
0.5
0.0
-0.5
-1.0
z en m
-1.0
-0.5
0.0
0.5
1.0
x en m
160
120
80
40
0

Fluorescence contrast

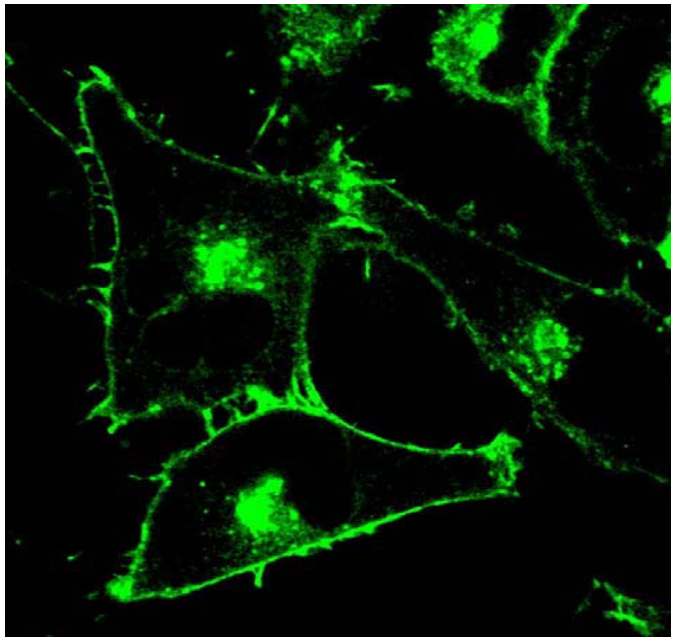

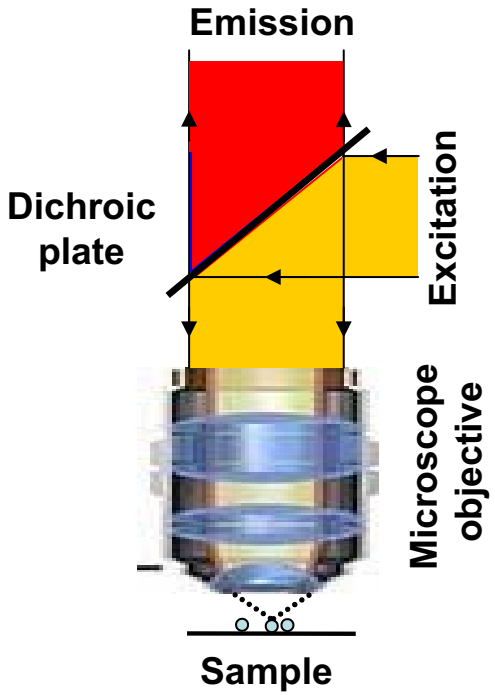

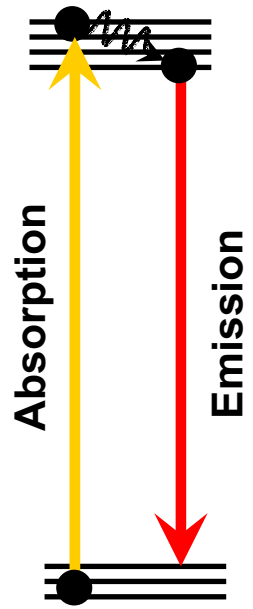

Fluorescence microscopy:

Advantages:	**Drawbacks:**
Chemical specificity	Staining step before observation
Very good SNR ratio	Staining induced cell's potential malfunctioning
	Photobleaching

Nonlinear contrast

(cf Mario Bertolotti tutorial on nonlinear optics)

$$\mathbf{P}(\omega) = \varepsilon_0(\chi^{(1)}\mathbf{E} + \chi^{(2)}\mathbf{E}:\mathbf{E} + \chi^{(3)}\mathbf{E}:\mathbf{E}:\mathbf{E} + \ldots)$$

$$P_i = \varepsilon_0(\chi_{ij}^{(1)}E_j + \chi_{ijk}^{(2)}E_jE_k + \chi_{ijkl}^{(3)}E_jE_kE_l + \ldots)$$

Einstein notation

Linear optics

Non linear tensor
Symmetry dependant

Introduction / mixing of frequencies
Need to be strong

Non linear optics requires strong optical field

-Hydogen atom, $E_{at} = \frac{e}{4\pi\varepsilon_0 a^2} \approx 5.10^{11}\ V.m^{-1}$; Bohr radius a=5.10^{-11}m

- Sun on earth: 10^3 *V.m*$^{-1}$, *linear optics regime*

- 10kW laser focused on a 10μm spot: 10^8 *V.m*$^{-1}$, *non linear optics regime*

- ***Non linear microscopy needs to focus the incident fields!!***

NLO contrasts in microscopy

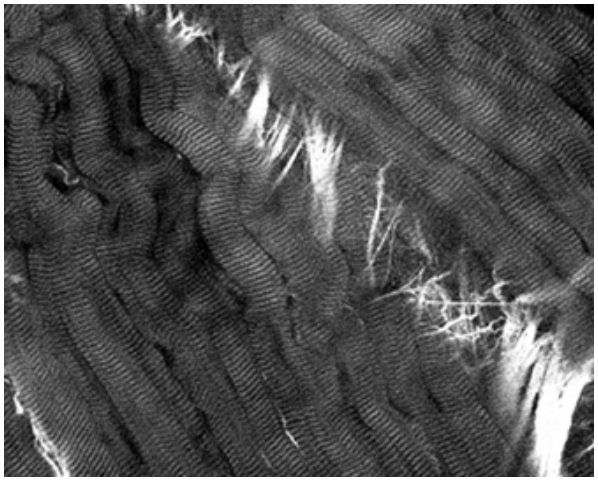

Muscle tissue (SHG)
(Webb lab)

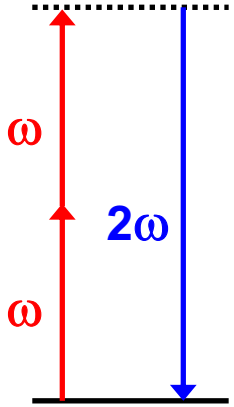

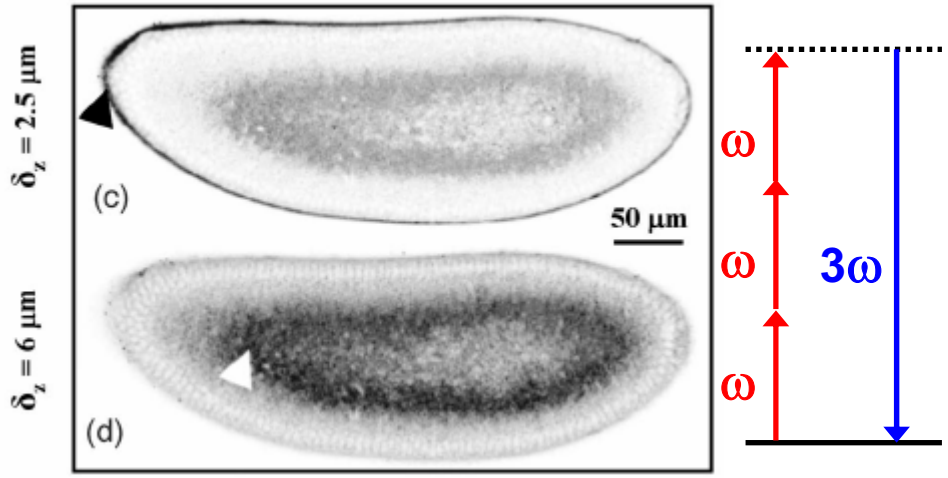

Débarre et *al.*, *Opt. Lett.* **30**, 2134 (2005)

SHG microscopy **THG microscopy**

$$\mathbf{P}(\omega) = \varepsilon_0(\chi^{(1)}\mathbf{E} + \chi^{(2)}\mathbf{E}:\mathbf{E} + \chi^{(3)}\mathbf{E}:\mathbf{E}:\mathbf{E} + \ldots)$$

SHG and THG microscopy

Advantages:	**Drawbacks:**
Useless staining	Non-Centrosymmetric media required (SHG)
No photobleaching	No chemical specificity

The challenge: a chemical selectivity without staining

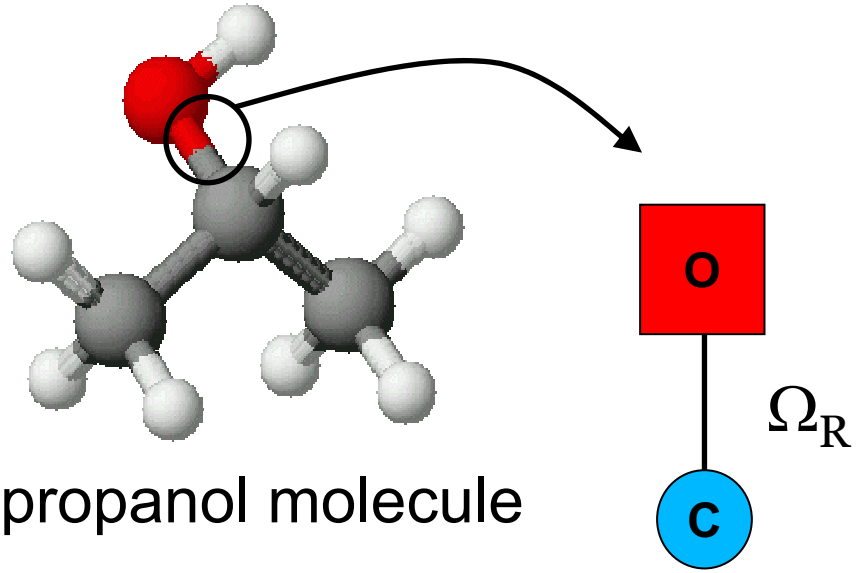

2-propanol molecule

CH3-CH(OH)-CH3

Modeling:

Assembly of oscillators with mode frequency Ω_R and mode energy $h\Omega_R$.

Specificity:

Ω_R specific to each vibrational mode.

Detecting vibrational levels: IR absorption microscopy

IR excitation

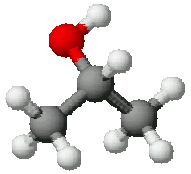

IR absorption spectrum

$1/\lambda=3300\ cm^{-1}$
$\nu=100\ THz$
$\lambda=3\mu m$

Ω_R

$1/\lambda=1000\ cm^{-1}$
$\nu=30\ THz$
$\lambda=10\mu m$

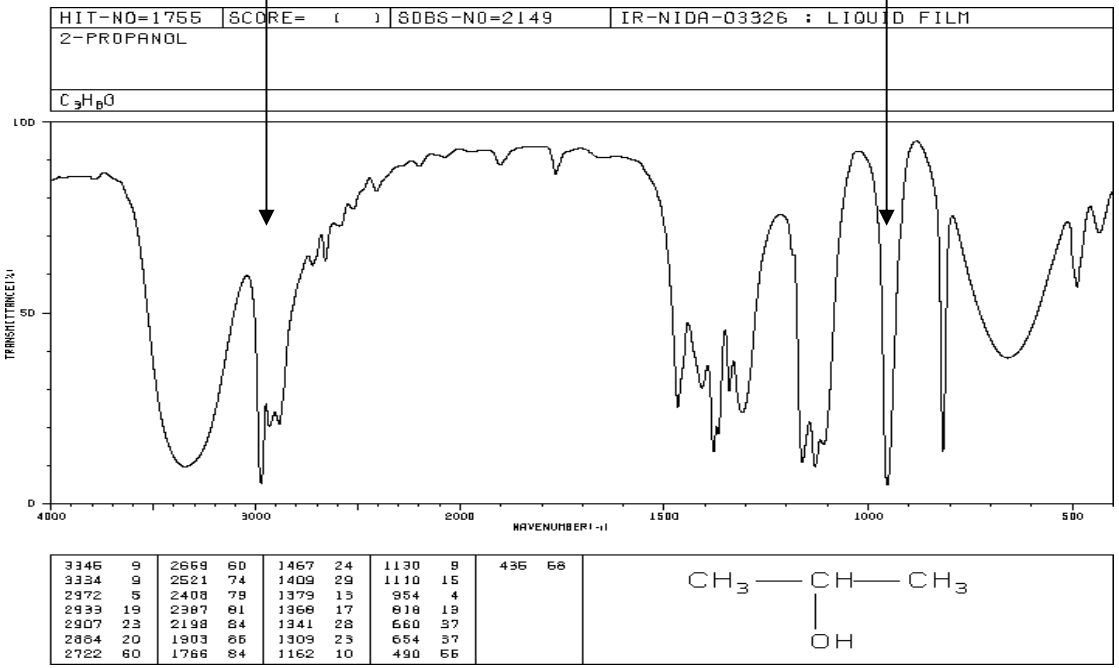

Source: http://www.aist.go.jp

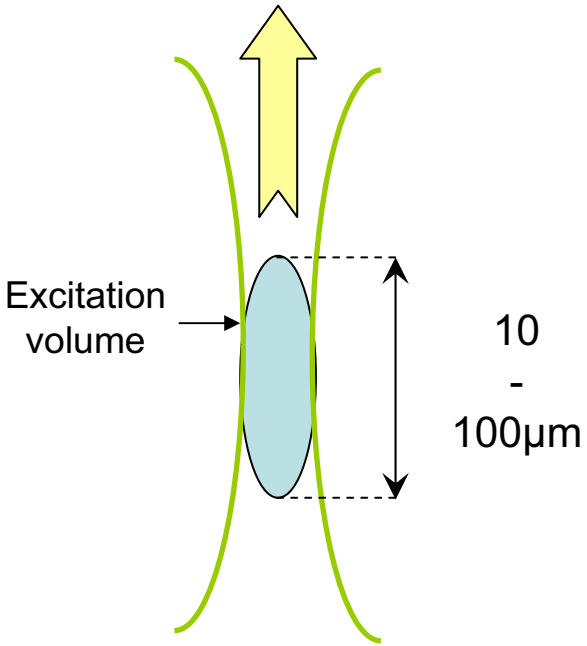

Main drawback:

bad spatial resolution

Detecting vibrational levels: Raman scattering basics (1)

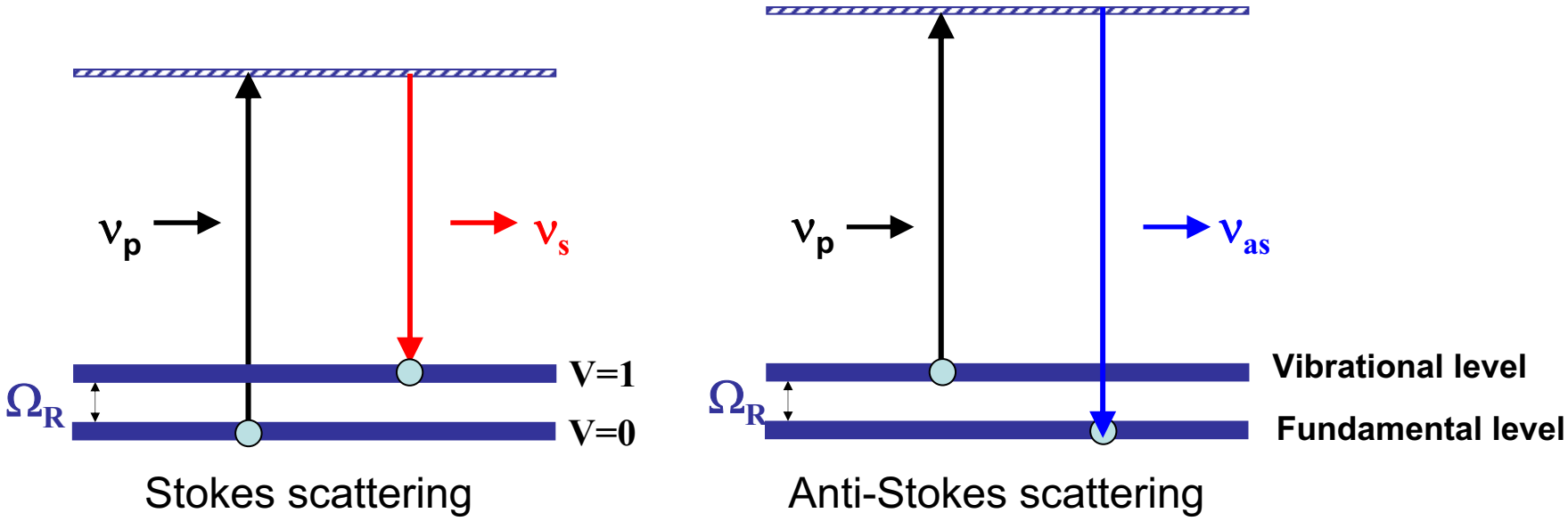

Spontaneous Raman scattering

Raman scattering basics (2)

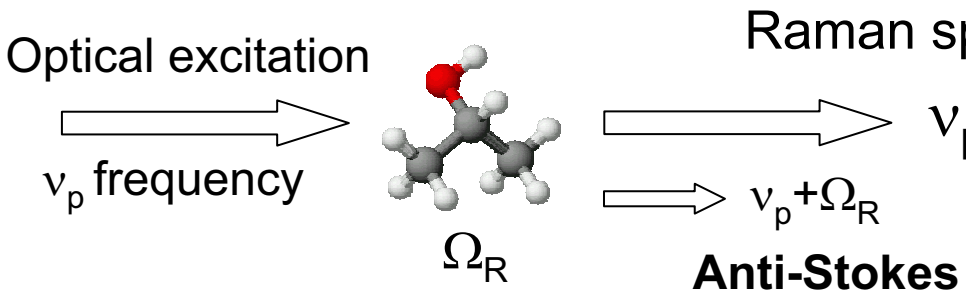

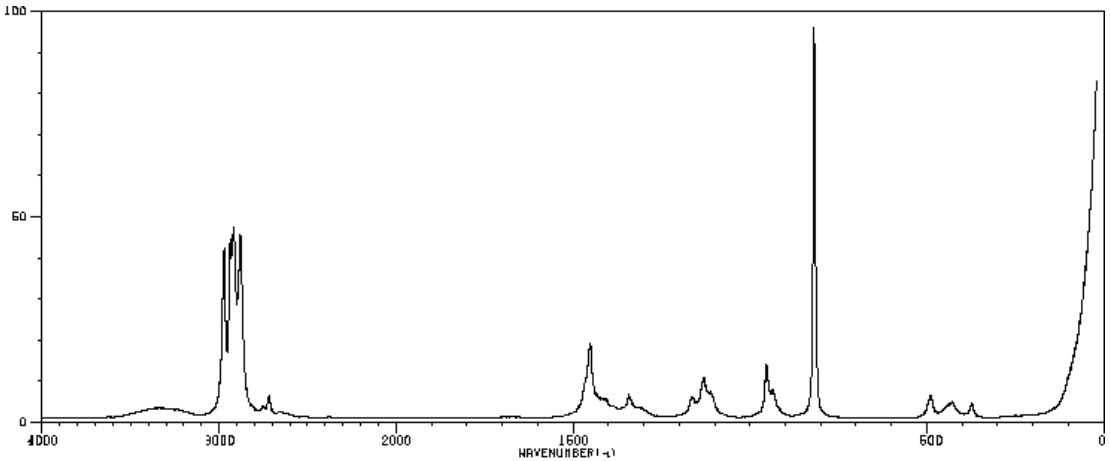

2-PROPANOL
SDBSNO = 2149 C_3H_8O RM-01-00029 : 488OA.15OM.LIQUID

2972	41
2938	44
2919	46
2881	45
1464	18
1132	10
955	13
820	95

Source: http://www.aist.go.jp

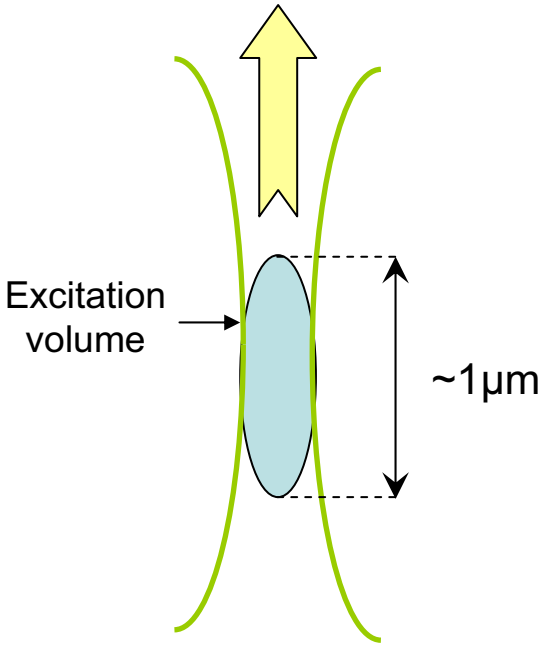

Main drawback:

Long acquiring time

$\sigma_R=10^{-14}\ \sigma_F$

Coherent anti-Stokes Raman Scattering

- Can we excite a specific molecular bond efficiently?
- Can we make an image at a sub-cellular level?

Coherent Anti-Stokes Raman Scattering Microscopy

CARS

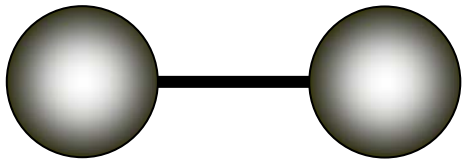

=

Bouncing the springs

$$\omega_0 = \sqrt{\frac{k}{m}}$$

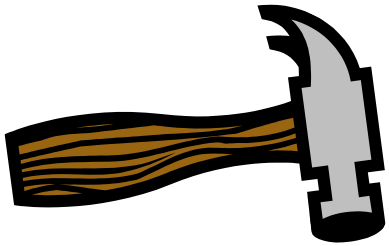

The CARS Hammer

Pump wave ν_P

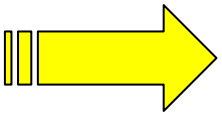

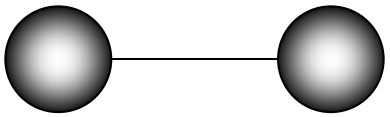

Ω_R

Anti-Stokes

$\nu_{AS}= \nu_P+\Omega_R$

Stokes $\nu_S= \nu_P-\Omega_R$

$\omega_P-\omega_S= \omega_P-(\omega_P-\Omega_R)=\Omega_R$

Coherent anti-Stokes Raman scattering: Energy view

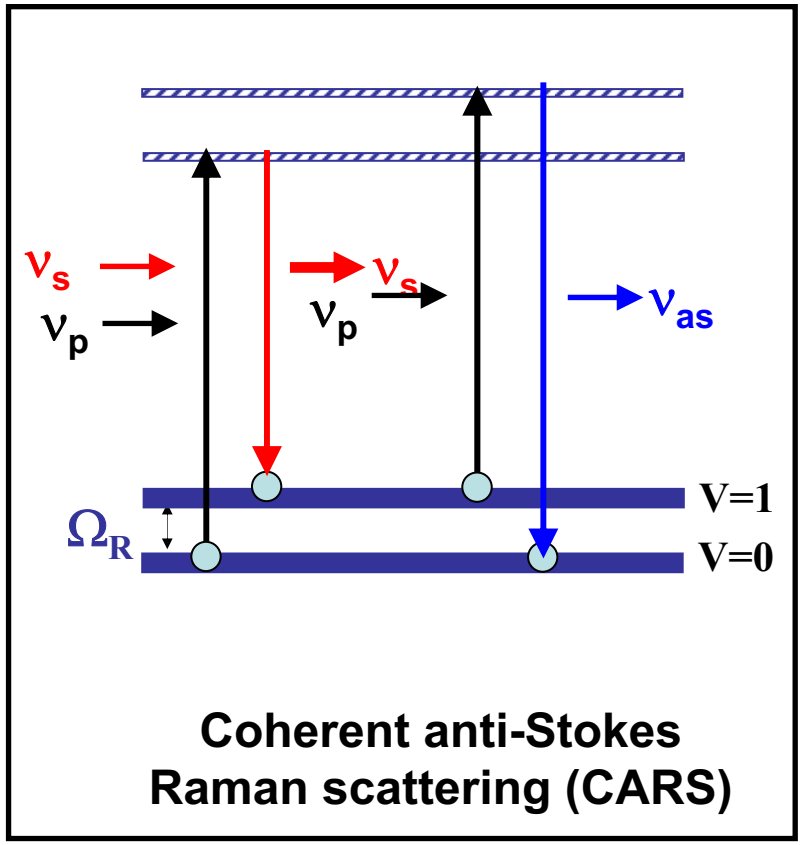

$\sigma_{CARS} = 10^6 \sigma_R = 10^{-8} \sigma_F$ (in microscopy)

Coherent anti-Stokes Raman scattering: $\chi^{(3)}$ view

$$\mathbf{P}(\omega) = \varepsilon_0(\chi^{(1)}\mathbf{E} + \chi^{(2)}\mathbf{E}:\mathbf{E} + \chi^{(3)}\mathbf{E}:\mathbf{E}:\mathbf{E} + \ldots)$$

Four waves mixing

$$\chi^{(3)}\ (\omega_1+\omega_1-\omega_3;\omega_1,\omega_1,-\omega_3,)$$

$$= \chi^{(3)}\ (2\omega_P-\omega_S;\omega_P,\ \omega_P,-\omega_S,)$$

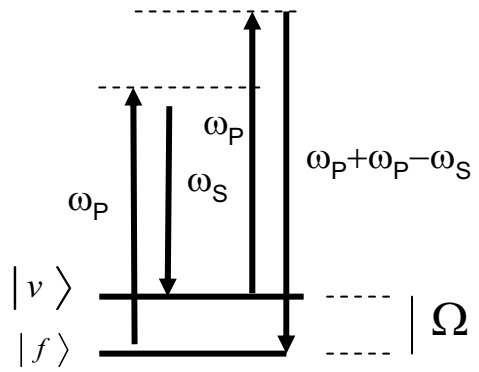

CARS / Raman Scattering

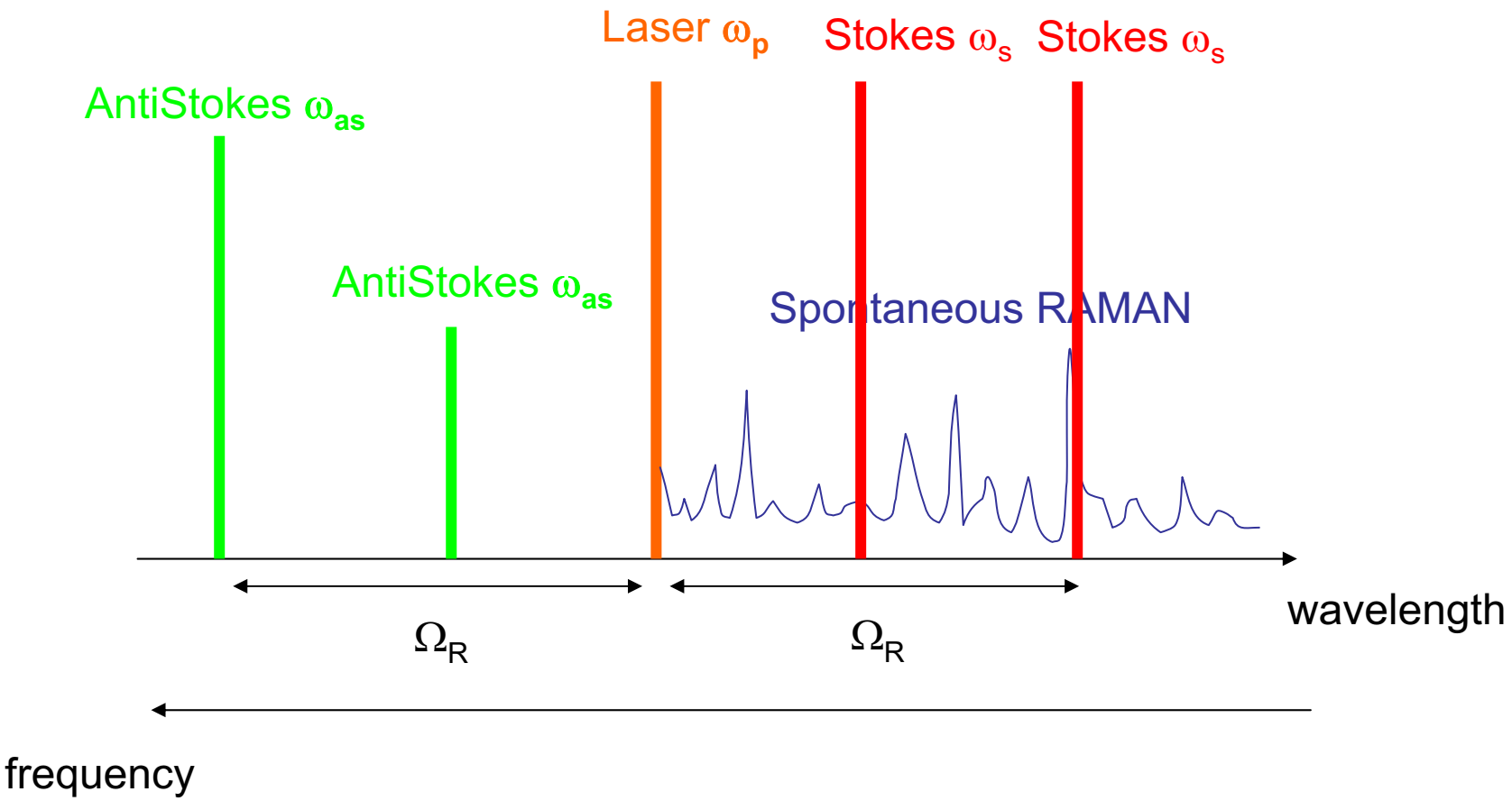

CARS microscopy: What do you need?

High sensitivity detectors

A first experimental set-up

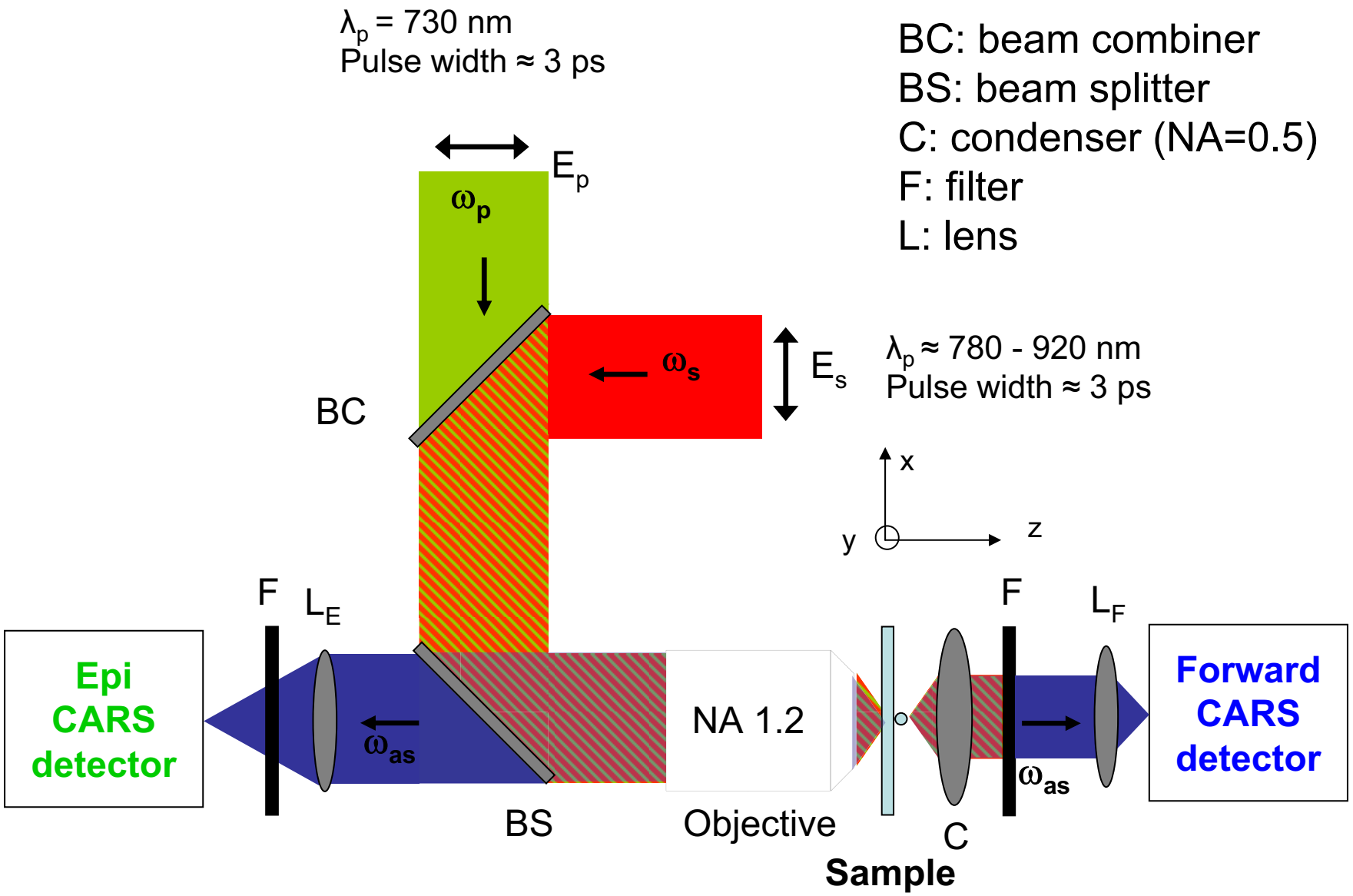

CARS microscopy: let's do a first experiment on GUV

Deuterated lipids

DMPC(D54)

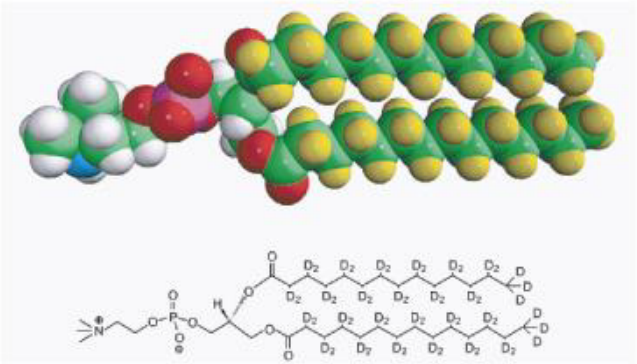

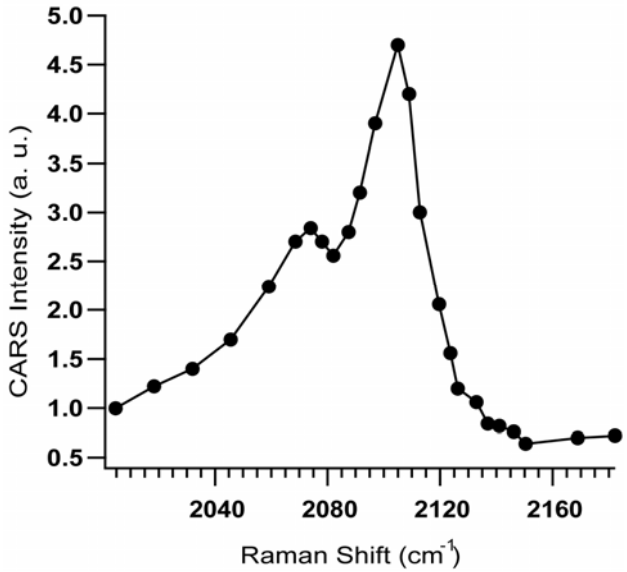

C-D bond Raman spectrum

Electroformation

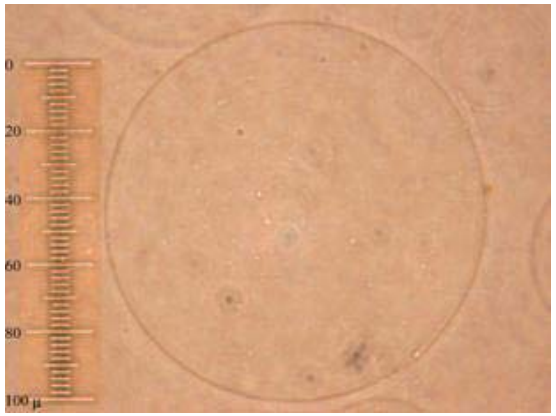

Giant unilamellar vesicles (GUV):
diameter: 5 -100 µm

CARS microscopy: a first experiment on GUV

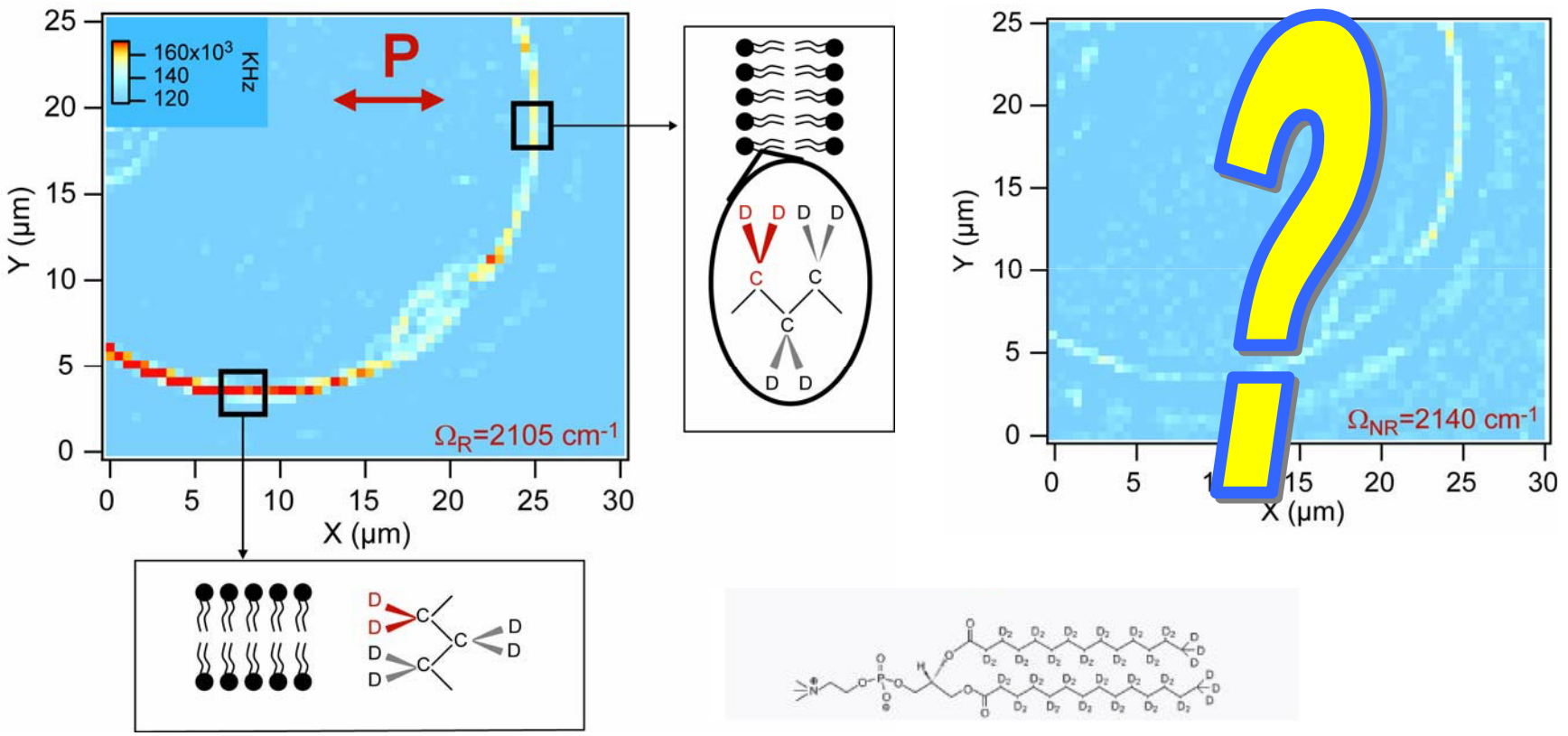

F-CARS images of GUV (Giant Unilamellar vesicle) DMPC[D54]

F-CARS GUV (DMPC-D54):
(60×60) pixels, 1ms/pixel.

Pump 730nm, Stokes 862nm: Power 800µW : rep rate: 4MHz

CARS: Resonant and non Resonant contribution

Two contributions to CARS generation

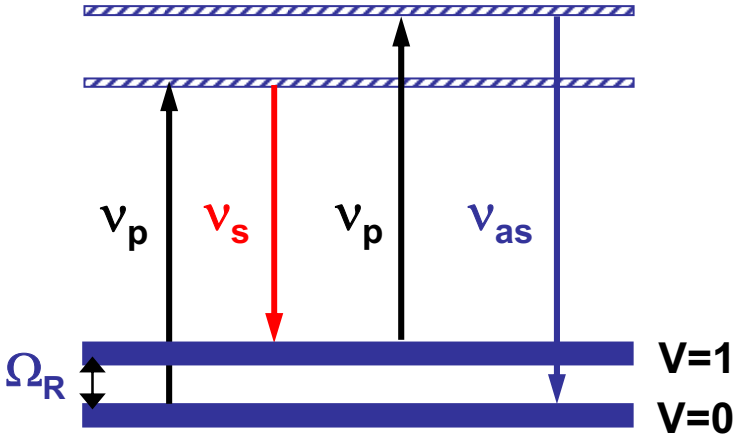

Resonant contribution ($\chi_R^{(3)}$)

(vibrational origin)

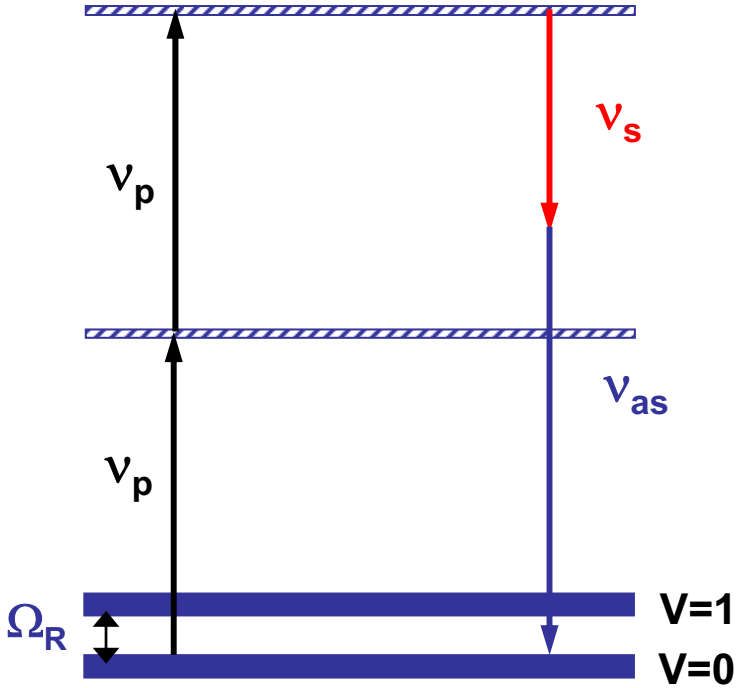

Nonresonant contribution ($\chi_{NR}^{(3)}$)

(electronic response of the medium)

Presence of molecules with oscillating vibrational mode Ω_R

➔ Enhancement of the signal at frequency ν_{as}

CARS: Resonant and non Resonant contribution

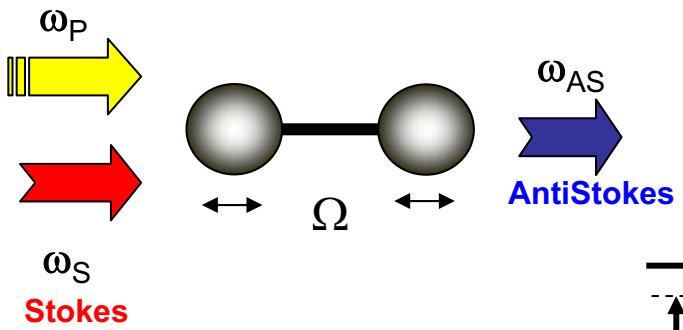

$$\omega_{as} = \omega_p + \omega_p - \omega_s = 2\omega_p - \omega_s$$

Degenerated FWM

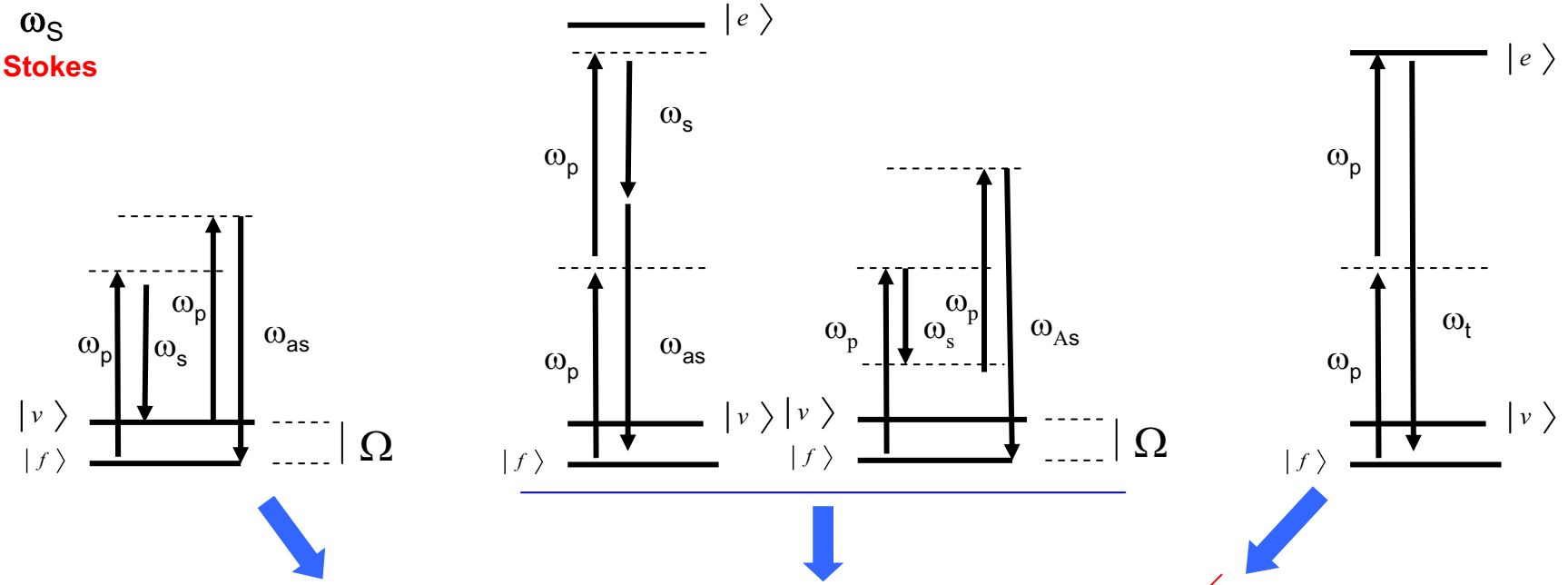

$$\chi^{(3)} = \underbrace{\frac{A_R}{\Omega_R - (\omega_p - \omega_s) + i\Gamma_R}}_{\chi^{(3)}_R} + \chi^{(3)}_{NR} + \frac{A_t}{\omega_t - 2\omega_p - i\Gamma_t}$$

Far from two photons absorption

Spectral behaviour of the $\chi^{(3)}$ tensor: $\chi^{(3)}_R$ and $\chi^{(3)}_{NR}$

CARS as a third-order nonlinear process:

$$\overrightarrow{P^{(3)}}\left(\vec{r},-\omega_{as}\right)=\overrightarrow{\overrightarrow{\chi^{(3)}}}\left(\omega_{as}\right):\overrightarrow{E_p}\left(\vec{r},\omega_p\right):\overrightarrow{E_p}\left(\vec{r},\omega_p\right):\overrightarrow{E_s^*}\left(\vec{r},\omega_s\right)$$

$$I(\omega_{as})\propto\left|P^{(3)}(-\omega_{as})\right|^2\propto\left|\chi^{(3)}\right|^2$$

$\chi^{(3)}$ decomposition into two parts : $\chi^{(3)}=\chi^{(3)}_R+\chi^{(3)}_{NR}$

For an isolated Raman line : $\chi^{(3)}_R=\dfrac{a}{(\omega_p-\omega_s-\Omega_R)+i\Gamma}$

- a → Oscillator strength
- Γ → Raman line half-width
- Ω_R → Vibrational frequency

Electronic response spectrally independent : $\chi^{(3)}_{NR}$ is real & constant

$\chi^{(3)}$ spectral behaviour

Spectral behaviour of the $\chi^{(3)}$ tensor: Interference term

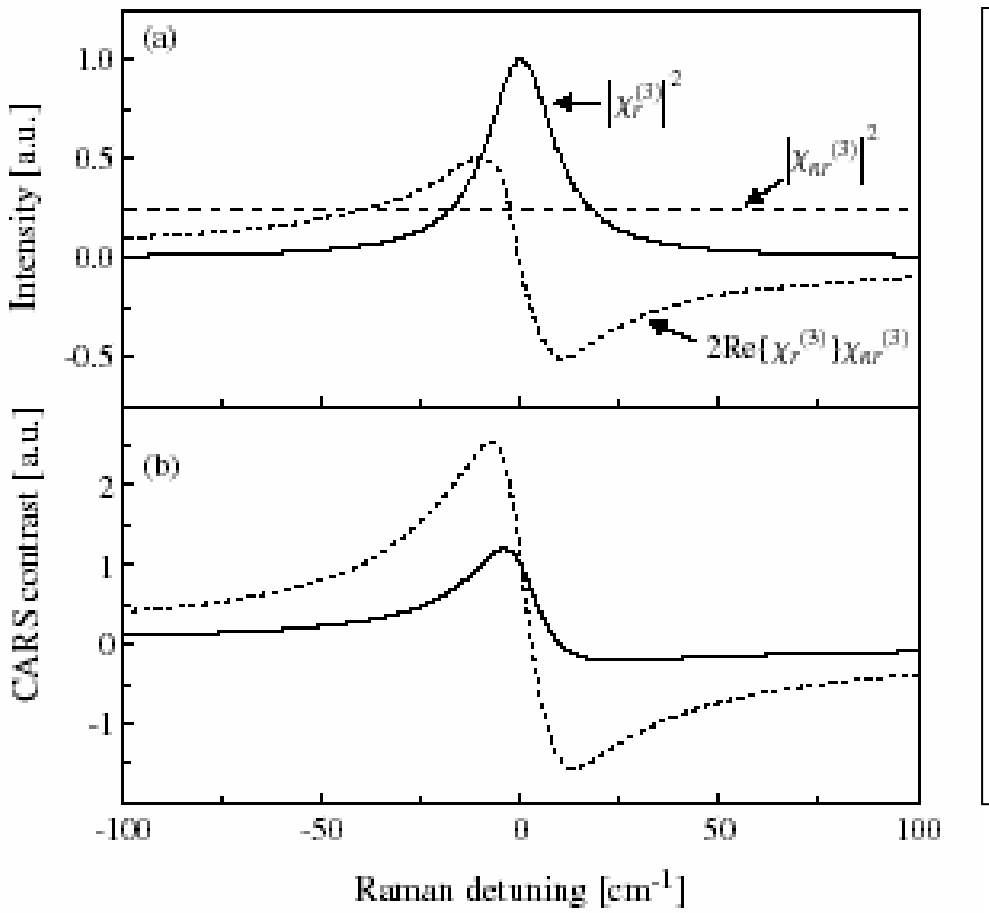

Potma et *al.*, *J. Raman Spectr.* **34**, 642 (2003)

$$I_{CARS} \alpha \left| \chi_R^{(3)} + \chi_{NR}^{(3)} \right|^2$$

$$I_{CARS} \alpha \underbrace{\left| \chi_R^{(3)} \right|^2 + \left| \chi_{NR}^{(3)} \right|^2}$$

Homodyne terms

$$+ \underbrace{2\,\mathrm{Re}\left(\chi_R^{(3)} \cdot \chi_{NR}^{(3)*} \right)}$$

Heterodyne terms

CARS resonance lineshape

Raman / CARS spectra

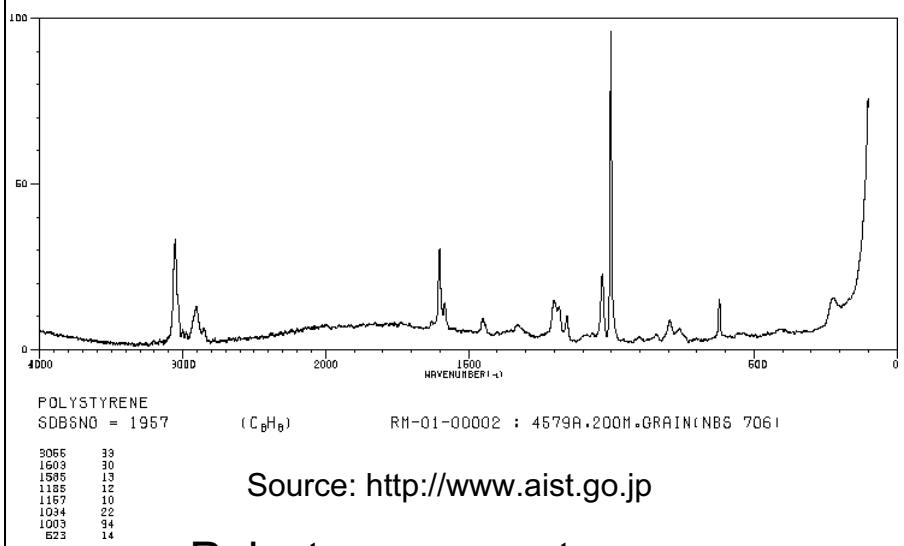

Source: http://www.aist.go.jp

Polystyrene spontaneous Raman spectrum

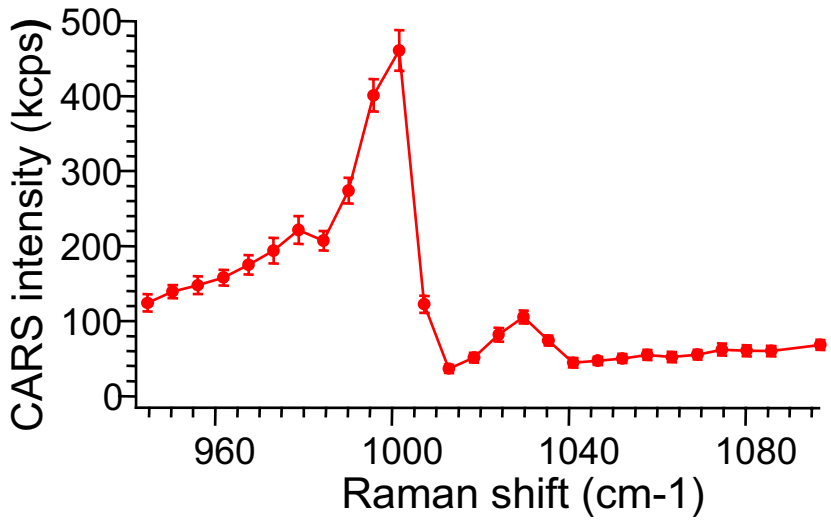

Polystyrene CARS spectrum

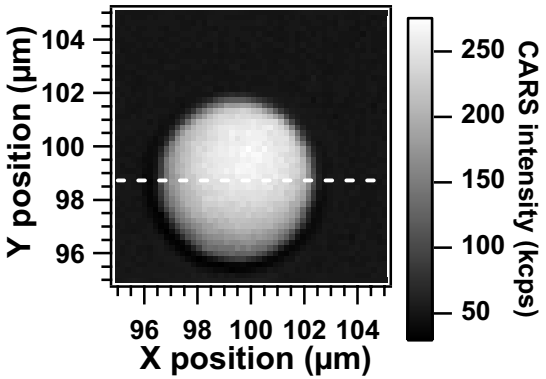

← CARS resonance

Off-resonance →

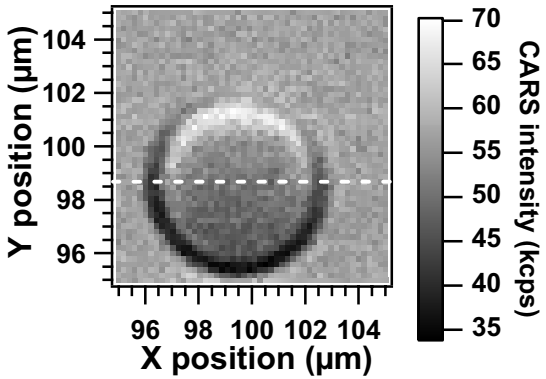

Experimental evidence

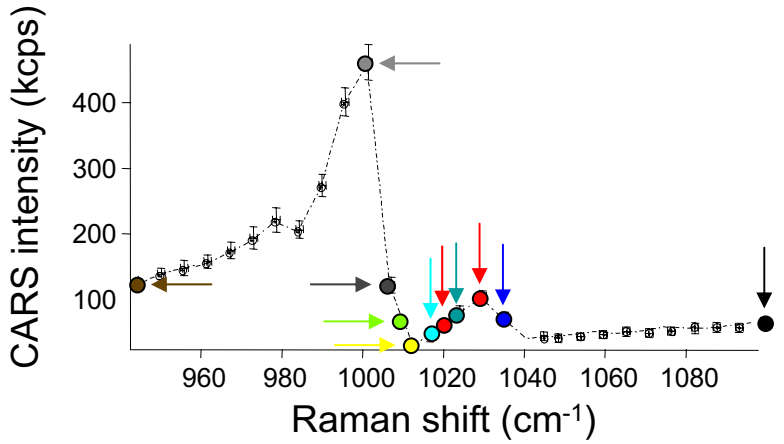

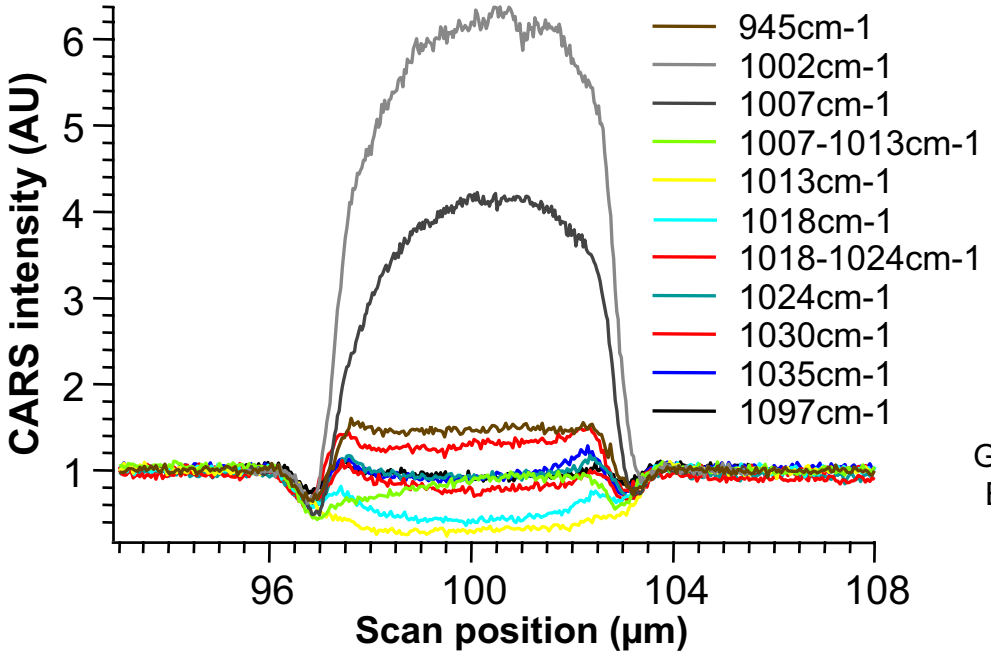

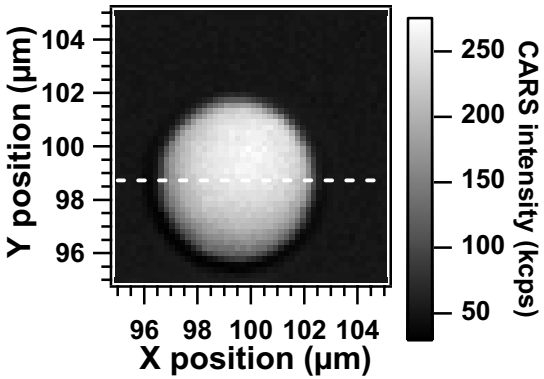

Gachet et *al.*, Optics Express **15**, 10408 (2007)

Bead experimental 1D scans

$$\chi^{(3)} = \chi_{\mathrm{R}}^{(3)} + \chi_{\mathrm{NR}}^{(3)}$$

$$\chi_{\mathrm{R}}^{(3)} = \frac{a}{(\omega_{\mathrm{p}} - \omega_{\mathrm{s}} - \Omega_{\mathrm{R}}) + i\Gamma} = \frac{a}{(\delta\omega - \Omega_{\mathrm{R}}) + i\Gamma}$$

Resonant contribution

$$\zeta = \frac{\delta\omega - \Omega_{\mathrm{R}}}{\Gamma}, \qquad \eta = -2\Gamma\frac{\chi_{\mathrm{NR}}^{(3)}}{a}.$$

$$\chi^{(3)}(\zeta,\eta) = \frac{\chi_{\mathrm{NR}}^{(3)}}{\eta(\zeta^2+1)}\left[\eta(\zeta^2+1) - 2\zeta + 2i\right]$$

$\chi^{(3)}$ can be expressed as a complex number: $\chi^{(3)}(\zeta,\eta) = \rho(\zeta,\eta)\exp\left[i\phi(\zeta,\eta)\right]$

Modulus:

$$\rho(\zeta,\eta) = \chi_{\mathrm{NR}}^{(3)}\left[1 + 4\frac{\frac{1}{\eta} - \zeta}{\eta\,(\zeta^2+1)}\right]^{1/2}$$

Phase:

$$\tan\left[\phi(\zeta,\eta)\right] = \frac{2}{\eta(\zeta^2+1) - 2\zeta}$$

Circle in the complex plane: $C = \left(\chi_{\mathrm{NR}}^{(3)}; \frac{\chi_{\mathrm{NR}}^{(3)}}{\eta}\right)$, $r = \frac{\chi_{\mathrm{NR}}^{(3)}}{\eta} = -\frac{a}{2\Gamma}$

$\chi^{(3)}$ in the complex plane

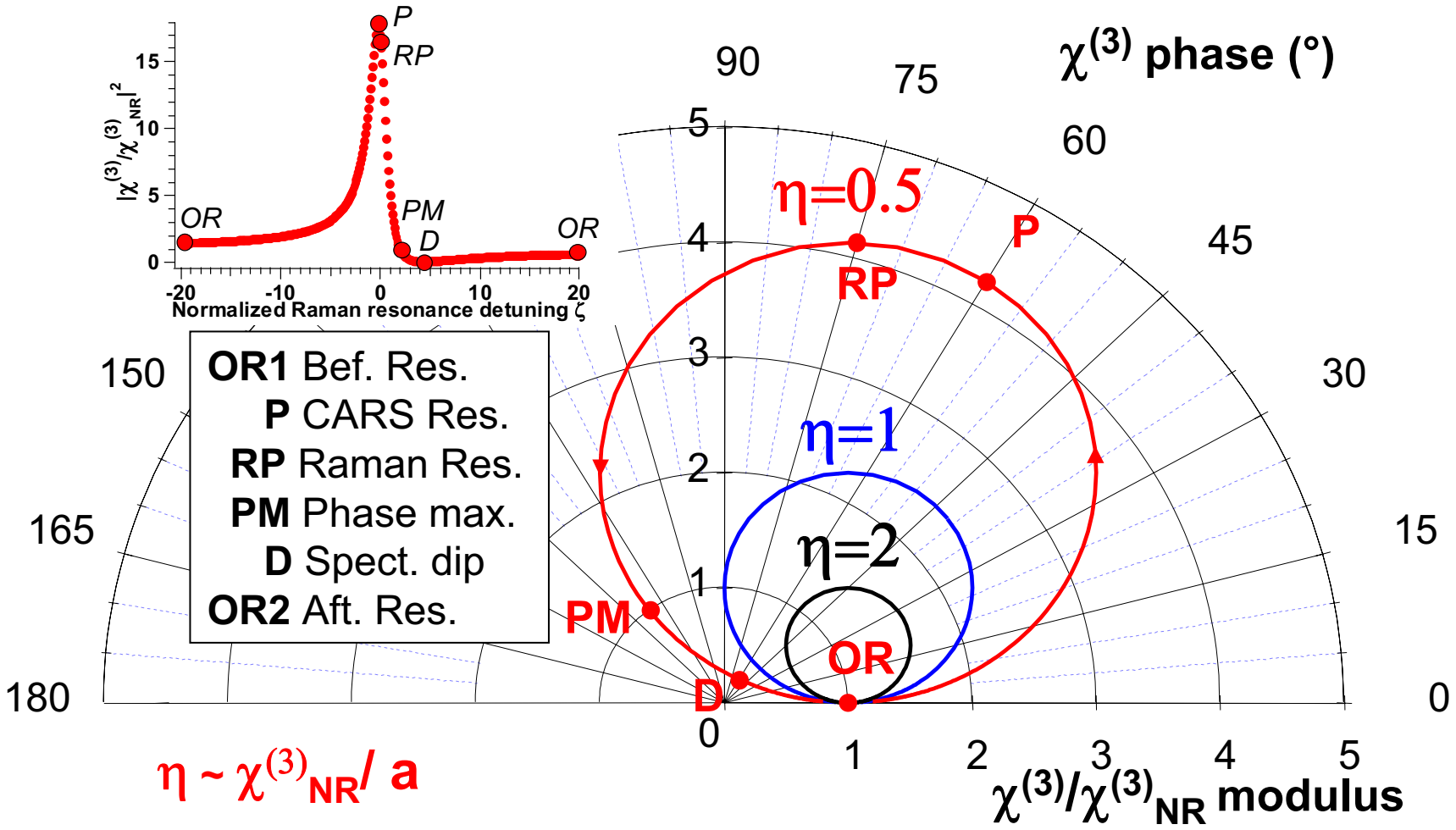

Representation of the resonance in the complex plane

$\chi^{(3)}$ drives the CARS antiStokes field

$$\overrightarrow{P^{(3)}}\left(\vec{r},-\omega_{as}\right)=\overline{\overline{\chi^{(3)}}}\left(\omega_{as}\right):\overrightarrow{E_p}\left(\vec{r},\omega_p\right):\overrightarrow{E_p}\left(\vec{r},\omega_p\right):\overrightarrow{E^*_{as}}\left(\vec{r},\omega_{as}\right)$$

$$P^{(3)}(-\omega_{as})\rightarrow\overrightarrow{E_{as}}$$

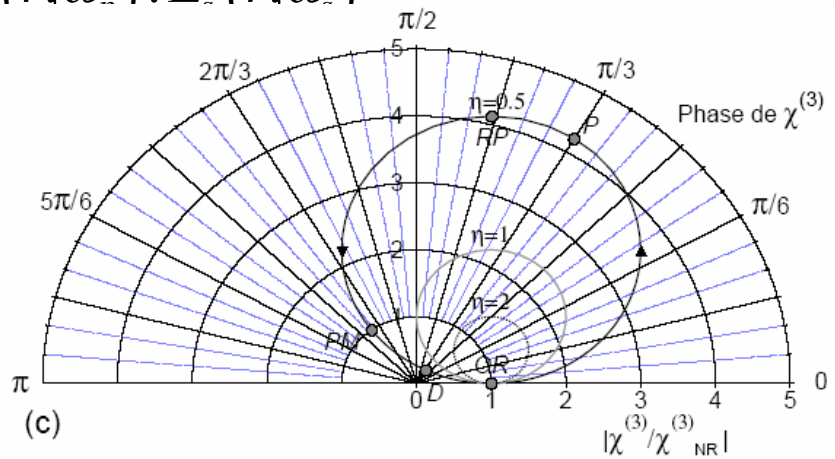

The amplitude and phase of $\chi^{(3)}$ drives the amplitude and phase of E_{AS}

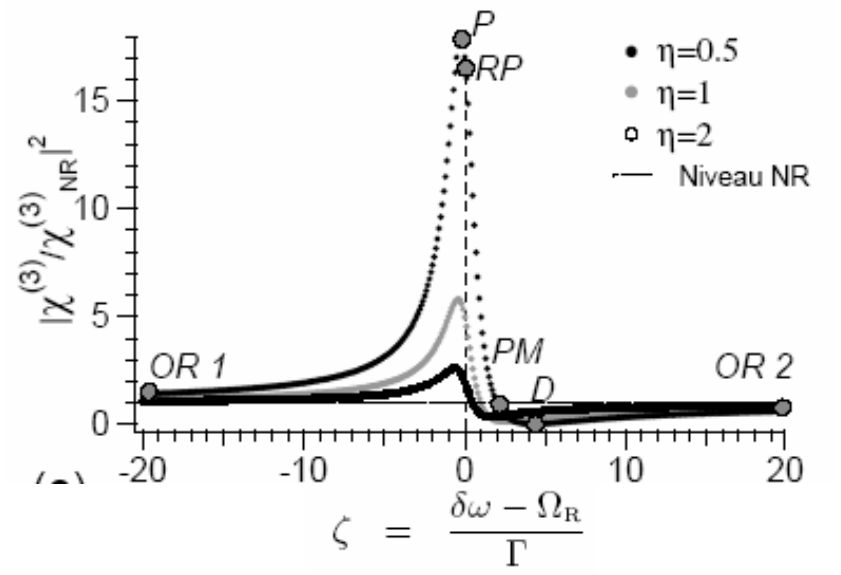

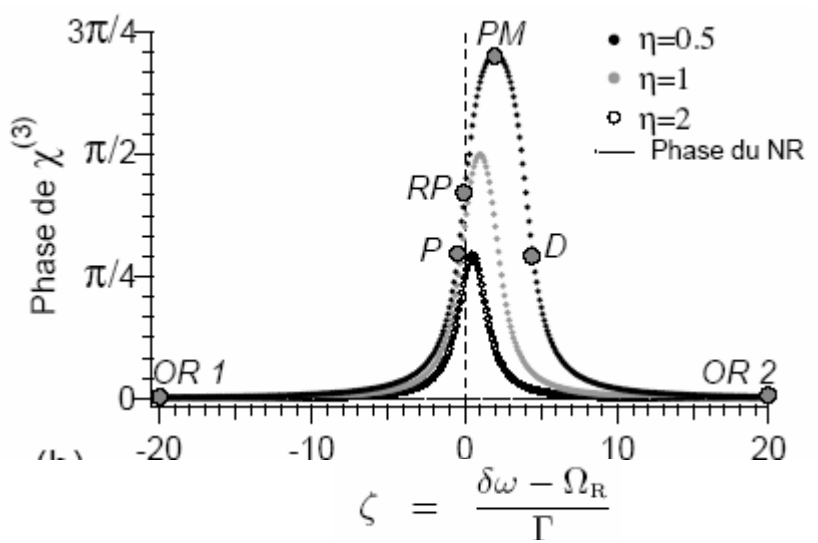

CARS step by step

1 Incoming fields $\overrightarrow{E_p}\left(\vec{r},\omega_p\right); \overrightarrow{E_s}\left(\vec{r},\omega_s\right)$

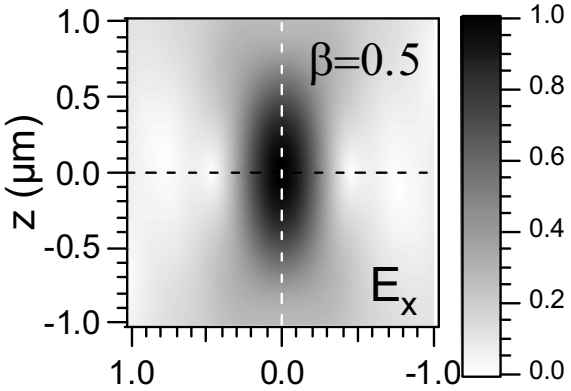

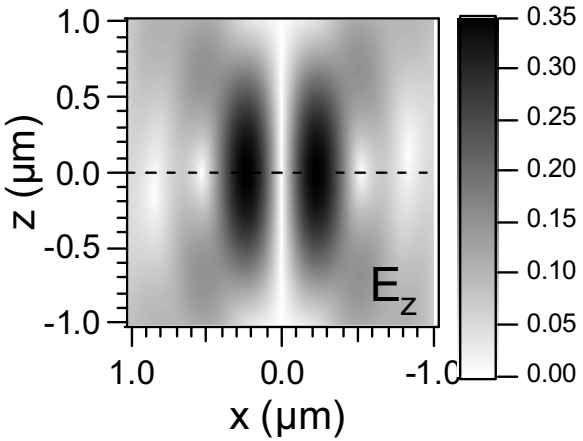

2 Induced polarization $\overrightarrow{P^{(3)}}\left(\vec{r},-\omega_{as}\right)=\overline{\overline{\chi^{(3)}}}\left(\omega_{as}\right):\overrightarrow{E_p}\left(\vec{r},\omega_p\right):\overrightarrow{E_p}\left(\vec{r},\omega_p\right):\overrightarrow{E_s^*}\left(\vec{r},\omega_s\right)$

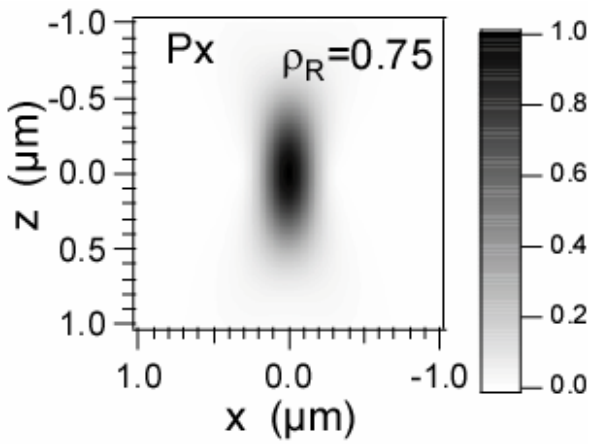

Phase of $\chi^{(3)}$

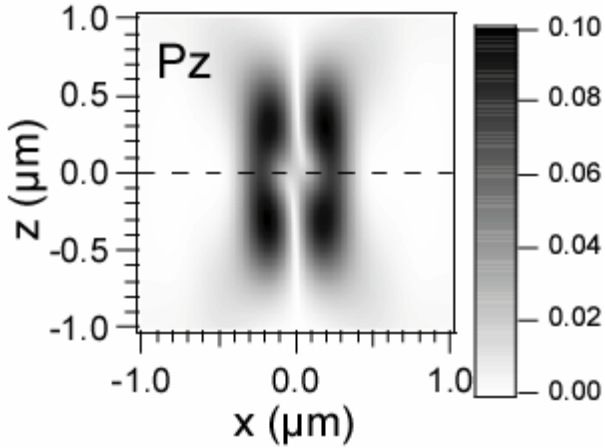

CARS step by step

1. Pump & Stokes fields
2. Induced nonlinear polarization
3. Dipolar emission
4. Summation over far-fields emitted in a particular direction

$$\overrightarrow{P^{(3)}}\left(\vec{r},-\omega_{as}\right)=\overline{\overline{\chi^{(3)}}}\left(\omega_{as}\right):\overrightarrow{E_p}\left(\vec{r},\omega_p\right):\overrightarrow{E_p}\left(\vec{r},\omega_p\right):\overrightarrow{E_s^*}\left(\vec{r},\omega_s\right)$$

Medium — Exciting fields

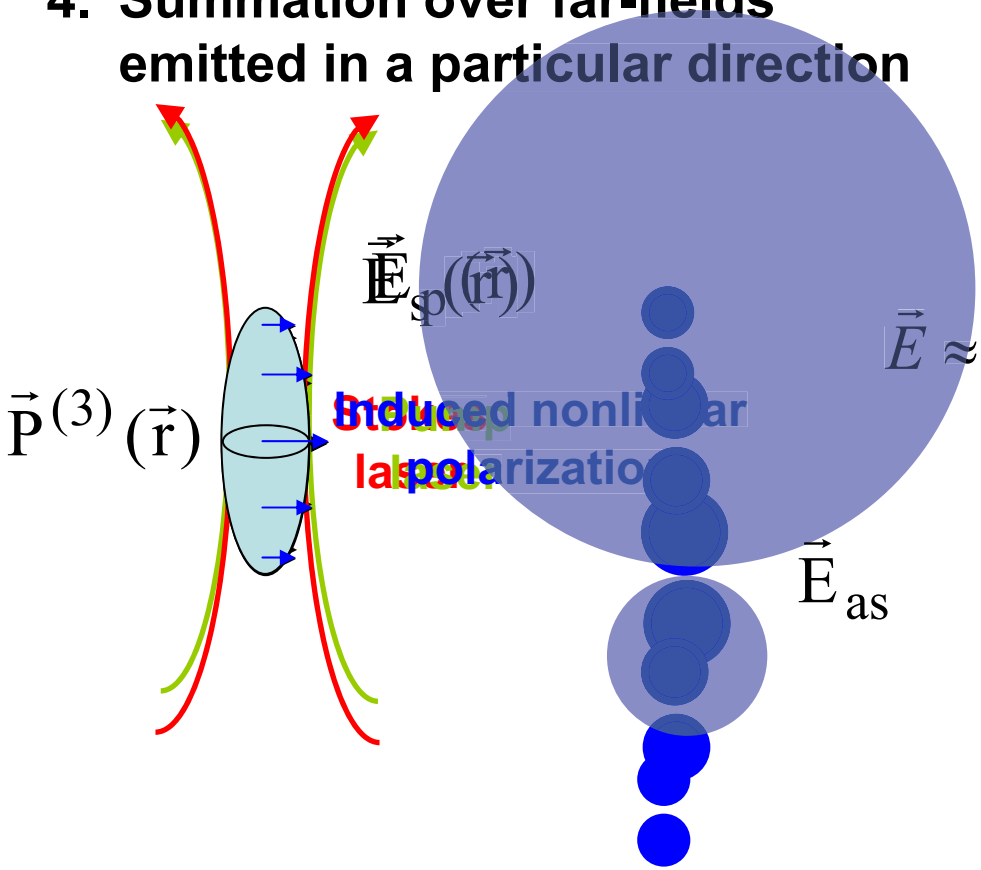

Far-field approximation

$$\vec{E}\approx\frac{1}{4\pi\varepsilon_0}\left(\frac{-k^2 p_0\sin\theta}{r}\right)\exp\left(i\vec{k}\cdot\vec{r}\right)\vec{e}_\theta$$

$$\vec{E}_{as}$$

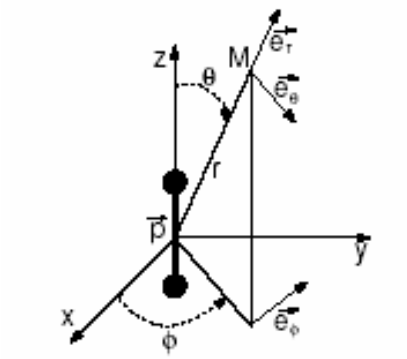

CARS field in direct and reciprocal spaces

Electric field E_{AS} in the direct space (x,y,z)

Coherent summation!

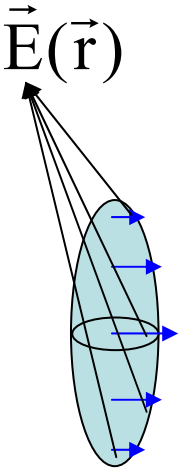

Induced polarization

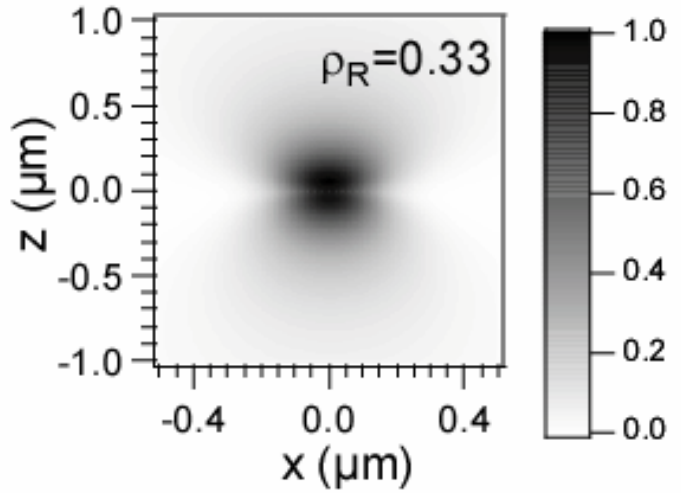

Electric field E_{AS} in the reciprocal space (k_x,k_y)

Coherent summation!

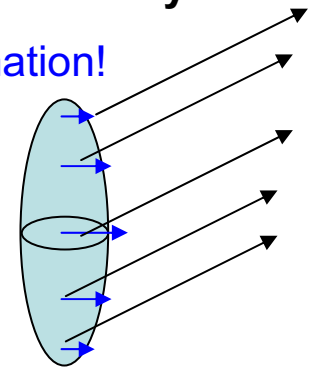

$\vec{E}(\vec{k})$

Induced polarization

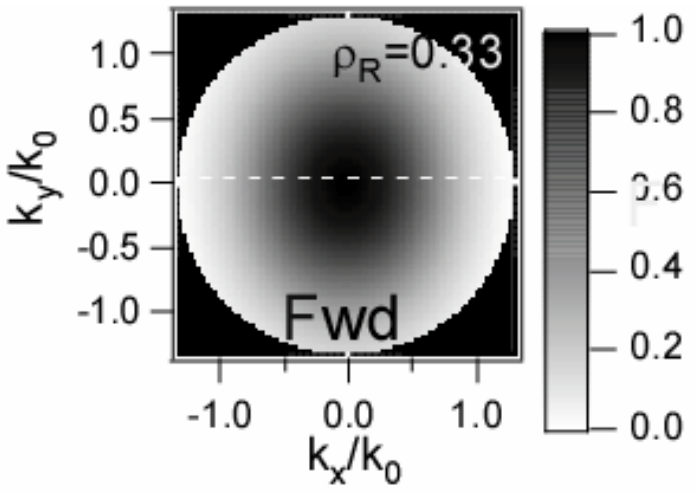

Far-field CARS radiation patterns in direct space

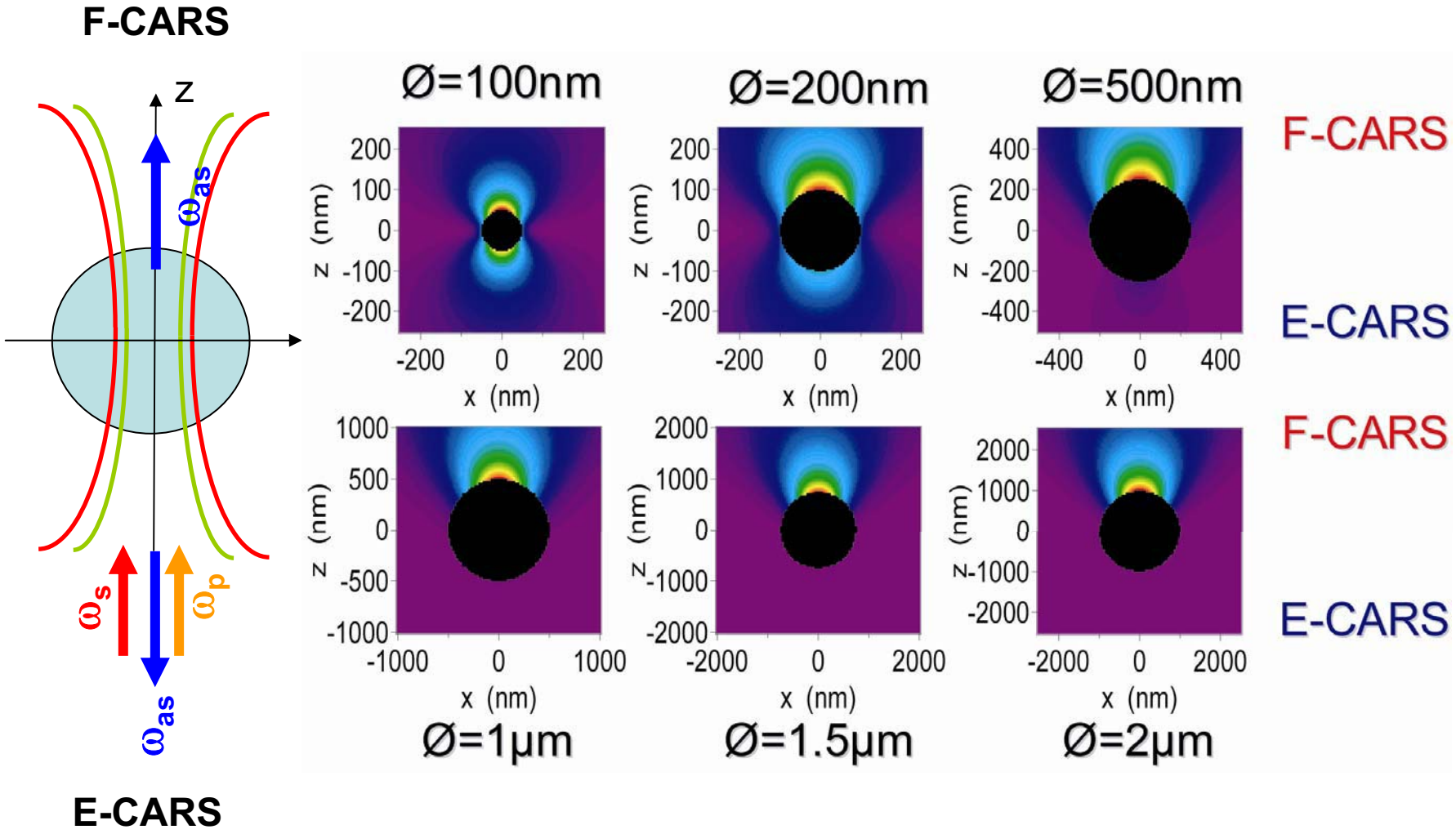

Gachet et *al.*, *Proc. SPIE* (2006)

Far-field CARS radiation patterns in k space

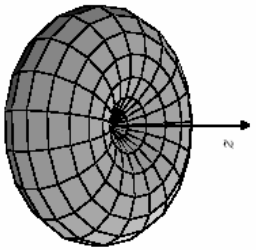

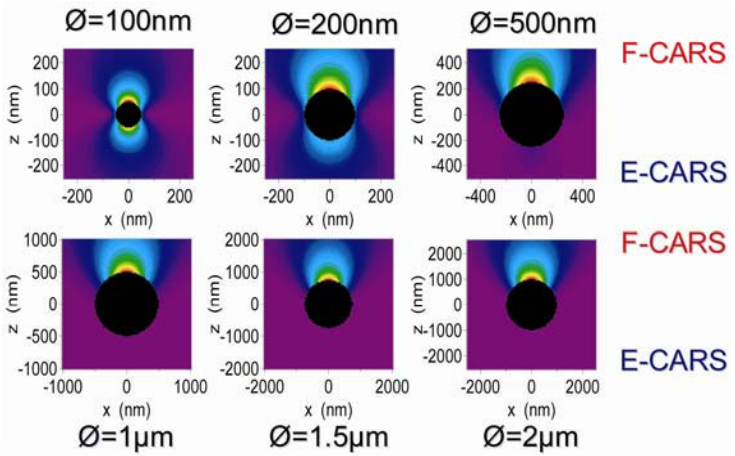

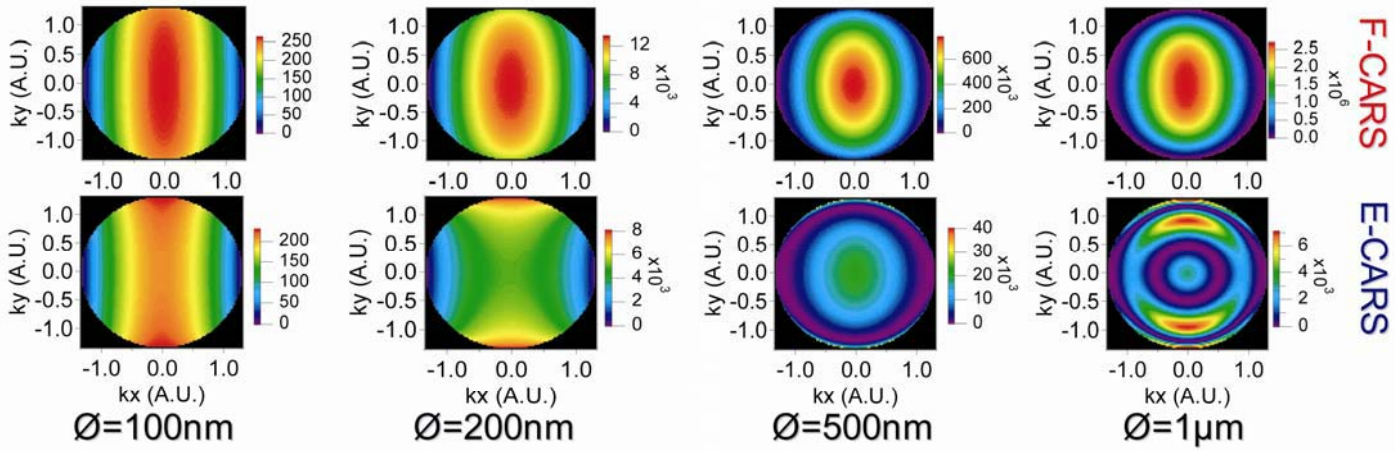

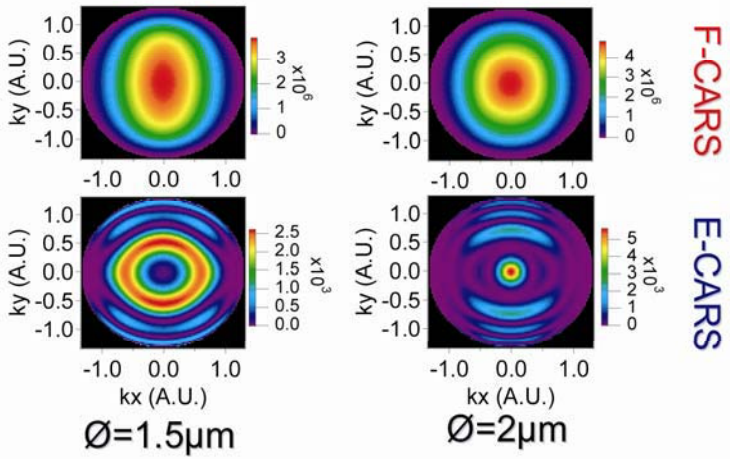

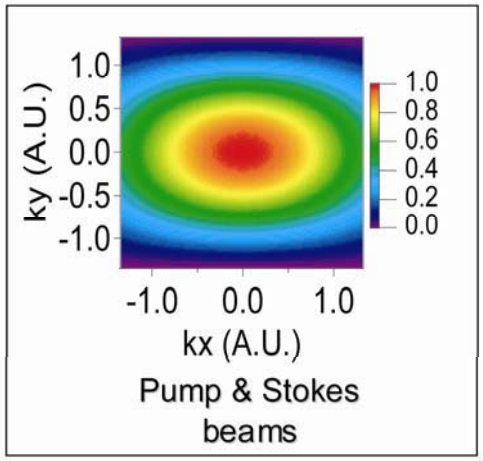

F-CARS emission more directive than the excitation beam along one direction

F-CARS / E-CARS radiation

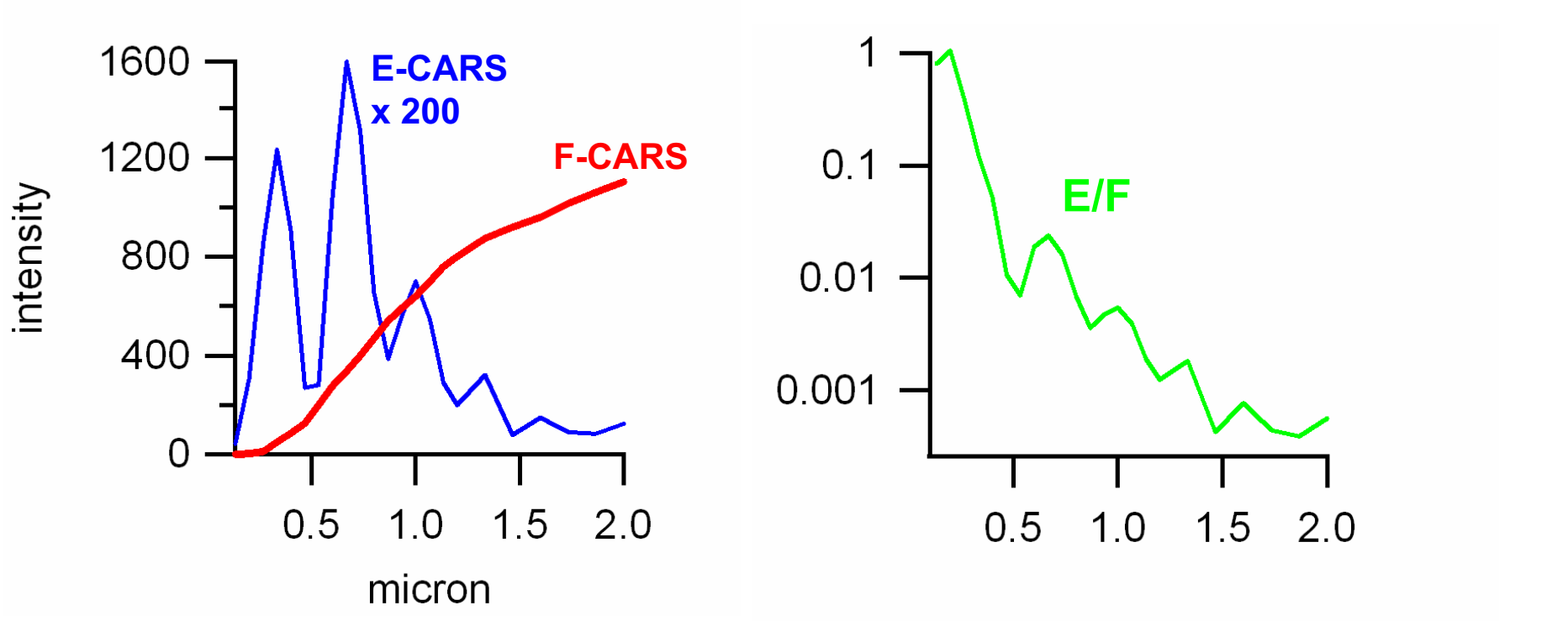

Volkmer et al. PRL (2001)
Gachet et *al.*, *Proc. SPIE* (2006)
Djaker et *al.*, *Appl. Opt.* **45**, 7005 (2006)

Epi-detected CARS: a way to visualize small objects

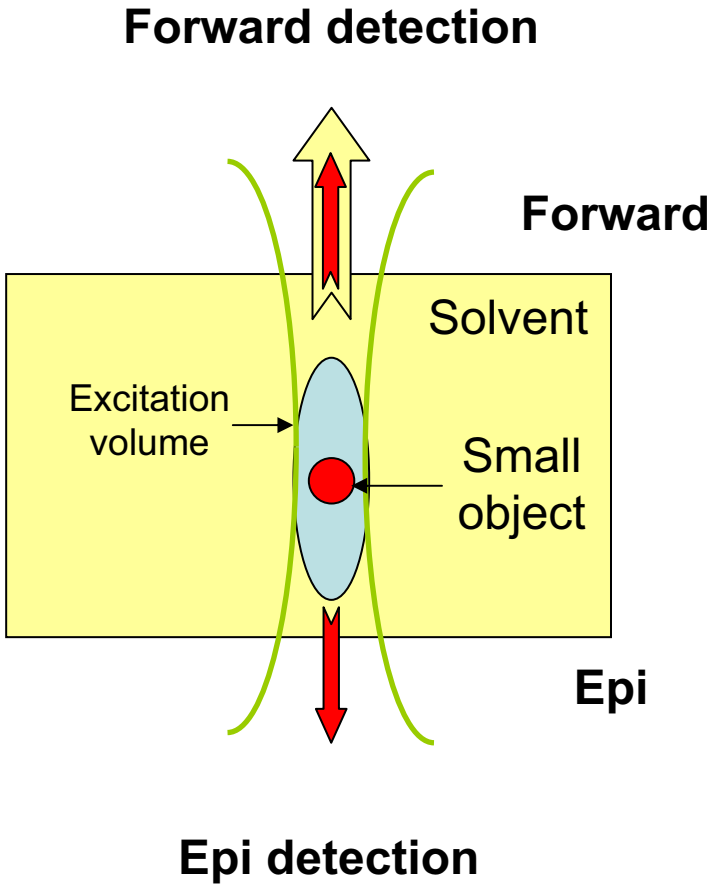

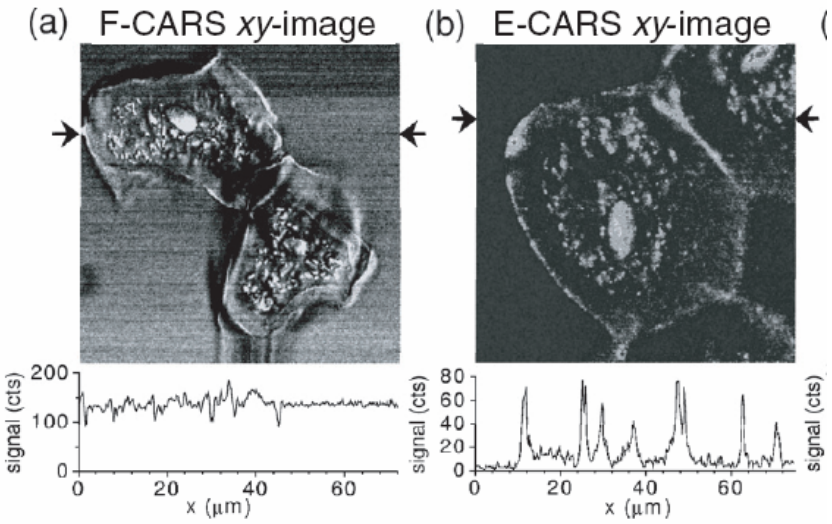

A. Volkmer, *J. Phys. D: Appl. Phys.* **38**, R59 (2005)

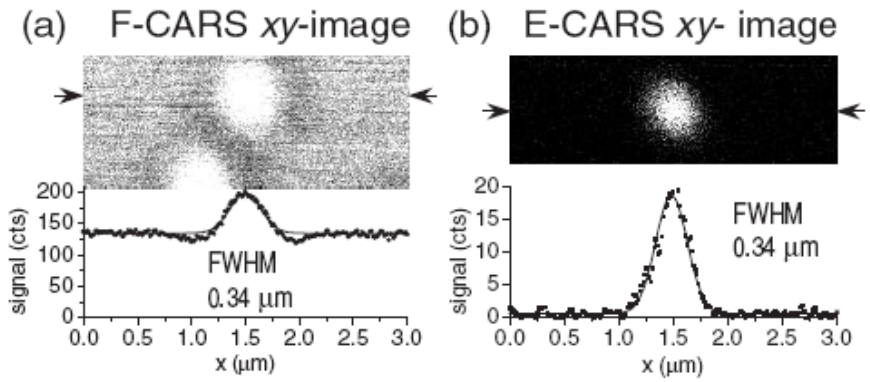

A. Volkmer, id.

Phase matching in NLO (SHG example)

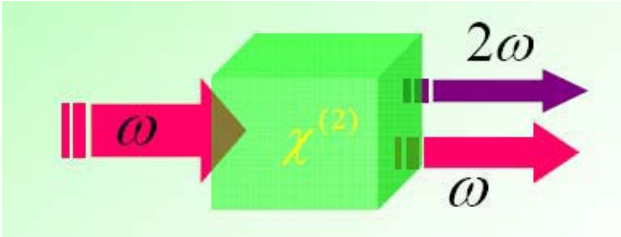

Cf lecture NLO Mario Bertolotti

$$P^{NL}(2\omega) = \chi^{(2)} E(\omega)^2$$

$$\frac{2\pi}{2\mathbf{k}_\omega} = \frac{\lambda/2}{n_\omega}$$

$P^{NL}(2\omega)$

$(2\mathbf{k}_\omega)$

$\mathbf{E}(2\omega)$

$2\omega)$

$$\frac{2\pi}{\Delta\mathbf{k}} = \frac{2\pi}{\mathbf{k}_{2\omega} - (2\mathbf{k}_\omega)} = \frac{\lambda}{2(n_{2\omega} - n_\omega)}$$

$l_{2\omega}$

$l_c = \frac{\pi}{\Delta k}$

x

$\mathbf{k}_{2\omega}$ l_c $n_{2\omega}$

Phase matching in CARS

$$P^{NL}(\omega_{AS}) = \chi^{(3)} E_P(\omega_P)^2 E_S(\omega_S)^*$$

$$\frac{2\pi}{2\mathbf{k}_P - \mathbf{k}_S} \approx \frac{1}{n}\frac{\lambda_P \lambda_S}{(2\lambda_S - \lambda_P)}$$

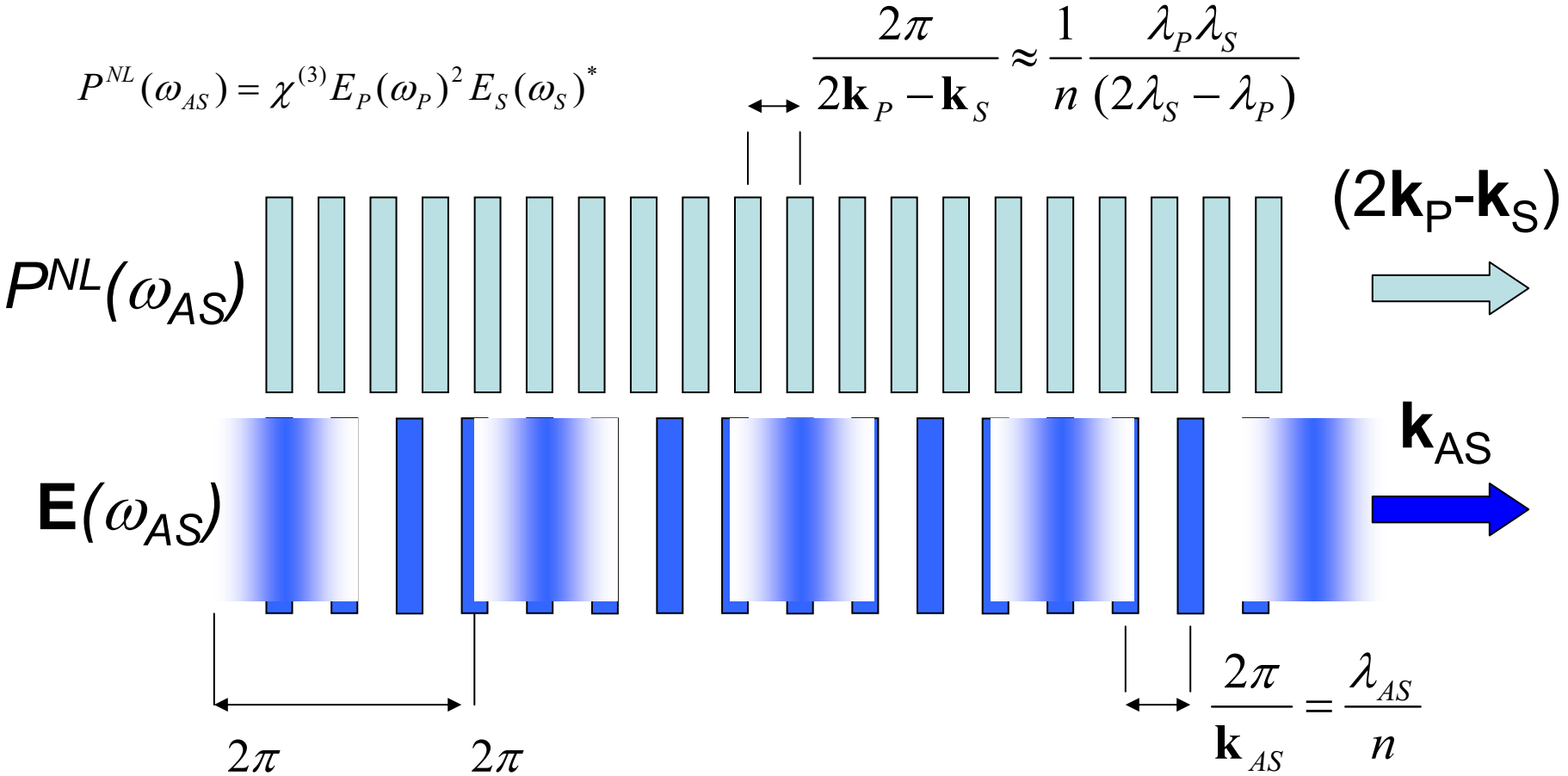

$$l_c = \frac{\pi}{\Delta k} = \frac{\pi}{k_{AS} - (2k_P - k_S)}$$

CARS phase matching: intuitive approach

Fwd-CARS

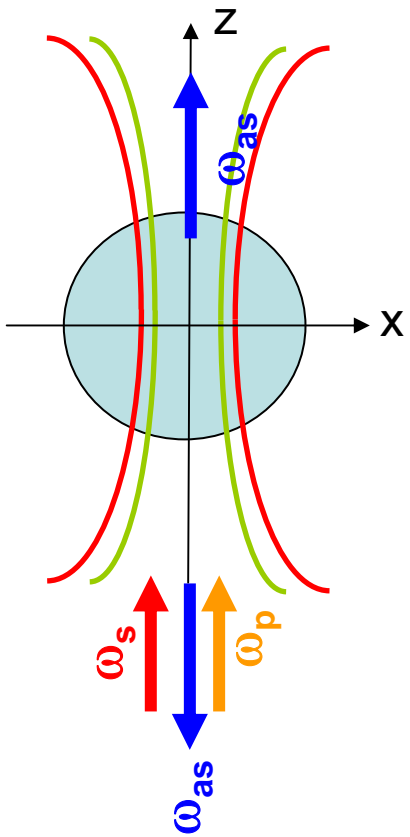

Epi-CARS

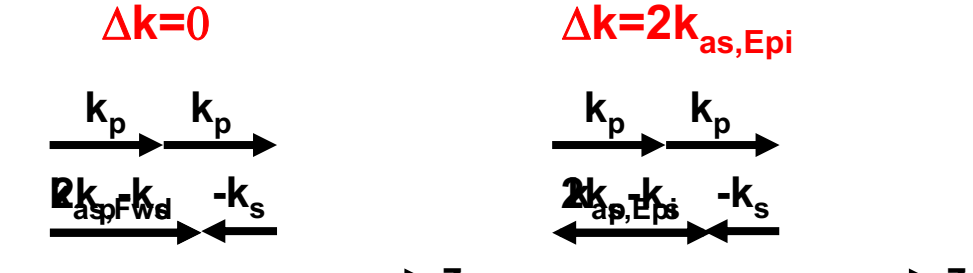

Phase-matching & CARS generation

$$I_{as}(\Delta k) \propto L^2 \frac{\sin^2(\frac{1}{2}\Delta kL)}{(\frac{1}{2}\Delta kL)^2}$$

$$l_c = \frac{\pi}{\Delta k} \longrightarrow \quad I_{as}\ \text{max}$$

Fwd-CARS: $\Delta k = 0;\ l_c \to \infty$

Epi-CARS: $\Delta k = 2k_{as};\ l_c = \frac{\pi}{\Delta k} = \frac{\pi}{2k_{as}} = \frac{\lambda_{as}}{4n(\lambda_{as})} \approx \frac{\lambda_{as}}{4}$

F-CARS / E-CARS radiation

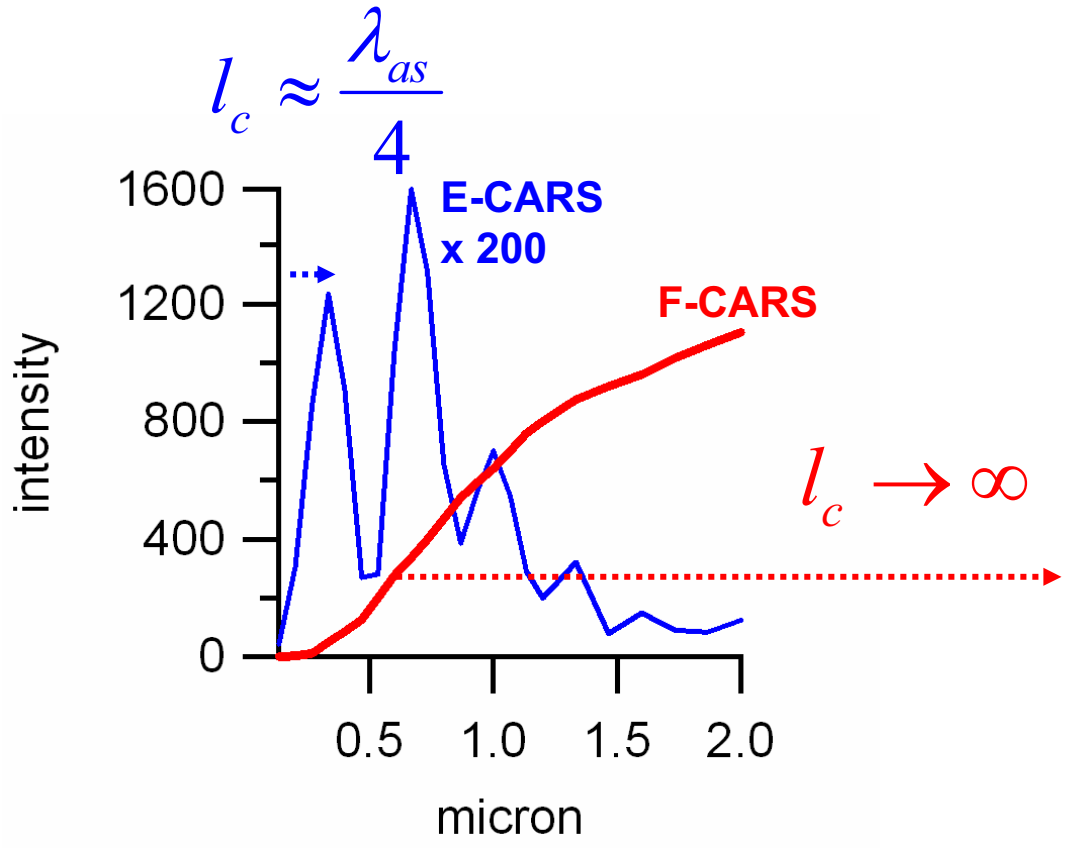

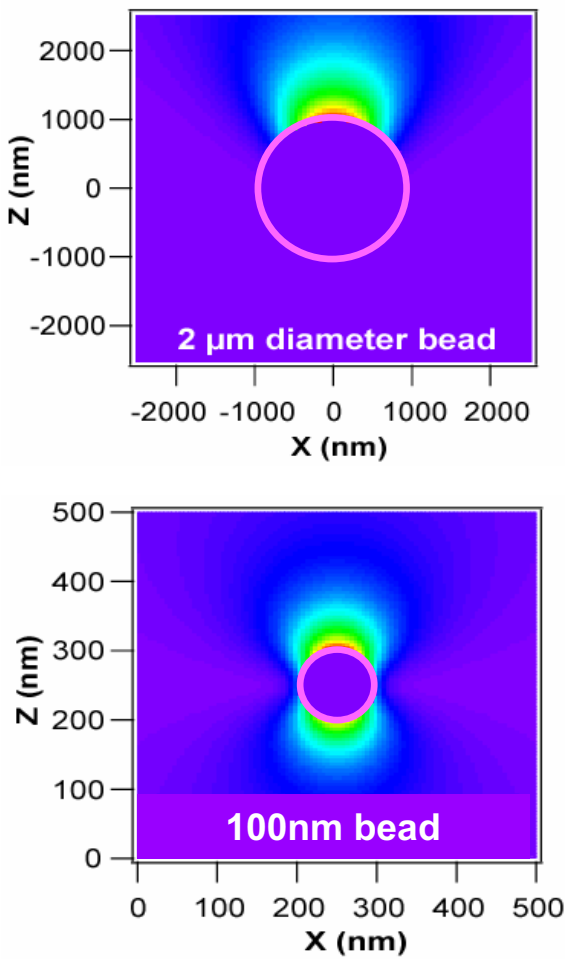

Gachet et *al.*, *Proc. SPIE* (2006)
Djaker et *al.*, *Appl. Opt.* **45**, 7005 (2006)

CARS instrumentation

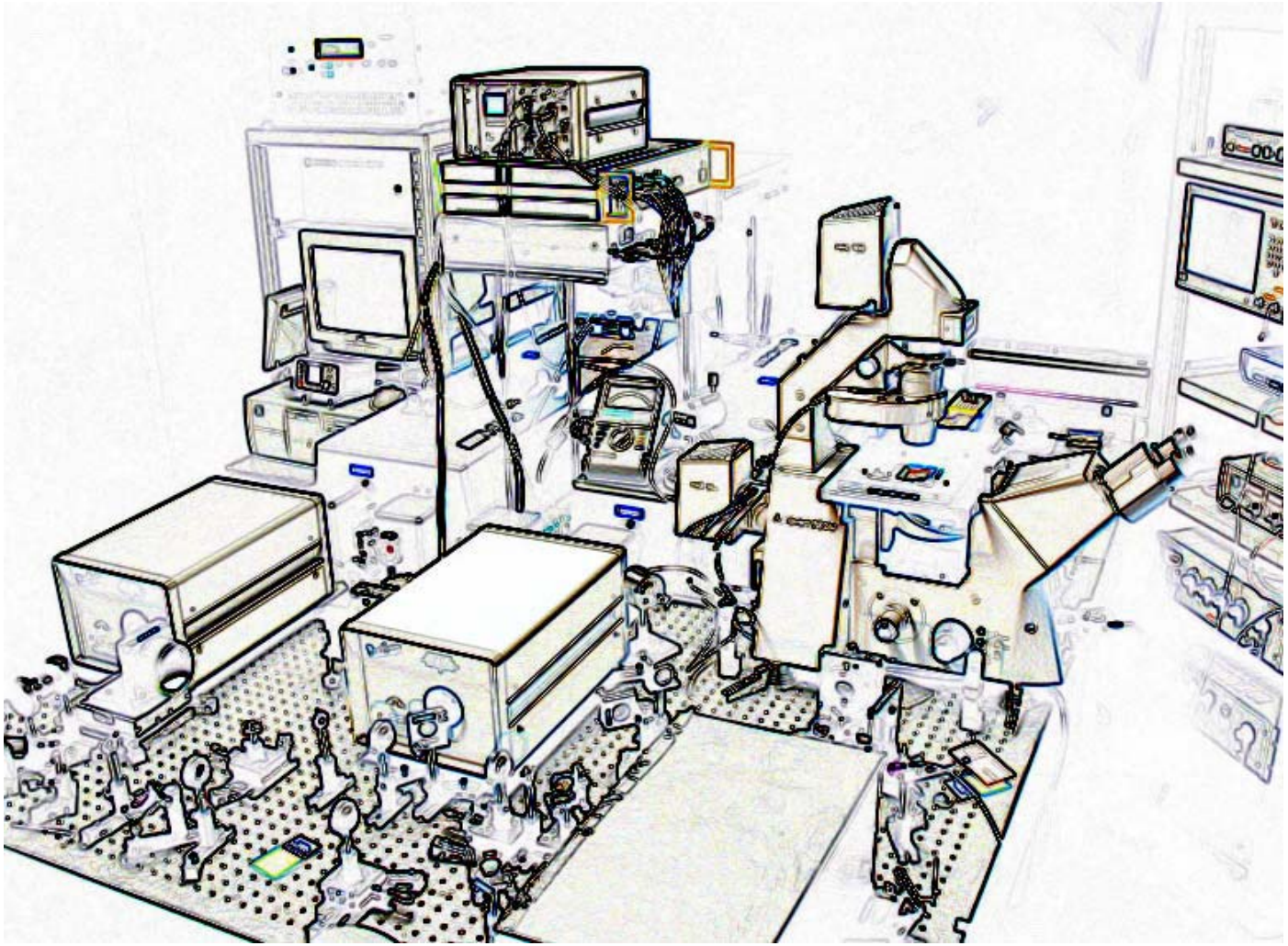

A first experimental set-up

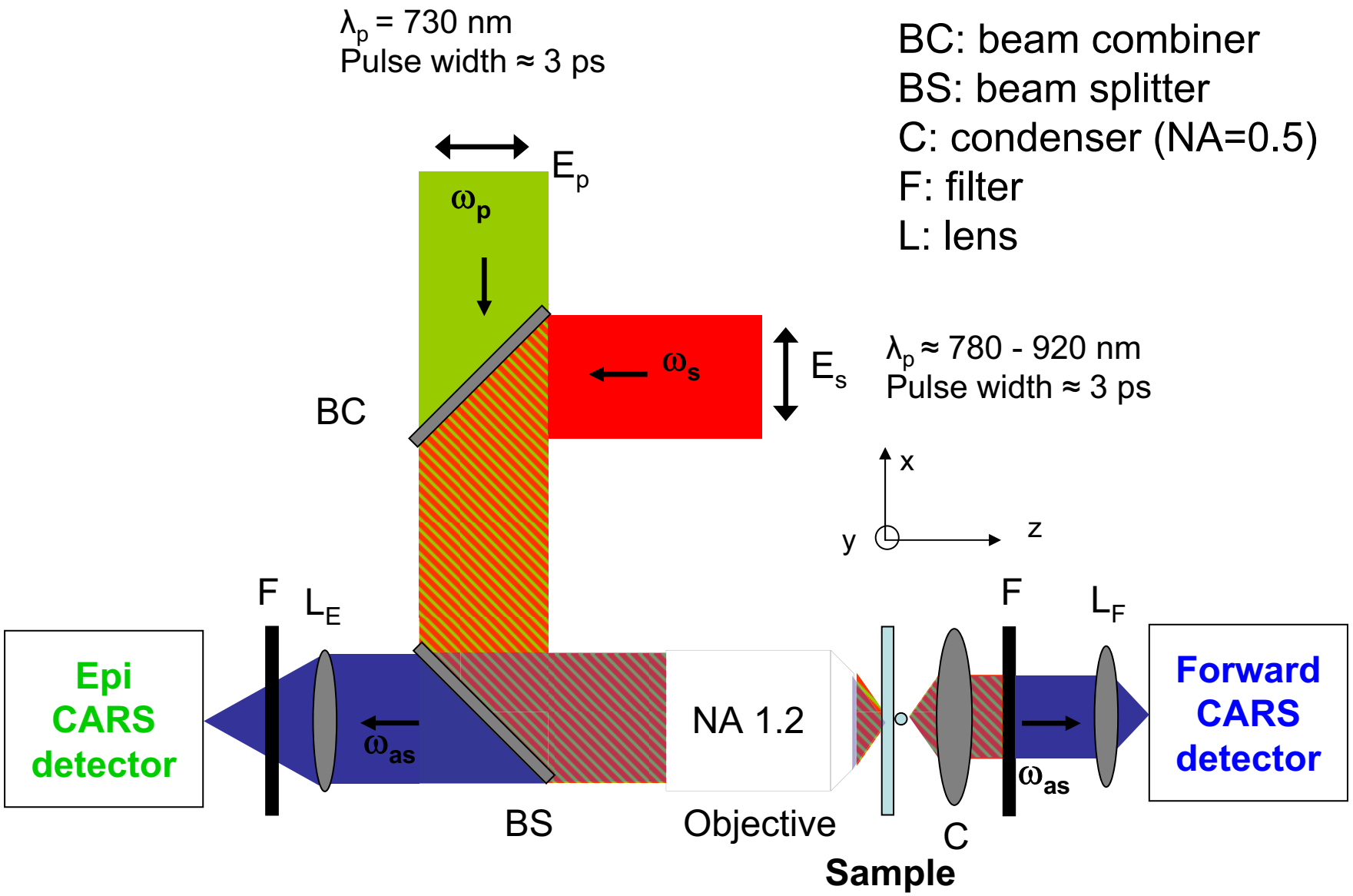

How to choose pulses temporal length?

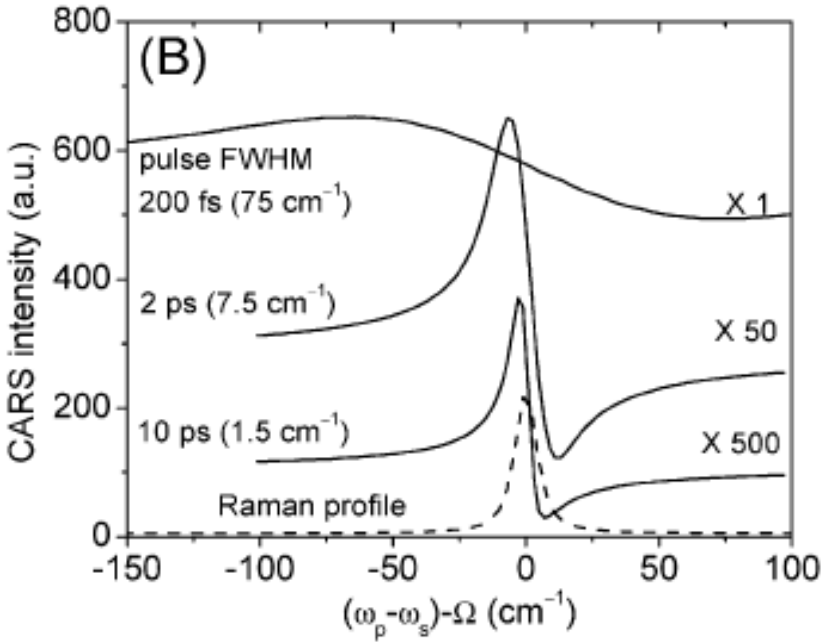

J.-X. Cheng et *al.*, J. *Phys. Chem. B* **108**, 827 (2004)

The dilemma:

- *Long pulses:*

+ good spectral selectivity

- poor CARS generation efficiency

- *Short pulses*:

+ efficient CARS generation

- low spectral resolution

Solutions:

- To spectrally match the studied Raman line →ps range

Laser Synchronization

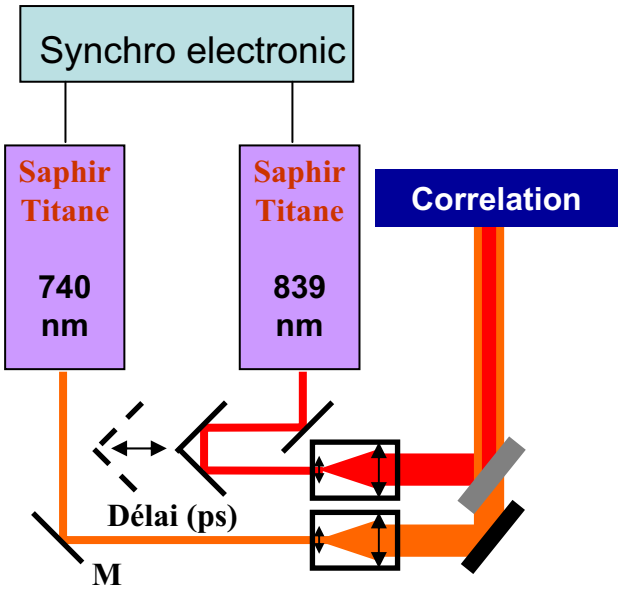

- Fast photodiodes
-/ Autocorrelator (SHG)
-/ 2P detector
- CARS signal

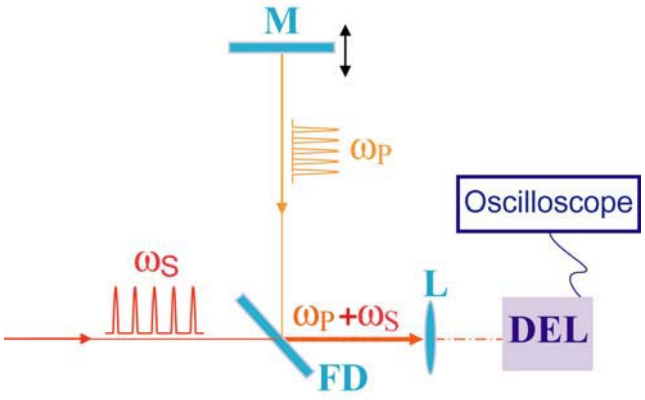

FD: filtre dichroïque, M: miroir

CARS signal

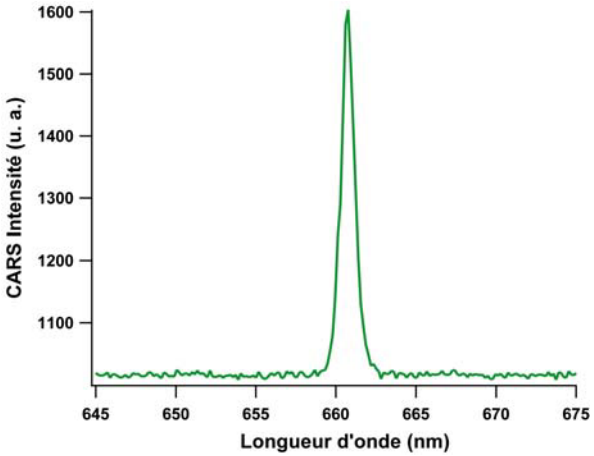

Cross-correlation

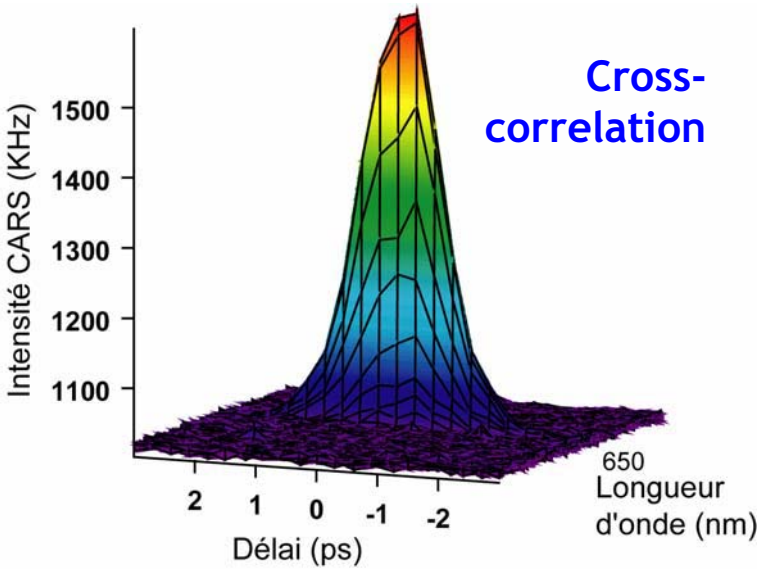

Potma Opt Lett 27 (2002)

Setup scheme pico/pico

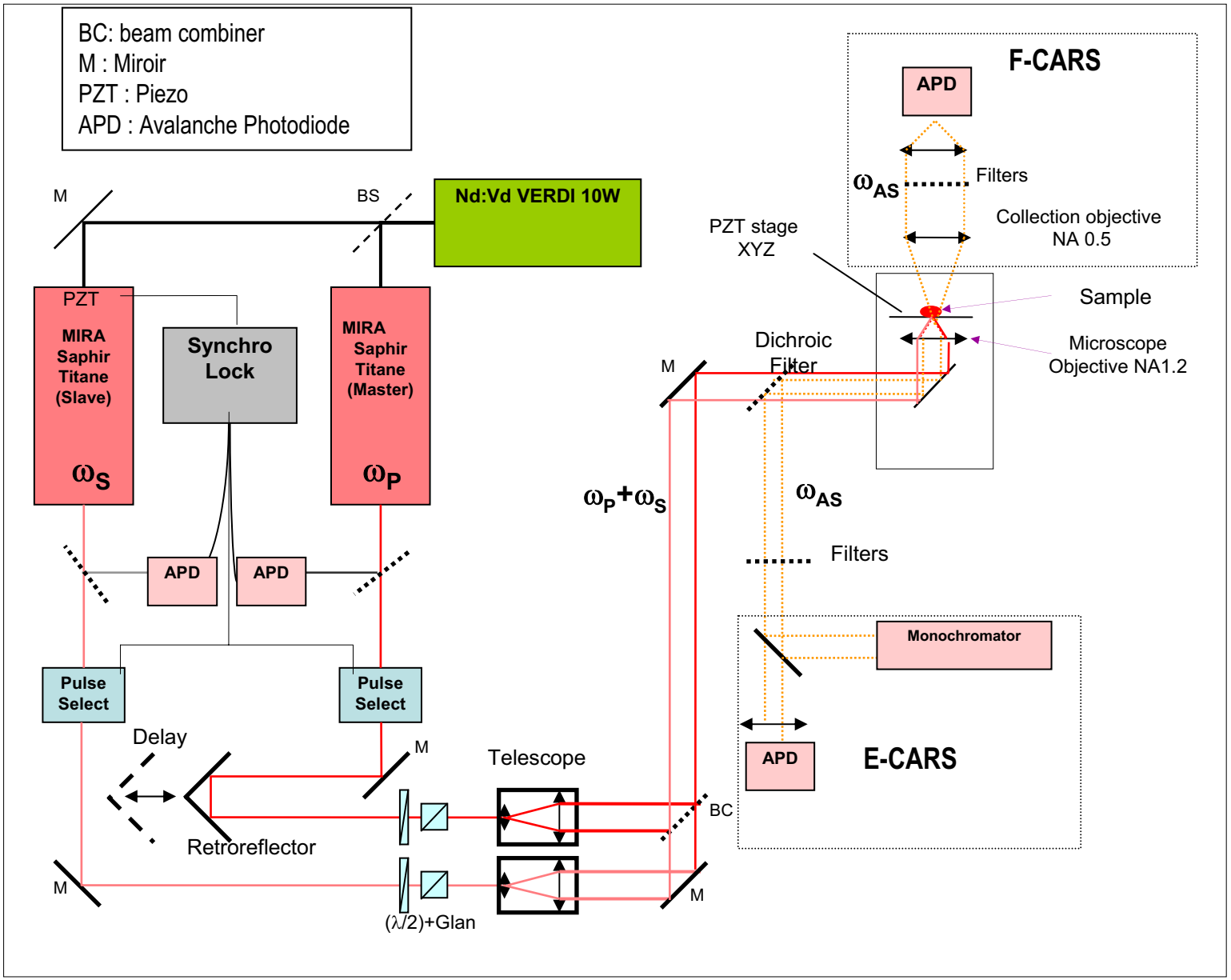

Two oscillators: pico / pico setup

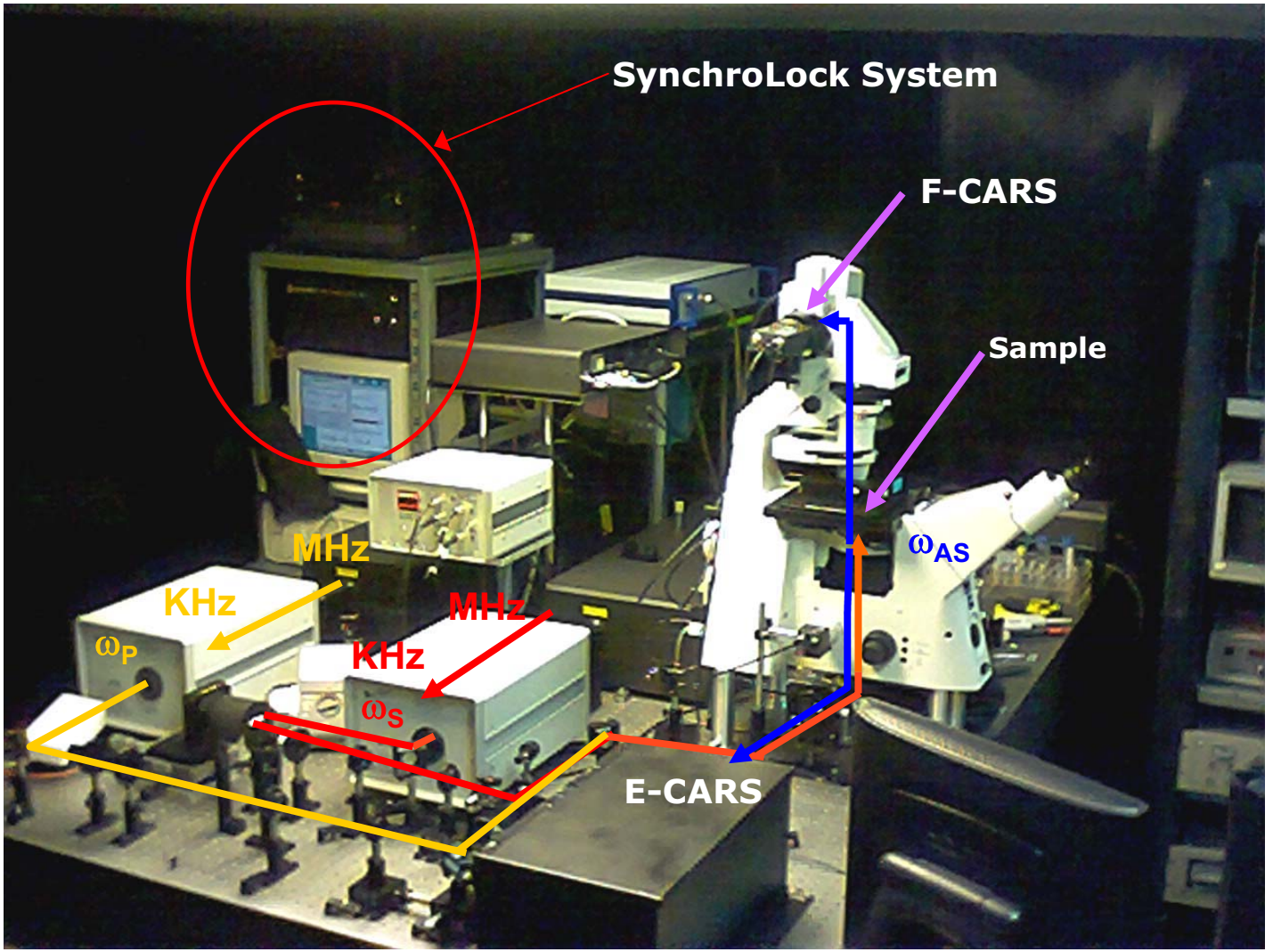

Two oscillators pico / femto = Multiplex CARS

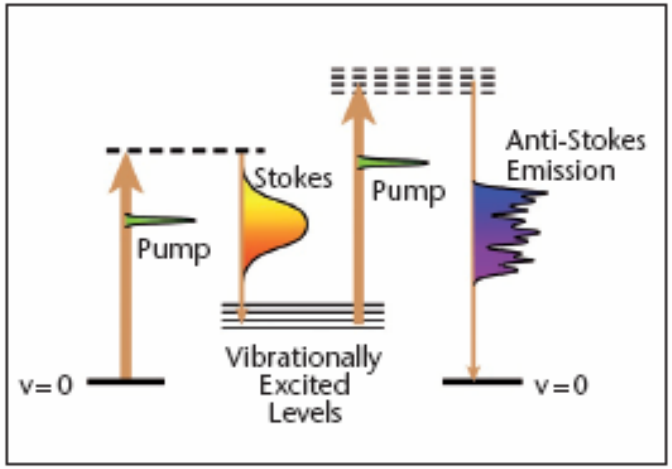

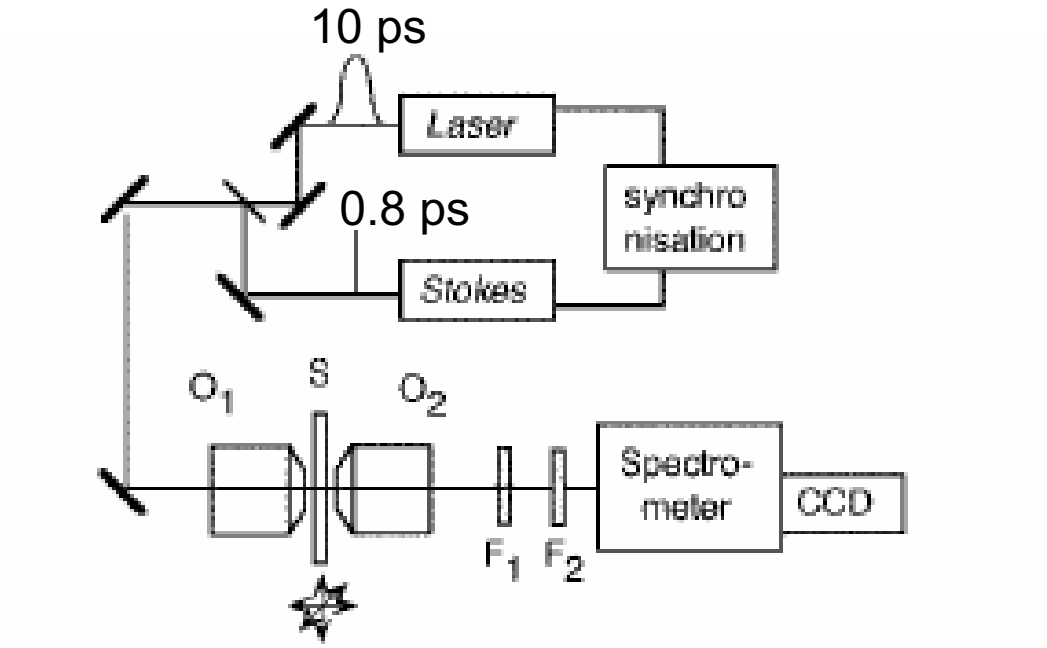

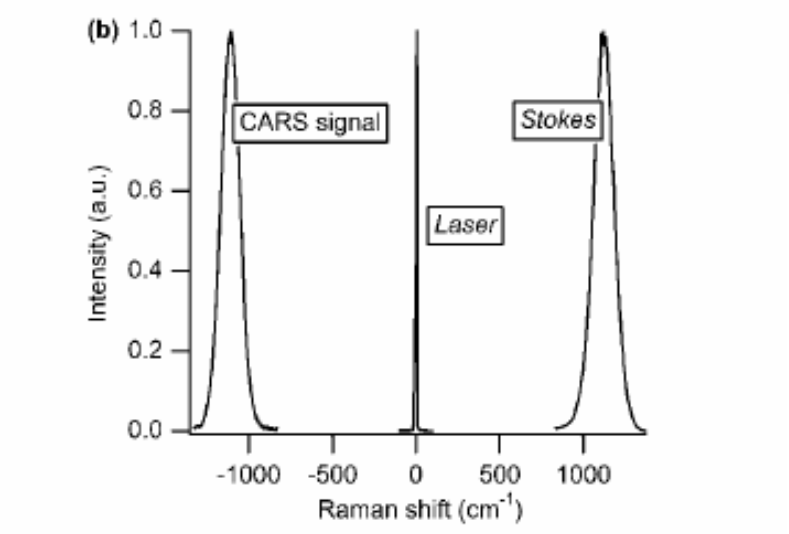

Pump: 10 ps
Stokes: 80 fs

Muller J. Phys. Chem B 106 2002

Multiplex CARS

Identification of the Thermodynamic State of Lipids in Multi-lamellar Membranes

From Müller, J. Phys. Chem. B. (2002)

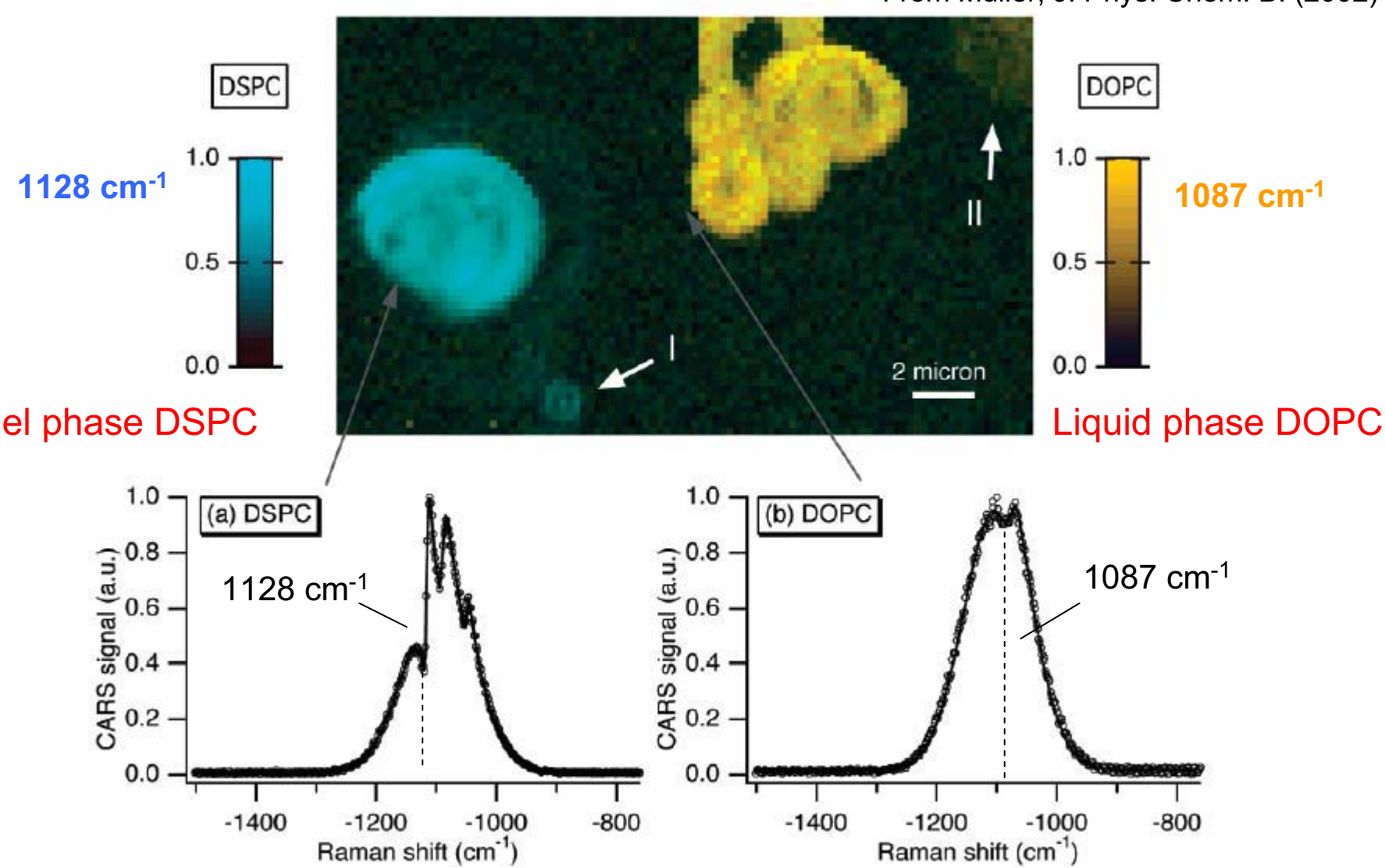

1 oscillator femto + PCF

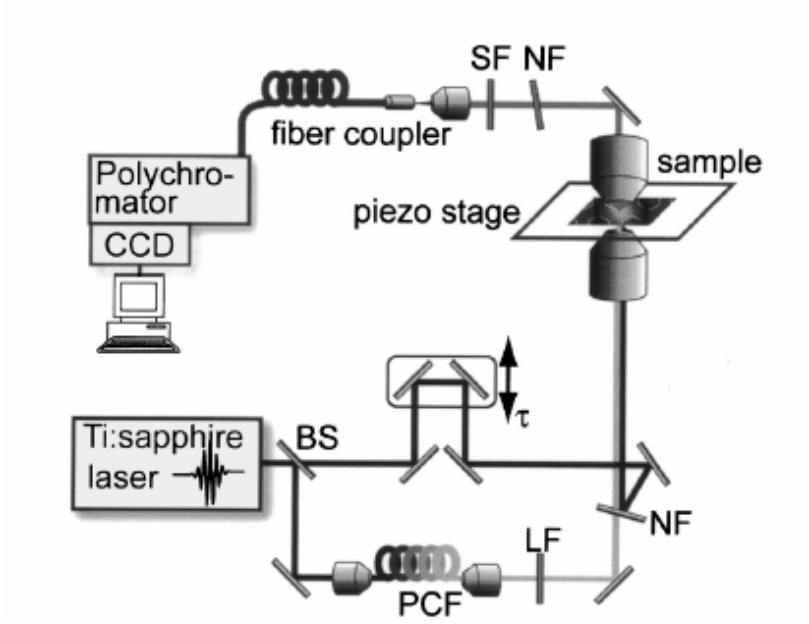

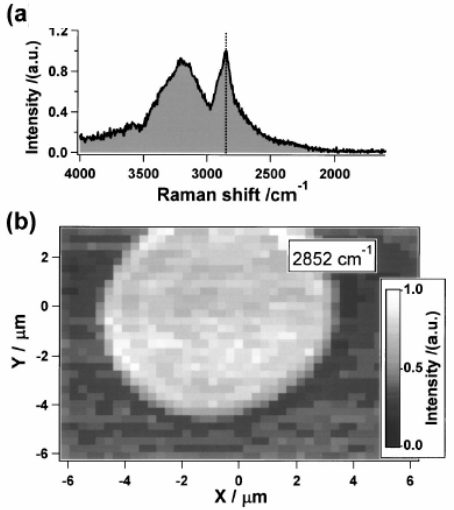

FIG. 4. (a) CARS spectrum of a multilamellar vesicle (MLV), (b) CARS lateral image of a MLV detected at 2852 cm^{-1}, which corresponds to the aliphatic C–H stretching vibrational mode. Brighter regions indicate greater signal intensities.

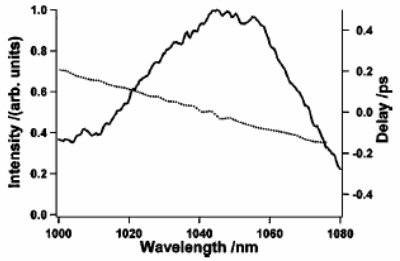

FIG. 2. Typical spectral profile of the supercontinuum in near-infrared region generated from a PCF without the sensitivity correction. The temporal chirp profile of the supercontinuum is also indicated (dotted).

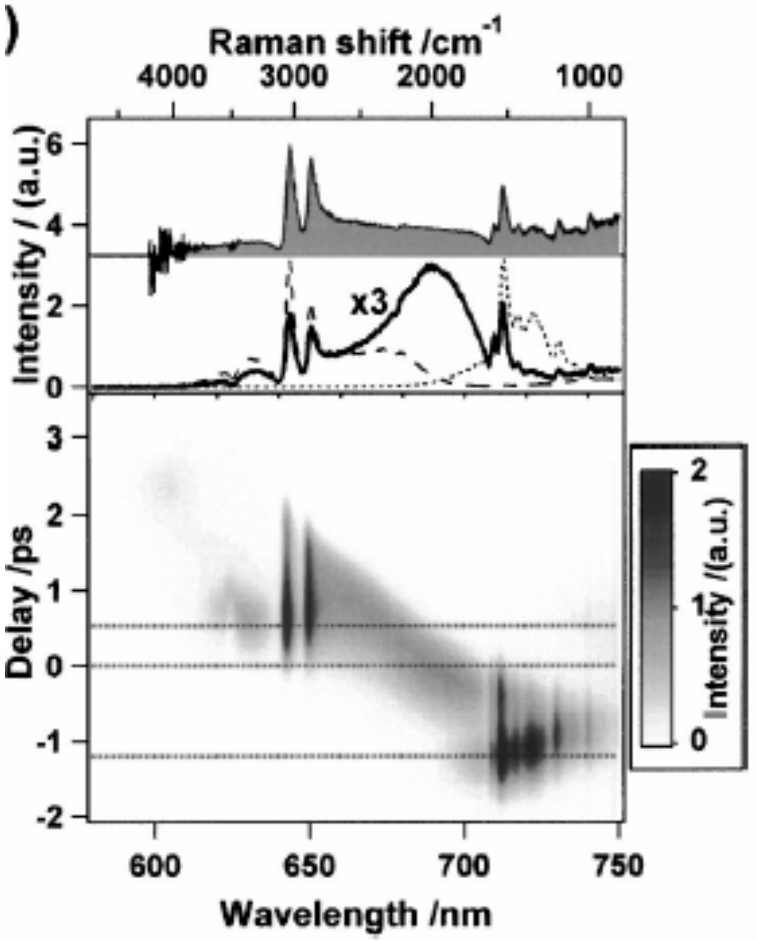

Kano et al. APL86 (2005)

What is an OPO (Optical Parametric Oscillator)

Recent advances in Optical Parametric Oscillators

A P E Berlin

Parametric generation $\chi^{(2)}$ $(\omega_3-\omega_1, \omega_3,-\omega_1)$.

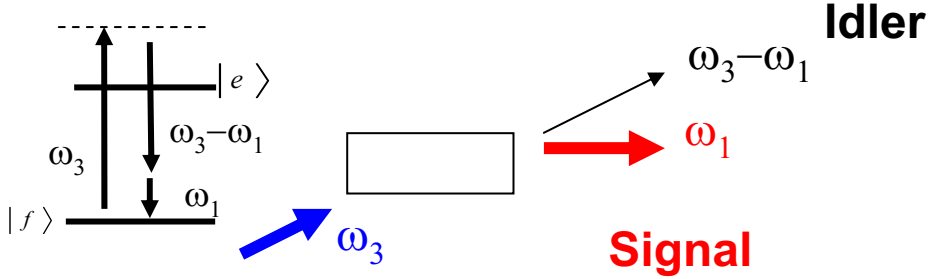

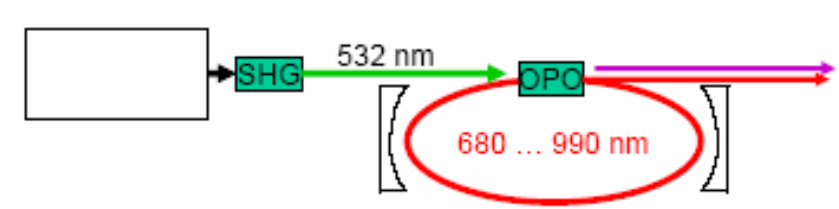

Parametric amplification $\chi^{(2)}$ $(\omega_3-\omega_1, \omega_3,-\omega_1)$.

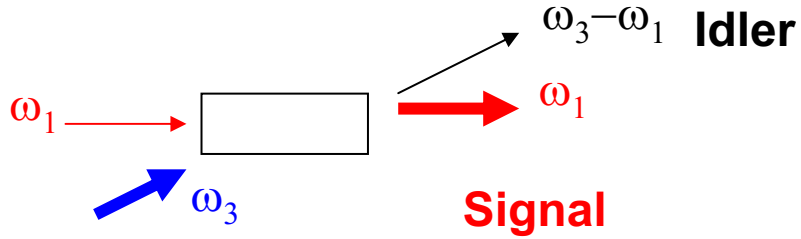

One oscillator + One OPO pico/pico

Pump ps 532nm

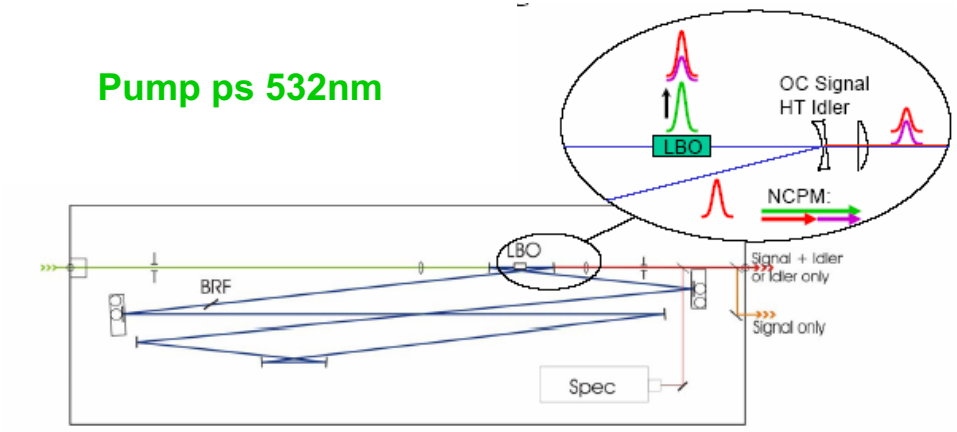

	Signal	Idler
• Tuning range	<690 … 990 nm	1150 … 2300 nm
• Energy difference (Signal - Idler)	1350 … 10000 cm^{-1}	

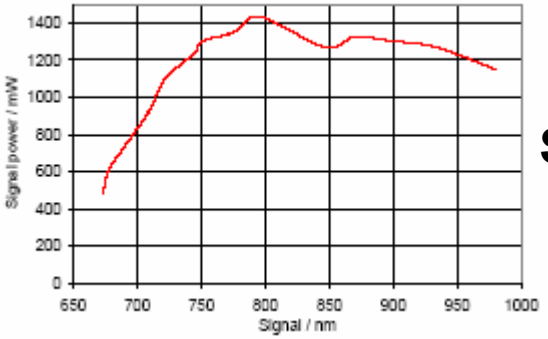

Signal

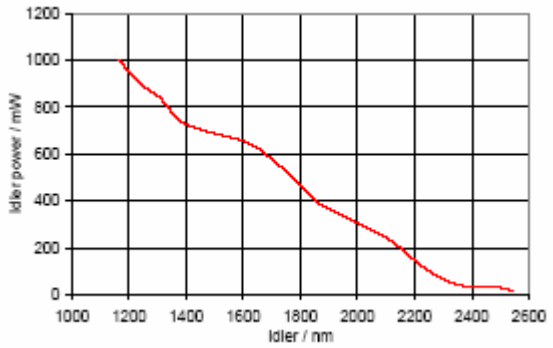

Idler

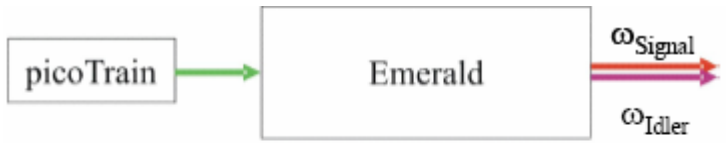

>1350 cm^{-1}

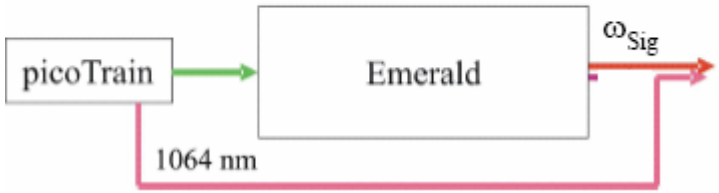

>700 cm^{-1}

Sensitivity improvement: FM CARS

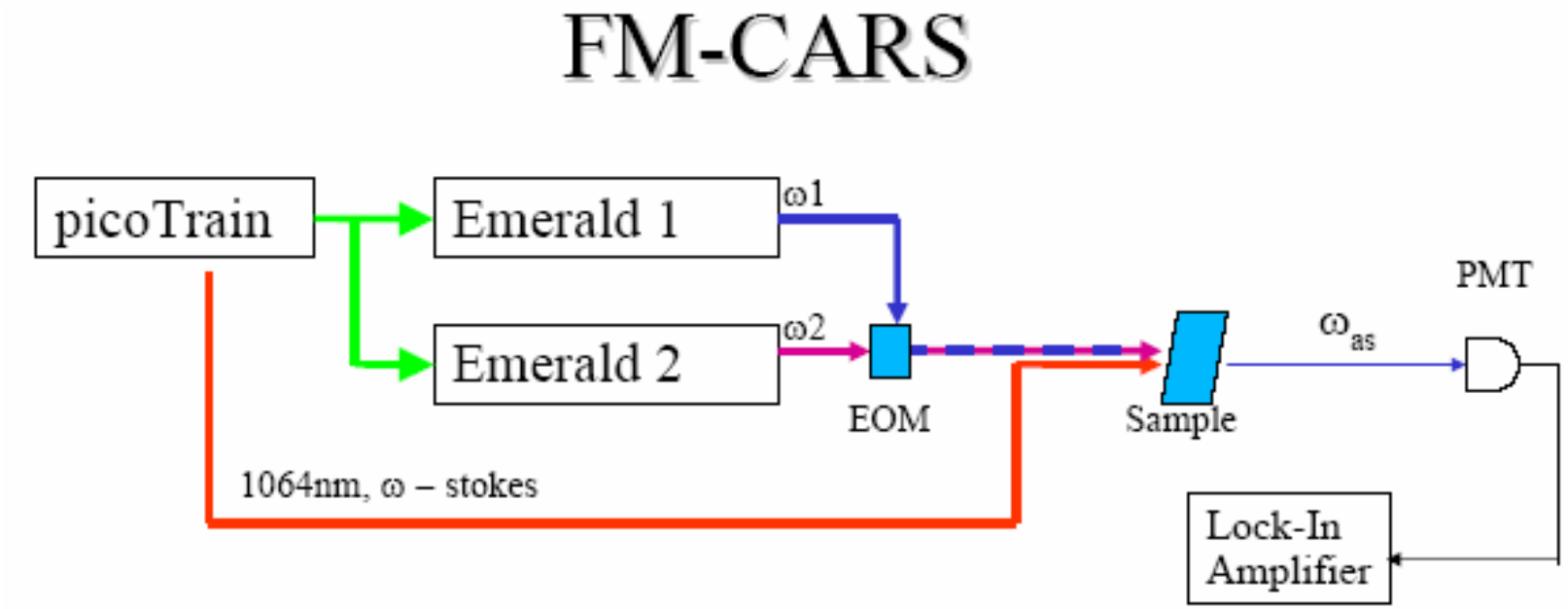

- 2 pump wavelengths, ω1 resonant, ω2 non resonant with switching speed of ~500kHz
  → lock in detection
  → non-resonant background subtraction
- →Sensitivity enhancement by factor 1000

Ganikhanov et al, Opt. Lett. 2006

Sensitivity improvement: H(eterodyne) CARS

Potma Opt. Lett. 31 (2006): LO generated in DMSO
Enable to recover real and imaginary part of $\chi^{(3)}$

$$S = |E_{LO}|^2 + |E_{as}|^2 + 2E_{LO}E_{EX}\{[\chi_{NR}^{(3)} + \mathrm{Re}\,\chi_R^{(3)}]\cos\Phi + [\mathrm{Im}\,\chi_R^{(3)}]\sin\Phi\},$$

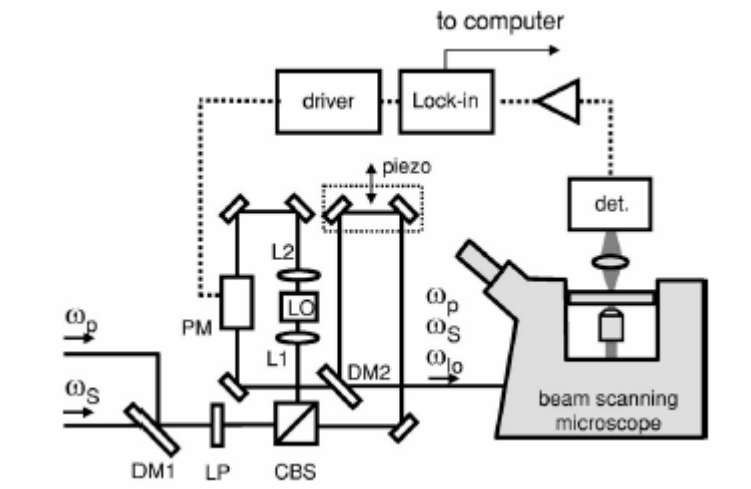

Lipid resonance 2845cm^{-1}

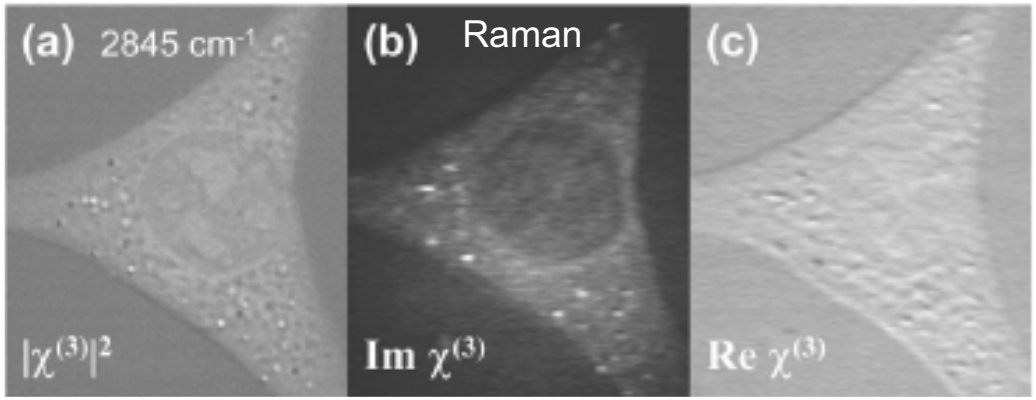

Off resonance

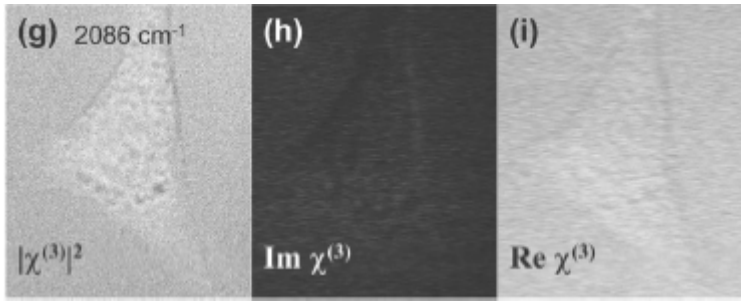

H(eterodyne) CARS with OPO!

$$I_{detector} = LO + CARS + \underbrace{2 \cdot \sqrt{LO \cdot CARS}}_{HCARS}$$

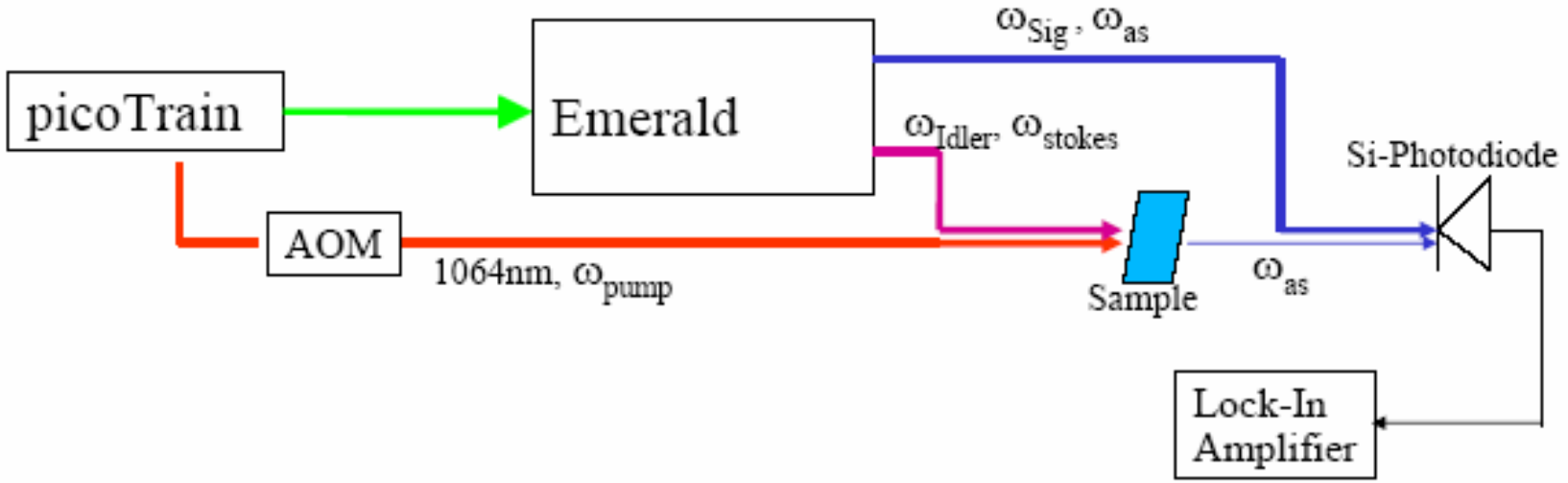

- $\omega_{as} = 2\omega_p - \omega_s$: with 1064nm = ω_p and ω_s as OPO-Idler ω_{idler}
- OPO pumed @ $2\omega_p$ (532nm) : $2\omega_p = \omega_{sig} + \omega_{idler}$
- → OPO ω_{sig} = CARS ω_{as}
- **Sensitivity enhancement by a factor of 5000**

Jurna Opt. Expr 15 (2007)

HCARS with interfaces

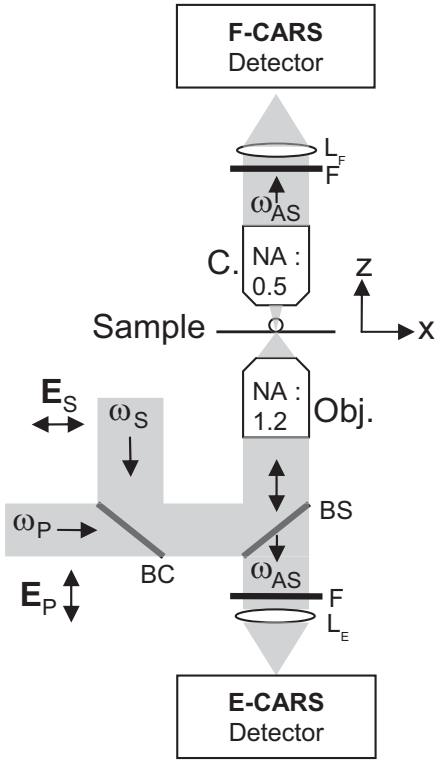

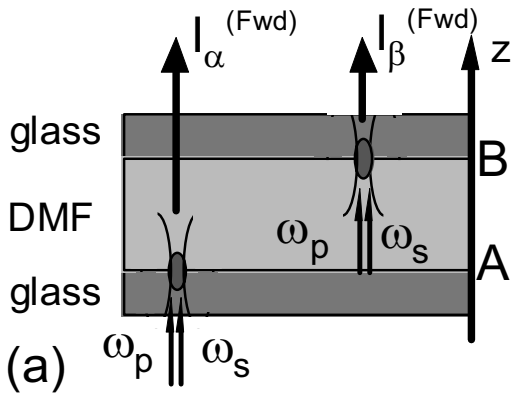

$$\Delta I^{(Fwd)} \propto 4\chi^{(3)}_{2NR}\,\Im\left(\chi^{(3)}_{1R}\right)$$

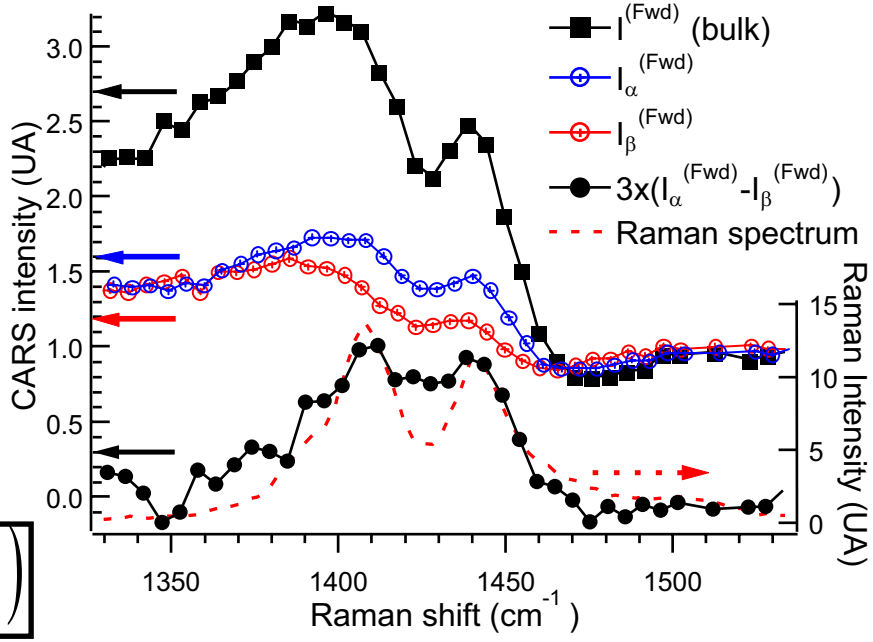

1. **Field symmetry permits to use non resonant CARS as a local oscillator**
2. **Raman spectrum recovery and heterodyne detection**

Gachet et *al.*, PRL (submitted)

Single pulse CARS

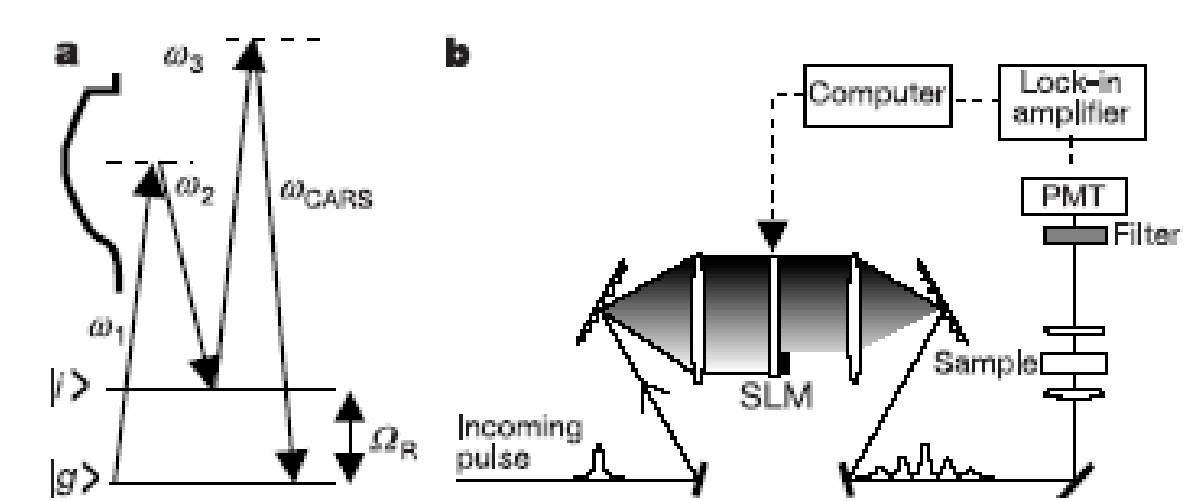

$$A(\Omega) = \int d\omega \epsilon_p(\omega)\epsilon_s^*(\omega - \Omega)$$

$$P_{nr}^{(3)}(\omega) \propto \int_0^\infty d\Omega \ \epsilon_{pr}(\omega - \Omega)A(\Omega)$$

$$P_r^{(3)}(\omega) \propto \int_0^\infty d\Omega \ \frac{\epsilon_{pr}(\omega - \Omega)A(\Omega)}{(\Omega_R - \Omega) + i\Gamma}$$

$\phi(\omega) = a_0 \cdot cos(\frac{\omega - \omega_0}{\Omega_m})$ $\tau_m = 2\pi/\Omega_m$ Can excite only a vibration with $T = \tau_m/N$

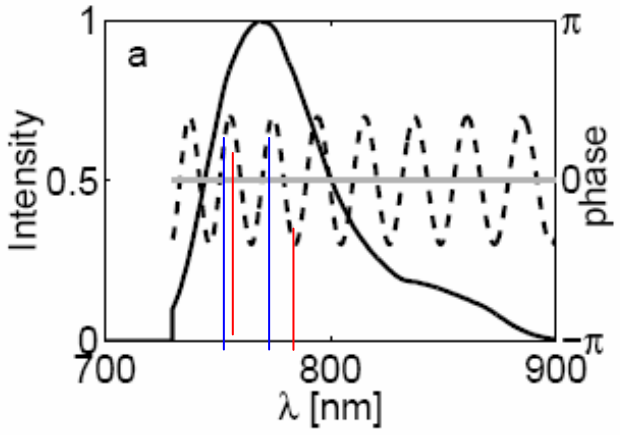

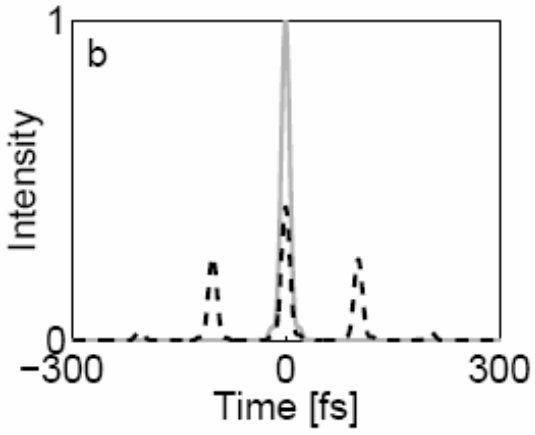

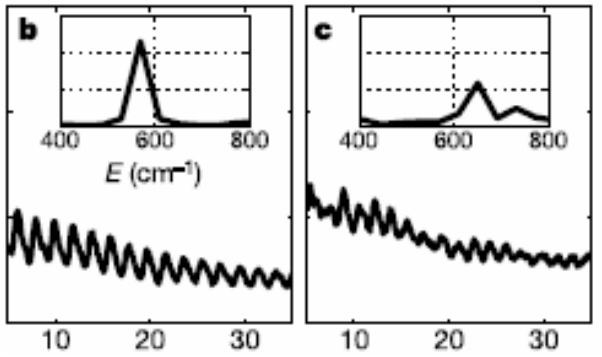

Number of oscillation across the SLM

CH_2Br_2 $(CH_2Cl)_2$

Dudovich, Oron, Sylberberg Nature 418 (2002)

Other scheme with a control of the probe beam: Oron PRL 89 2002

CARS Application: a stain free microscopy

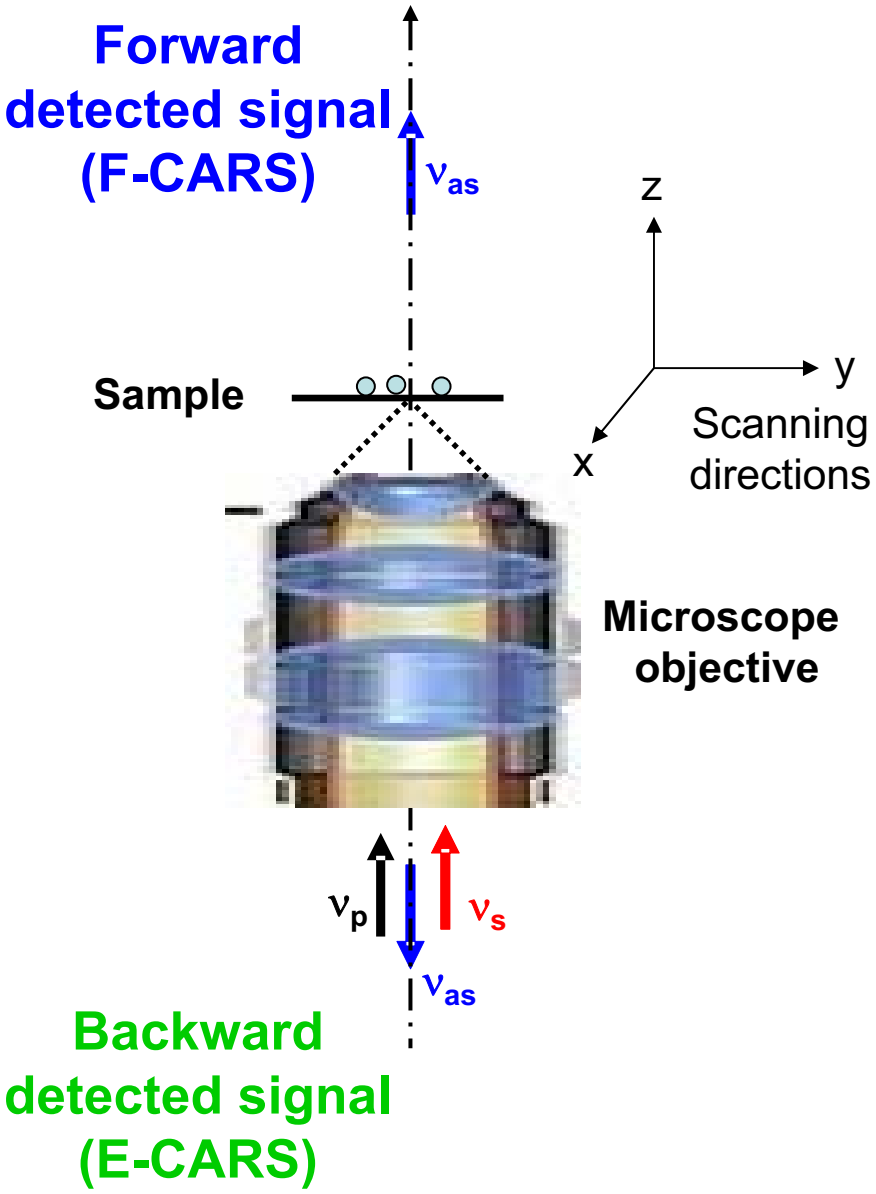

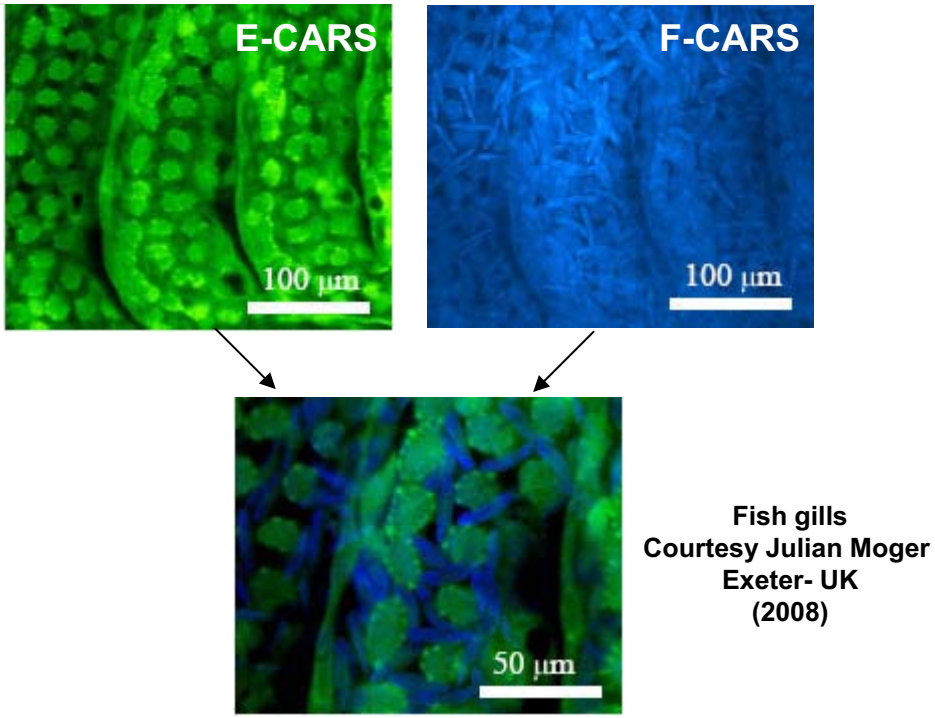

Fish gills
Courtesy Julian Moger
Exeter- UK
(2008)

Advantages:

1. Fluorescent staining useless.
2. Chemical selectivity of the contrast.
3. Intrinsic 3D imaging.

Imaging lipids in cell

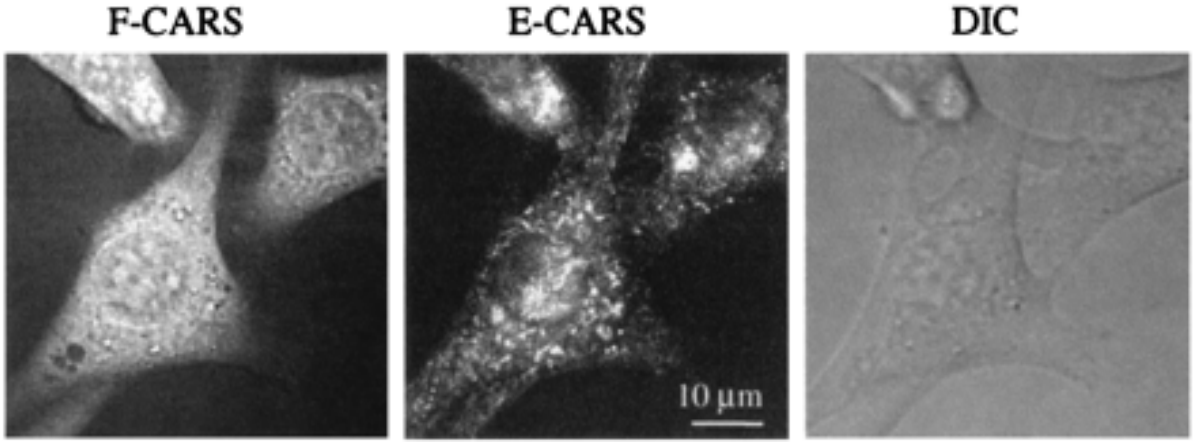

NIH 3T3 cells in interphase. Aliphatic C-H stretching 2970 cm^{-1}
Pump 14054 cm^{-1}(711nm) and the Stokes 11184 cm^{-1}(894nm). P: 40mW; S: 20mW

Cheng et al Biophys. J. **83**, 502 (2002)

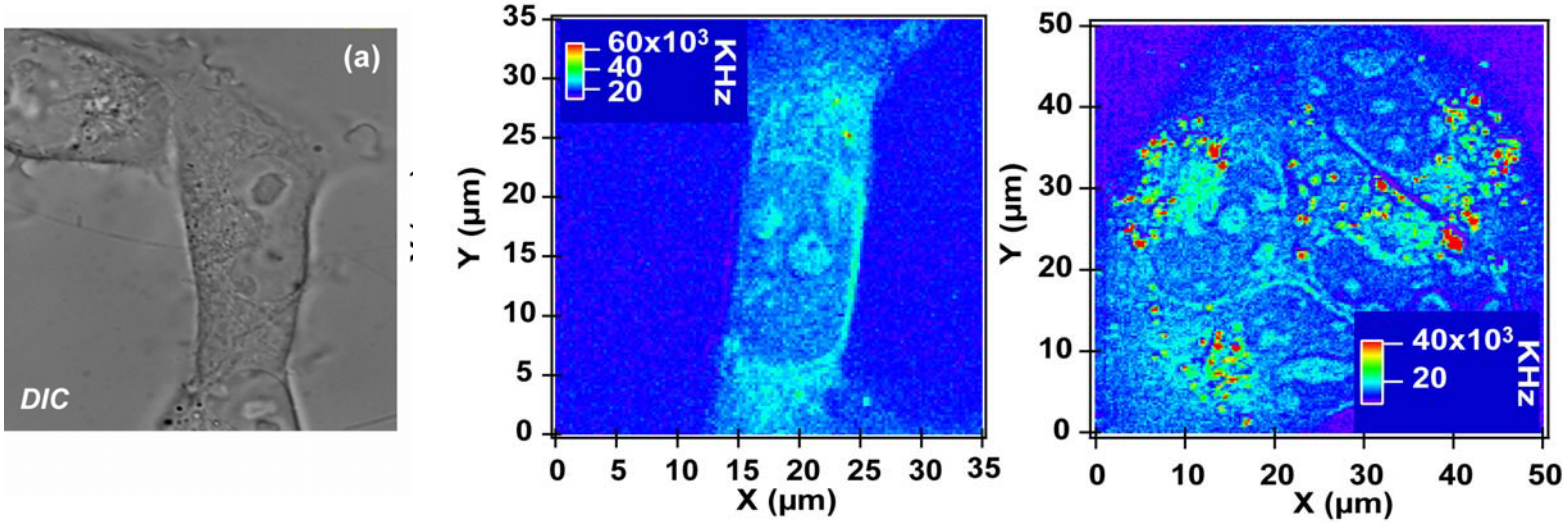

N.Djaker et al, Medecine & science – (2006)

3D sectioning capability of CARS

Three dimensional distribution of lipids in epithelial cells.
CH_2 stretching vibration (2845 cm^{-1}).
Lipid granules and plasma membranes.

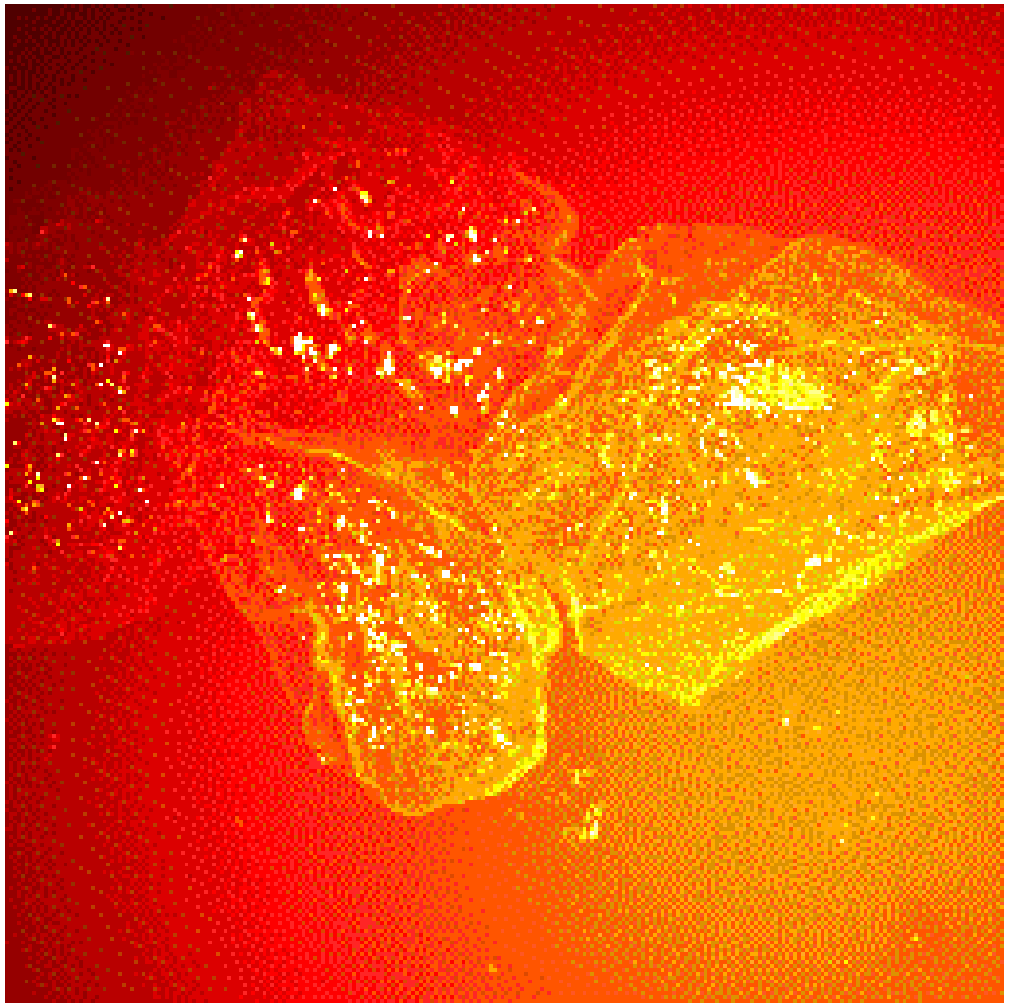

http://bernstein.harvard.edu/research/cars.html

Raman Spectrum of the cell

Potma, E.O. et al. *Optics and Photonics News*, 2004, *15*

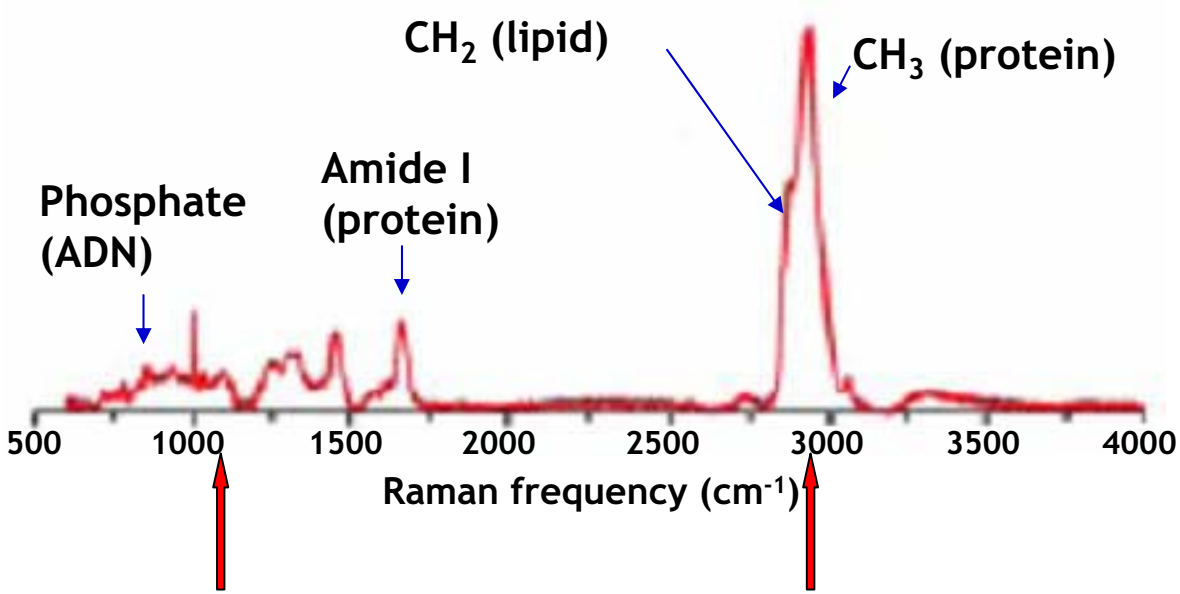

CARS image

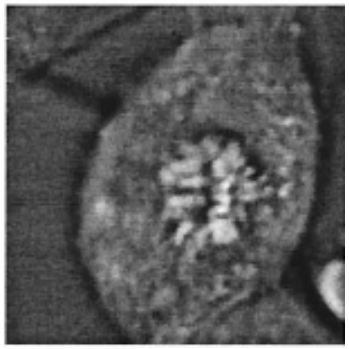

PO_2^-symmetric stretching vibrational frequency at 1090 cm^{-1}

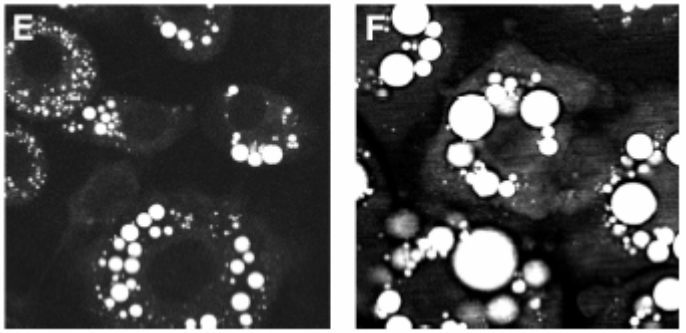

Lipid droplets in 3T3 cells (Xie group)

Imaging H_2O in cell

OH strech 3300 cm^{-1}
OD strech 2800 cm^{-1}

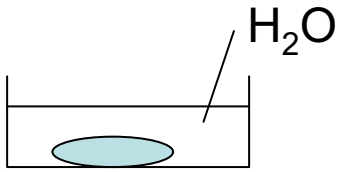

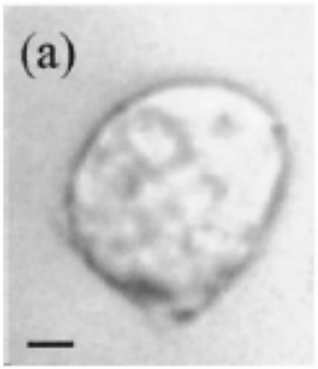

3300 cm^{-1} OH strech

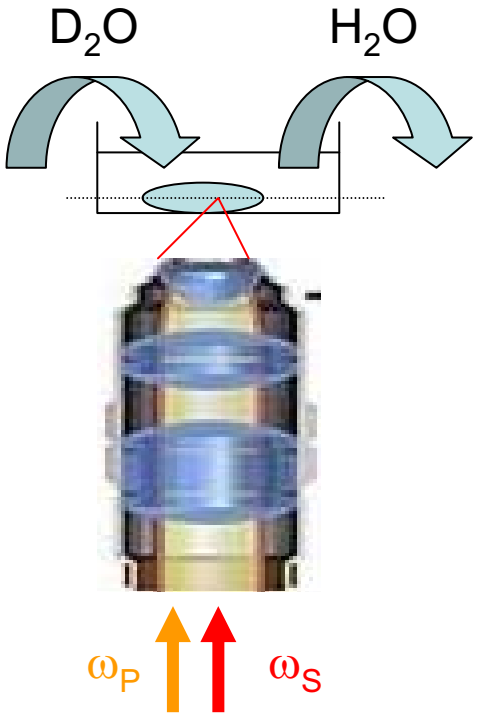

living *D. discoideum* cells

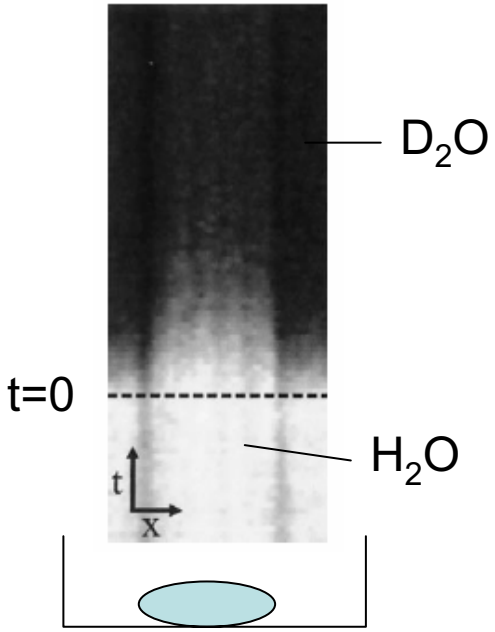

Permeability of the plasma membrane P_d=2.2 μm/s
D_w=5 $\mu m^2/s$ (10%-20% of the cell diameter)
D_w>500 $\mu m^2/s$ (central cell region)

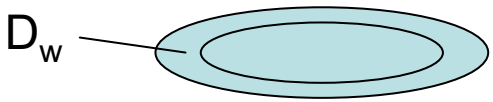

Exceptionally low D_w due to the presence of densely packed actin filaments in this region that provide an additional barrier in the process of water diffusion.

From Potma PNAS **98**, 1577 (2001)

F-CARS back reflected in scattering tissue

CARS imaging in scattering media

Evans et *al.*, *PNAS* **102**, 16807 (2005)

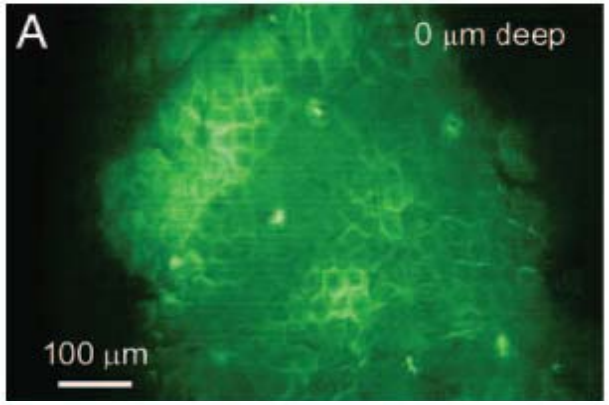

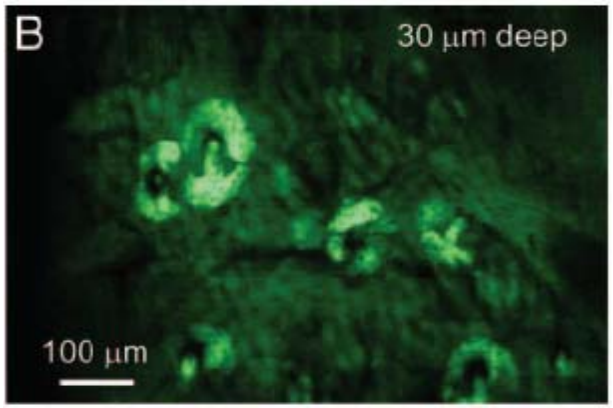

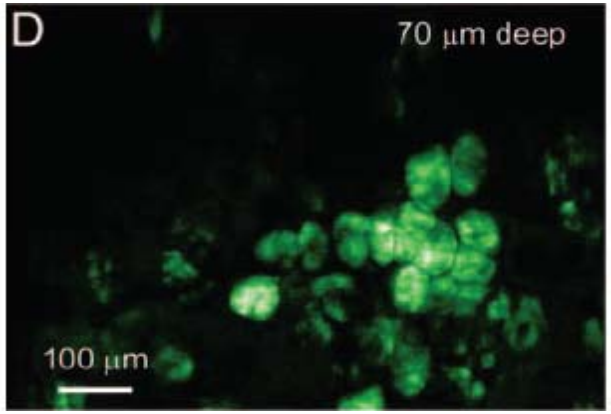

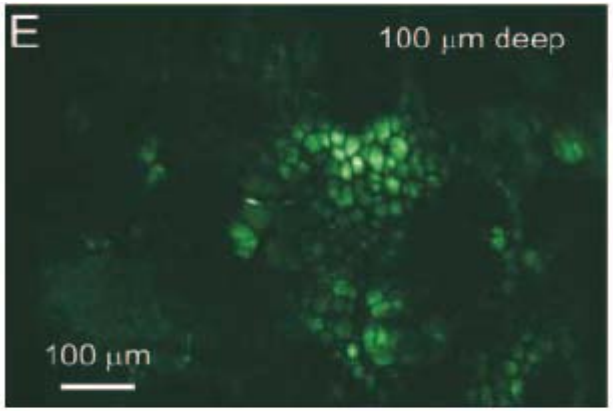

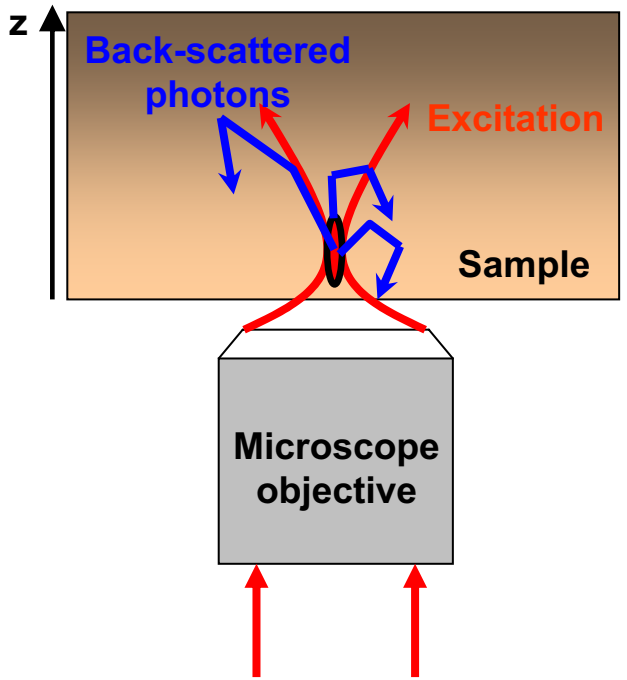

Imaging Tissue

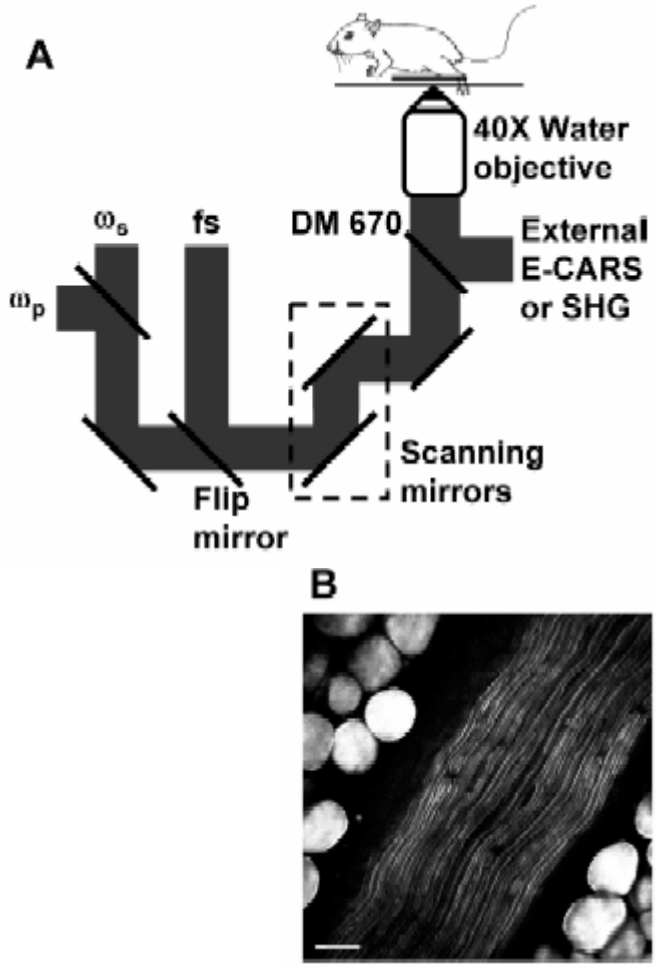

Experimental Setup and *in vivo* E-CARS images. (A) Experimental setup for combined **E-CARS and SHG imaging** of a live mouse. (B) E-CARS image of parallel **myelinated axons in the sciatic nerve** and the surrounding fat cells. Scale bar = 25 μm.

Huff, Cheng, J of Microscopy 225 (2007)

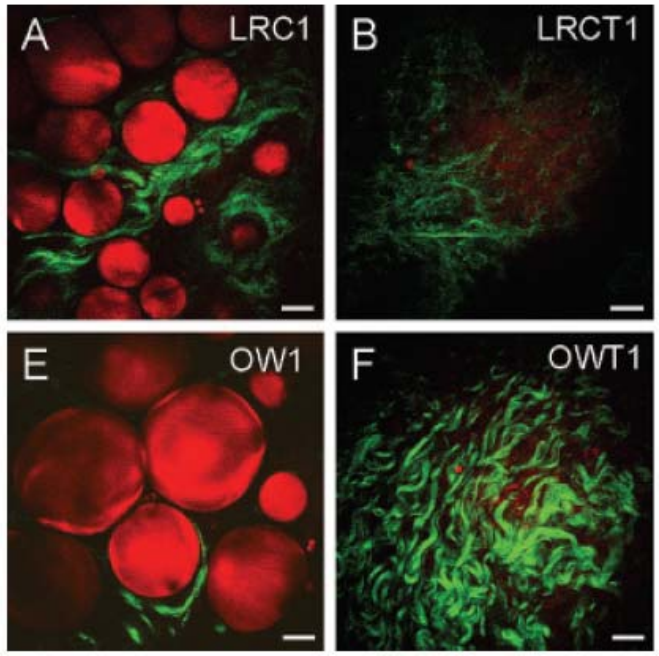

Coherent anti-Stokes Raman scattering imaging of **adipocytes** (red) and second harmonic generation imaging of **collagen fibrils** (green) to evaluate the impact of obesity on **mammary gland** and **tumor stromal** composition.

Le et al., Molecular Imaging 6 (2007)

Imaging the skin: Rat skin

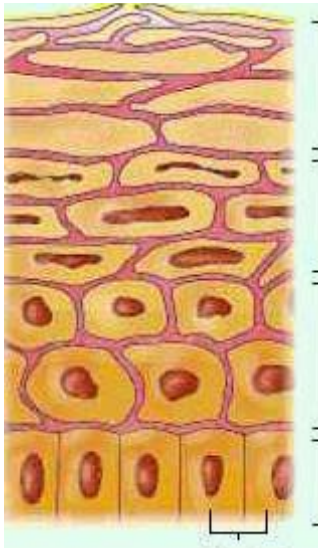

Stratum corneum

Depth: 0 µm

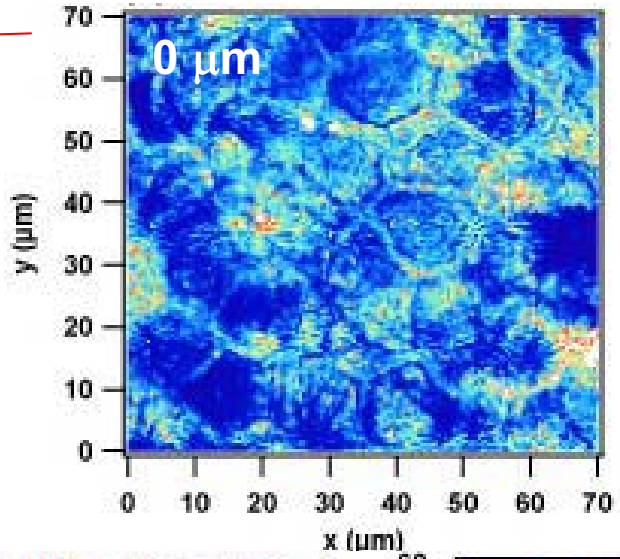

Marseille

Depth 15 µm

Adipocytes of the dermis

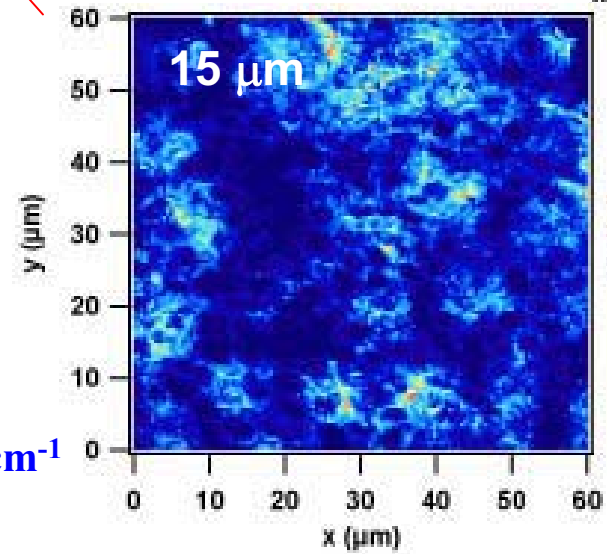

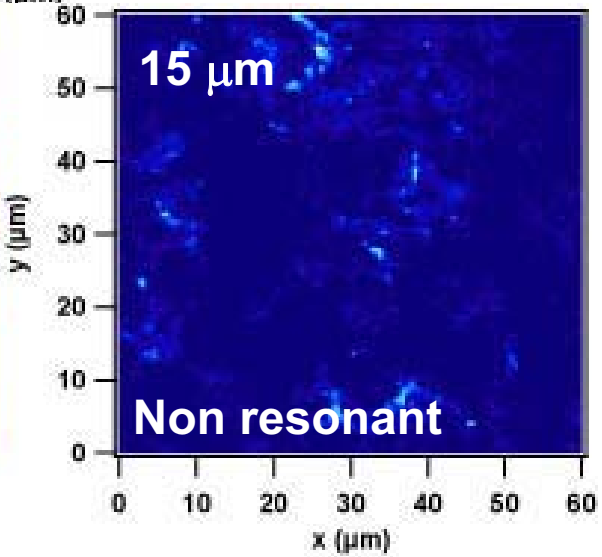

E-CARS rat Skin. CH strech 2845cm^{-1}
(200×200) pixels - 1ms/pixel.

Pump 730nm, Stokes 920nm: Power 800µW, rep rate: 4MHz

Imaging the skin: Stratum Corneum

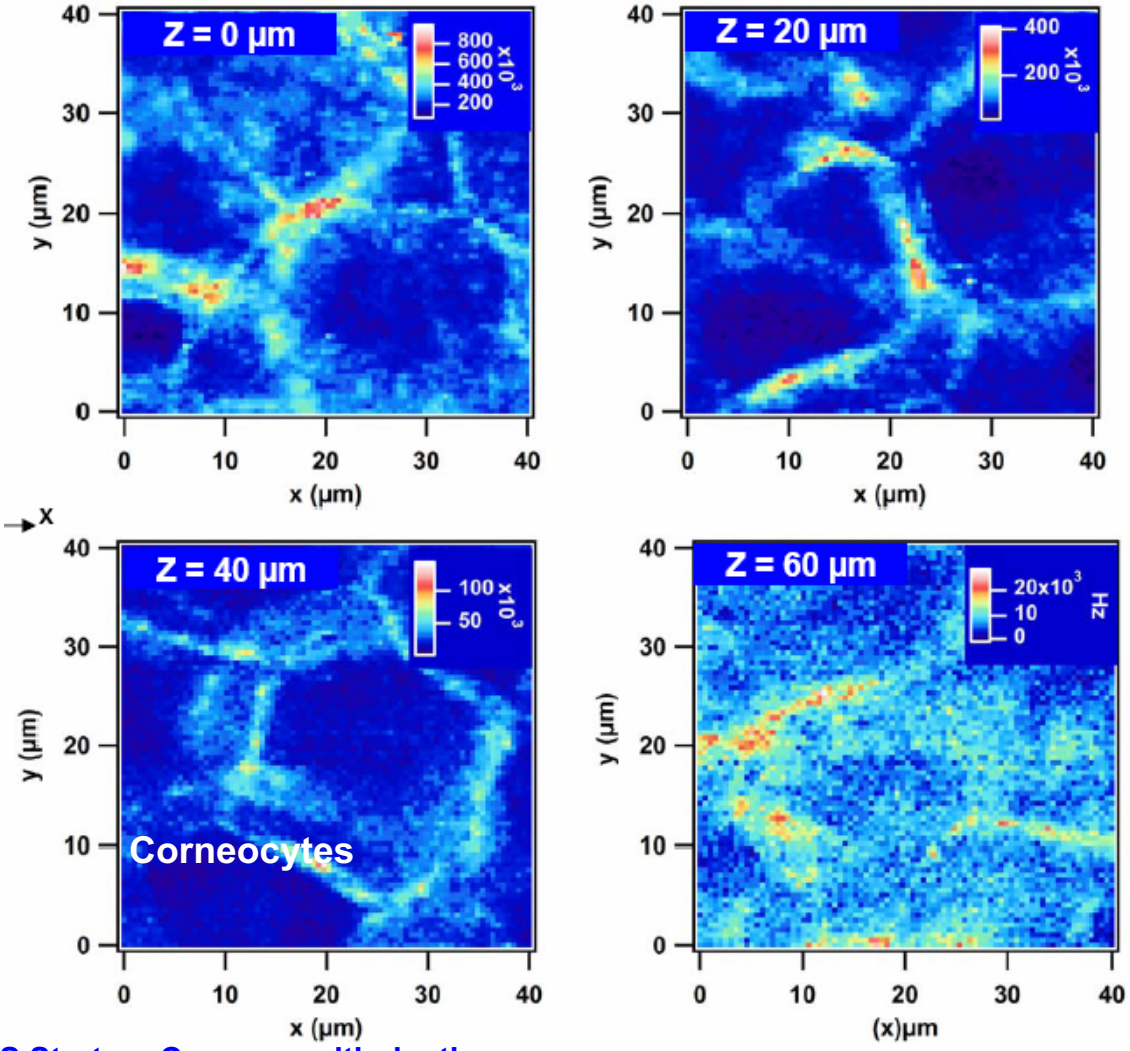

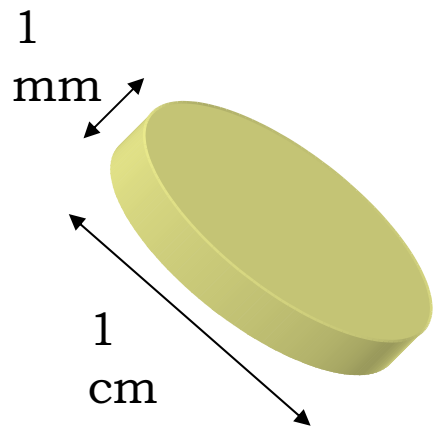

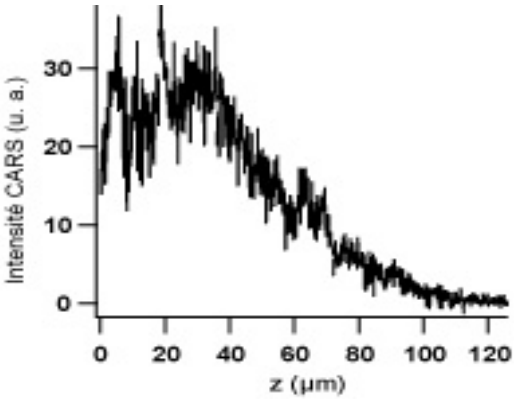

E-CARS Stratum Corneum with depth.

Ω_R=2829cm^{-1} (C-H bond)

(200×200) pixels - 1ms/pixel.

Pump 730nm, Stokes 920nm: Power 800µW, rep rate: 4MHz

A polarization sensitive technique

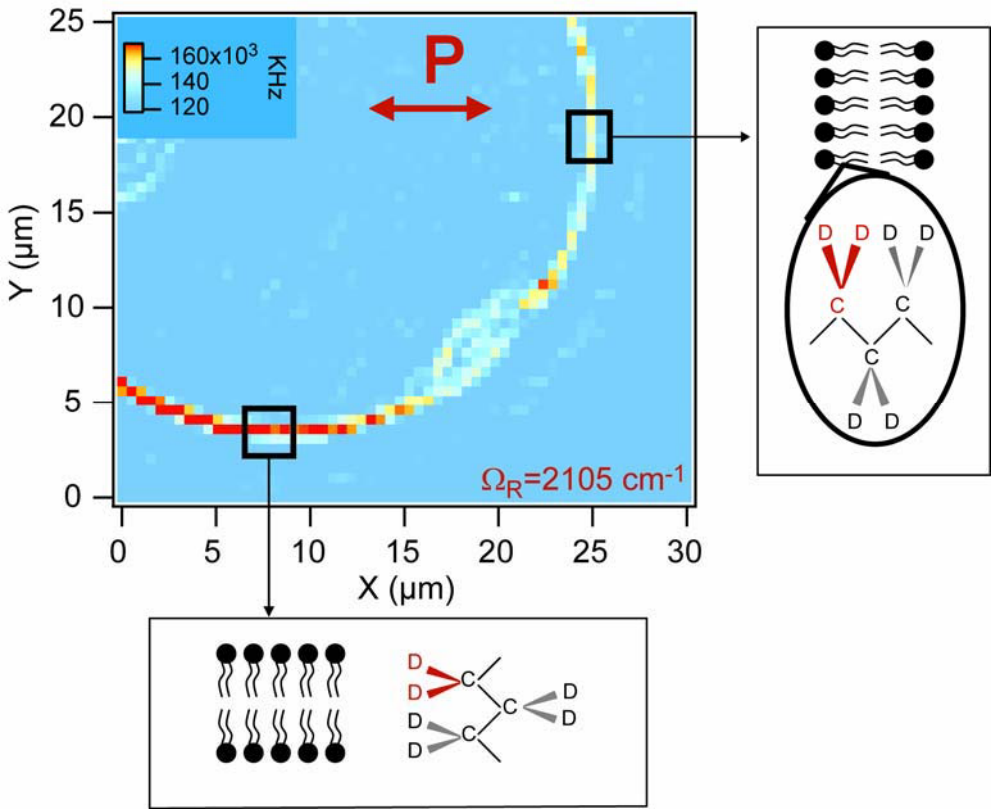

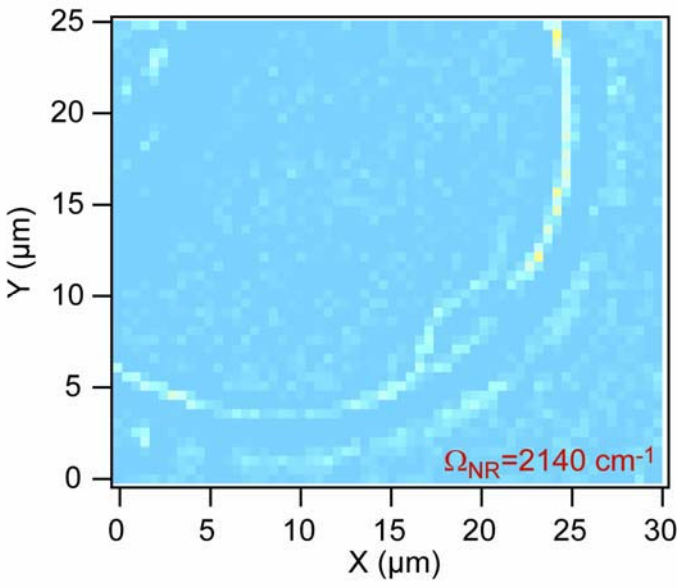

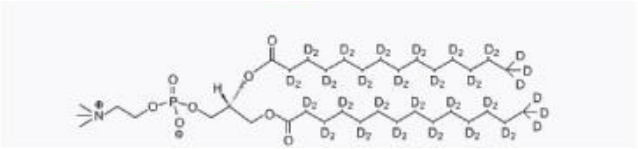

Djaker et *al.*, *Médecine / Science* **22**, 853 (2006)

F-CARS GUV (DMPC-D54):
(60×60) pixels, 1ms/pixel.

Pump 730nm, Stokes 860nm: Power 800µW : rep rate: 4MHz

Forthcoming

Investigation in polarization CARS microscopy

Conclusion

1. CARS addresses molecular intrinsic vibrational transition and does not require staining with fluorophore or radioactivity.

2. CARS is a coherent process which builds an anti-Stokes wave on a large number of molecular bonds. This coherent process permits to obtain a signal orders of magnitude larger than spontaneous Raman scattering. Small laser powers (1mw) can be used which are compatible with biological samples.

3. CARS is selective of a certain molecular bond (by adjusting the detuning between laser and Stokes beam) (spectral selectivity)

4. CARS is a non linear process which takes place only at the focal point of the microscope objective (diffraction limited) . Therefore no confocal pinhole is needed to obtain 3D imaging of biological samples.

5. Working in IR limits the absorption and diffusion of bio- tissue. Images as deep as 0.3mm can be obtained in living tissues.

6. CARS is an elastic process which does not store energy into the system. It is therefore insensible to photobleaching.

7. Finally, CARS is not affected by endogenous fluorescence because the anti-Stokes signal is at lower wavelength than the pump lasers.

Mosaic project

When photonics meets life

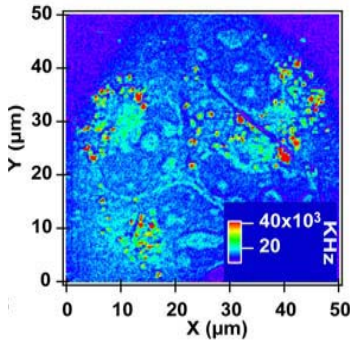

CARS

http://www.fresnel.fr/mosaic

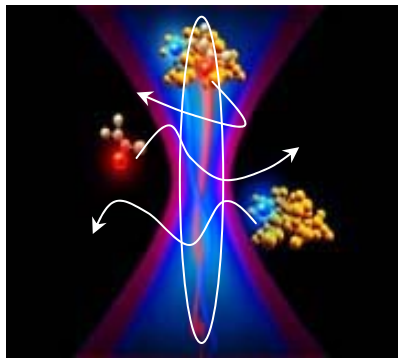

FCS

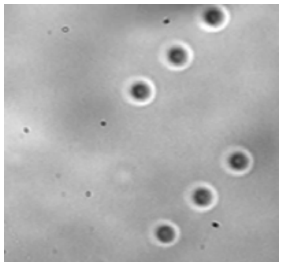

Dynamic organization
of living cells and tissues

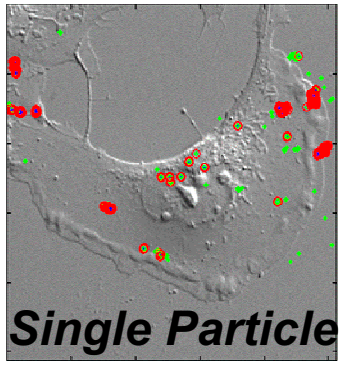

Single Particle
Detection

Dynamic Multiple
Optical Tweezers

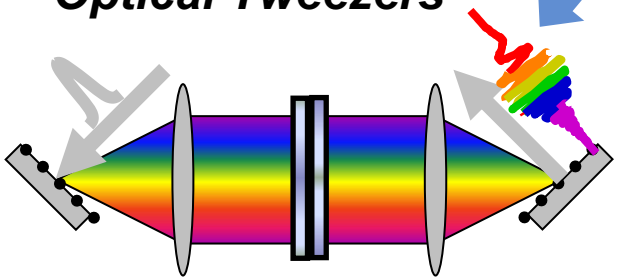

Pulse shaping
imaging

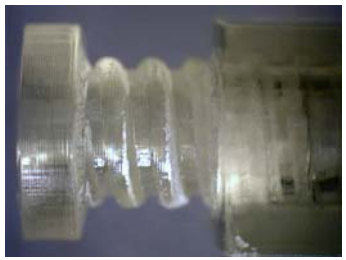

Micro-stereolithography

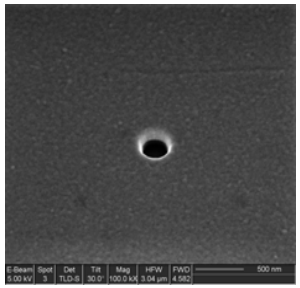

Nanostructures

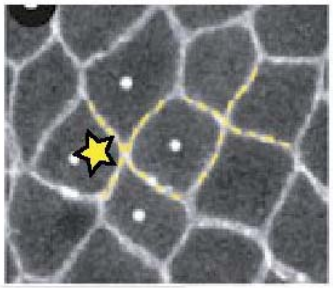

Laser nanoscissors